We appreciate the time and energy that all three reviewers put into the evaluation of our manuscript. Their comments and questions were insightful and addressing them has improved the quality and the clarity of the presented science. We have arranged our response by 1) reiterating the comments of the reviewers (black text) 2) providing our response (dark red, indented text) and clarifying where the comment was addressed in the revised manuscript. We address the points raised by each reviewer in order (Reviewer 1, 2 and 3).

Author Response to SE-2017-117-RC1 (P.A. van der Beek, 2017)

Gilmore et al. present a sensitivity analysis for a recently developed modelling approach in which structural restoration is combined with forward thermal-kinematic modelling to predict thermochronometer ages in fold-thrust belts, and subsequently use these ages to constrain the timing and rate of thrust-(sheet) motion in such settings. This is a promising approach, which h is being developed by several research groups separately (e.g., Almendral et al., 2015; Erdös et al., 2014; McQuarrie and Ehlers, 2015; 2017). However it still faces challenges, in particular how to take into account the topographic evolution through time and how to handle the large degree of freedom in the models. The present manuscript explores some of these challenges, in particular the effect of material properties (heat production rates), reconstructed geometry and kinematics, and the topographic history, which all influence the predicted thermal histories significantly but are very difficult to constrain. It is therefore a useful contribution to the still small but growing number of papers on this subject, and I would recommend publishing this in Solid Earth after moderate revisions.

I have two major comments and a number of smaller, more specific comments on this manuscript. The first major comment concerns the context of this study and what is exactly new in it. When I started reading this, this was not very clear for me. Long et al. (2012) presented the structural cross-section and thermochronology data used here, as well as similar data for the parallel more westerly Kuri Chu cross-section. McQuarrie and Ehlers (2015) modelled the data for the Kuri Chu cross-section in a similar manner to what is done here. What is new in this manuscript is the modelling of the (eastern) Trashigang cross-section. This is a valuable exercise in itself, and the comparison of the outcomes of the two modelling exercises in enlightening (see below), but I think it would be useful if the authors presented this context and the relationship of this study with previous work straight up in the introduction, so that readers are not left wondering what is new or different here with respect to previous work by the same group of authors.

> Introduction was revised to highlight new contributions and improve context with previous work. In particular we describe what is new in the introduction; p. 2 lines 13-21.

My second comment concerns the inferred history of shortening rates; in particular the strong variability in these rates that the analysis suggests. I have been intrigued by this outcome since the initial paper by Long et al. (2012). I reviewed that paper at the time and already queried the authors about the robustness and implications of that finding but am still struggling to understand it. Starting from what we know (and progressing toward lesser constrained inferences): the modern convergence velocity

between India and Tibet is ~20 mm/y; the total India-Asia convergence rate is about twice that. If we accept the results of Molnar & Stock (2009), India-Asia convergence rates have decreased since 20 Ma; from 54-83 mm/y before 11 Ma to 34-44 mm/y after that, for points in the NW and NE corner of the Indian subcontinent respectively. That total India- Asia convergence rate should be distributed between far-field deformation in the Tibetan plateau and its northern borders, shortening in the Himalaya, and underthrusting of the Indian plate beneath Tibet. It is interesting, and reassuring, to note that most of the tested models predict shortening rates in the order of 5-6 mm/y in the last ~10 Ma, which is consistent with estimated "overthrusting" rates in simpler thermokinematic models used to predict thermochronology ages (e.g. Brewer and Burbank, 2006; Whipp et al., 2009; Robert et al., 2009; 2011; Herman et al., 2010; Coutand et al., 2014, and others). Any increase in shortening rates up to the total India- Tibet convergence rate of ~20 mm/y could potentially be explained by temporally variable partitioning between "overthrusting" and "underthrusting"; since these concepts are really defined by a particular frame of reference only (which is in my view controlled by the erosional efficiency in the Himalaya), that could be plausible and possibly linked to temporal variations in erosional efficiency. If one wants to invoke further increases up to the India-Asia convergence rate, that would only be possible by temporally transferring far-field deformation to the Himalaya, but it remains in the realm of possibilities. The inferred rates of ~70 mm/y during building of the Upper Lesser Himalayan duplex are more problematic, because – if true – they would necessarily imply north-south extension in other parts of the Himalaya-Tibet system, for which there is very little evidence. The inferred reconstruction requires significant amounts of shortening to build this duplex (at least 150 km or ~1/3 of the total shortening since 20 Ma according to Fig. 3) and I wonder whether a more conservative structural solution would not be possible to fit the surface observations for this duplex. In any case, the preferred models with variable shortening velocities pose significant questions, which should be addressed more directly. The reader is really left wondering how well resolved these shortening histories are, given the significant number of unconstrained parameters in the models. Some of the specific comments below refer to these unknowns.

> We agree that the fast rate from ~ 13- 8 Ma are unexpected, and yet this is a robust part of the model and is a function of the suite of ZHe ages that are all 8.5-10 Ma in the Kuru Chu area and 9.5 to 11 Ma in the Trashigang area. These rocks cool through the ZHe closure temperature as the Baxa duplex forms, and accommodates 155-165 km of shortening. 160 km in 2 Myr is 80 mm/yr. That is essentially the problem. We appreciate the suggestion for a more conservative structural solution to reduce the shortening expressed by the Baxa Duplex. However, this is a region where the shortening amount is remarkably well constrained. Shortening magnitude in its simplest sense identifies an area (a box), and calculates the length of a unit with thickness X necessary to fill that box. The Kuru Chu and Trashigang sections from Long et al. (2011b) show how well-constrained this box is. Unlike sections in Nepal, the Baxa duplex in this area is almost entirely exposed and fault bedding plane relationships show the hanging wall cut-offs for the Baxa faults have (almost all) been eroded (implying more shortening possible). Yet, there are erosional remnants of the Paleoproterozoic Shumar/ Daling rocks carried by the Shumar Thrust exposed in fault klippe almost all of the way to the MBT (Long et al., 2011). These fault klippe define the top of the box as being essentially immediately above the erosion surface. There is

just enough space to erode the hanging-wall cut offs of the Baxa faults. The base of the box is defined by the décollement. The décollement depth for the Long et al., (2011) cross sections in the region of the Baxa duplex is directly between the 2 permissible depths estimated by Coutand et al., (2014) and matches geophysical constraints in the region (Mitra et al., 2005; Singer et al., 2017). If anything, estimates of the décollment depth are deeper (Coutand et al., 2014) which would just exacerbate the problem. The only variable left is the thickness of the Baxa, which can be observed in the field, as can the faults that repeat it. Field observations provide several thickness estimates that all fall between 2.1 and 2.5 km and well constrained shortening estimates of 150-165 km.

Thus in both the Ehlers and McQuarrie (2015) and in this manuscript, we have tried to figure out what is an acceptable age range that does not violate the data. Shortening rates can viably increase up to the India-Asia convergence rate of 40-45 mm/yr. The expectation is that during that window of time the Himalayas are taking up the entire magnitude of convergence. Shortening rates above that (45-70 mm/yr do require coeval extension to be viable.

We have conducted more simulations looking at the sensitivity of shortening rates, particularly using the new geometry. Due to limited measured cooling ages between 70 -100 km from the MFT there is more flexibility in the Trashigang section than the Kuru Chu and rates as low as 45 mm/yr (at plate tectonic rates) are permissible. Our new thoughts are that a revised geometry for the Kuru Chu section (two ramps) may facilitate more exhumation in this region and thus lessen the need for excessively fast rates (55-75 mm/yr) for that section.

Intriguing enough (because I (McQuarrie) have never been a huge fan of extrusion or channel flow) the age of this rapid shortening in the Baxa duplex overlaps with the age of the STD in this portion of the Himalaya --12.5 Ma (Th-Pb monazite age from Kula Kangri at the border of Bhutan and Tibet) and 7 Ma (ZHe ages)(Edwards and Harrison, 1997; Coutand et al., 2014). Although shortening rates should not be faster than plate convergence rates, it is permissible if it is accompanied by fault parallel normal faulting, such as is postulated by channel flow models. To me (McQuarrie), one of the strongest arguments for channel flow/ extrusion like behavior is thrust faulting rates above plate tectonic rates. The observed thrusting rate would be the shortening rate plus the extension (extrusion) rate.

Numerous changes were made to the manuscript in section 5.3 to address this comment and our new simulations.
(1) Without relating all of the justifications for the cross-section, we have included the statement that the cross section itself is a minimum shortening estimate and that any change to the cross-section will increase the shortening. We referred again to the Long et al. (2011b) paper where the details are laid out. (p. 22 ~l. 30)
(2) The manuscript includes revisions to discussion evaluating the permissible ranges of deformation ages and rates based on our simulations (~p. 23 l. 5-8)
(3) To present these new simulations in the paper, a new figure 11 has been created and introduced in this section, and table 3 updated.

(4) Comparison of the Trashigang section to the Kuru Chu section, thermochrometer data available along the sections, and reasons for differences between rates proposed by this study and by McQuarrie and Ehlers (2015) are included. (p. 23 ~l. 19-35)
(5) Because so many of the permissible shortening rates are above plate tectonic rates we have also expanded on our discussion of modeled rates to include their relationship to convergence rates in section 5.3. (p. 24 , l. 15-25)

Overall, the paper is fairly well written and illustrated. On a number of occasions, phrases don't run because a verb is missing or because of singular/plural confusions. A certain number of typos also remain. All of these can be weeded out by some careful editing. The use of some internal "modelling jargon" like "Python topography", "Split KT" etc. does not add to the general understanding of the manuscript – the authors might want to find some more eloquent terms to describe these modelling settings.

The manuscript has been edited to correct typos and clarify wording in areas that are currently mistyped or confusing. We changed the topographic estimations from Python Topography and Template Topography to Responsive Topography and Static Topography respectively. Since "Split KT" refers to Kakhtang Thrust motion at two different periods of time (versus all early or all late), we could not find a word that was more descriptive or more accurate and that would improve the readability of the paper. If you have a suggestion, we would be more than willing to incorporate it.

Specific comments, tied to page and line number:

p. 1 l. 7-10: the first two phrases of the abstract do not really set up the problem in a very clear manner or "draw" the reader into the problem – you may want to consider rewriting these into something more clear and specific.

Abstract was revised. Comments about the first two sentences of the abstract were raised by multiple referees.

p. 2 l. 13-20: this first paragraph of the "Geologic background" section looks a bit lost on its own; it is not very informative (why is the onset of motion on the MCT important here?) and could easily be combined with the following "Tectonostratigraphy" section. The Daniel et al. (2003) and Tobgay et al. (2012) references are missing in the reference list.

The geologic background was removed and the critical information was included in section 2.1 on tectonostratigraphy. Daniel et al. (2003) and Tobgay et al. (2012) was added to the reference list.

p. 3 l. 20-21: how were the data exactly projected into the cross-section? This is a critical step, as the ages (in particular for the low-temperature systems) will be influenced by the local topography. See further comments below.

In order to maintain structural context along the cross section, all of the data (including data from Coutand et al., 2014) were projected onto the cross-section along-structure (i.e. in the direction of the trend of fault while maintaining distance from structures as possible). The exceptions to this in the original manuscript were minor and have been corrected. We have corrected all figures data projected along the section to be consistent with the along-structure projection method, and text in section 2 describes this projection.

Since most samples were not taken exactly along the line of section, the elevations of most samples vary from the elevations at these projected location. However, our models do not use present-day elevation in the models either (discussed below in response to RC1 comment on p. 8 l. 15-19). We have plotted all of the data with respect to elevation and limited age elevation trends emerge strongly suggesting the ages are controlled by structural uplift and minimally modified by topography – this is clarified in the manuscript in section 2.2.

p. 3 l. 30: why do the ZHe ages require "rapid" cooling? This inference can only be drawn by comparing them to other thermochronometer data, or by assessing age-elevation profiles for instance.

There is no a priori reason to indicate rapid due to the age and the adjective has been removed.

p. 3 l. 32: three ZHe cooling ages north of the MCT are shown on the cross-section (but only two on the map?). Also, the cross-section of Fig. 2 gives the impression that the samples between ~57-65 km are from the lower Greater Himalayan sequence, while the map shows they are from the upper. Maybe you should sketch in some of the geology above the topography to make this clearer. This also brings us back to the question above of how these data were projected into the cross section. What was their imposed elevation? Simply plotting them on the topography in the cross-section puts them on a much lower structural level than where they actually are!

As explained above, this was a plotting error and has been corrected in figures and in text where fit has changed because of the re-projection. Overall results are not impacted by this revision. Since the modeled ages are all predicted at the surface, projecting the samples in the air would have limited applicability to match modeled results. Where discrepancies between modeled and measured ages exist we do examine both the structural and topographic elevations that the samples are from. For example see new text in section 5.3, p. 23 l. 5-10

p. 4 l. 5-9: why do you take this approach? It is easy enough to model the individual data using the combined Move/Pecube approach . . .

At the scale we are evaluating predicted versus measured ages and what is controlling the change in ages, these samples plot basically on top of each other, particularly when projected into the cross section. In the version of Pecube we use, the ages plot as the age trend shown on figures 5, 6, etc. In our view, they represent a true variability in sample age and can be considered a clustered datum rather than several data for our purposes. The one minor caveat to this is the cluster of AFT age in structurally higher Greater Himalayan rocks. As expanded on

in our responses to reviewer 3, (and included in the text at the end of section 2) there is a modest age elevation trend here. However the exhumation rate given by the age-elevation differences is 0.4 mm/yr while an average 3.5 Ma AFT age suggests more of a 1-1.7 mm/yr exhumation rate. Additional details of possible age elevation relationship are mentioned at the end of section 2.2.

p. 4 l. 17-18: the question here is obviously: "how was the new topography obtained?" this is discussed further on – you may want to refer the readers to this later discussion here.

We mention where the approach is discussed further in the first paragraph of section 3.1.

p. 4 l. 26-27: Note that a subsequent similar model by the same authors (Hammer et al., GRL 2013) comes up with much lower estimates for the elastic thickness in Bhutan (< 25 km) than in Nepal.

Yes, the very low values (in Hammer et al., and in Berthet et al., 2013) are in part a function of their approach for estimating EET that varies spatially (something that we are unable to mimic using the flexural algorithms in Move). In addition, the solution is for modern EET, which for Bhutan is strongly depending on the narrow width between the MFT and Shillong Plateau. 1) Our EET is a much longer-term average and, 2) is not meant to be viewed as a calculation of the EET in the area. However we can state with confidence that using low (25-40 km) EET values in the flexural-kinematic model will not reproduce the foreland basin thickness, the modern dip of the décollement or the geology exposed at the surface today. This section has been modified appropriately.

p. 5 l. 2: here you could reference some of the previous studies using the same approach.

Although there has been a suite of groups moving forward with linking cross-sections to advection diffusion models the details of the kinematic model are not always clear particularly if or how flexural loading and erosional unloading were accounted for. A good example of the potential influence is Erdős et al. (2014). They noted that a cooler crustal thermal structure was needed to match the measured high-temperature cooling data (than the lower temperature data) in the Pyrenees. Alternatively, their model could be restoring the rocks to a position that is too deep (thus becoming too warm) because thrust-related isostasy was not taken into account, or perhaps accurately accounted for as the section was retro-deformed backwards in time. What this paper highlights is that accounting for flexure (and erosion) in the kinematic model is a critical and necessary component.

We added text addressing this in section 3.1 as well as 3.1.1. In both sections, references to work using this approach were added. We added more detail in section 3.1 to discuss the kinematic modeling process, in particular how different groups account for flexure, erosion, and thus paleodepths, because these decisions are going to control the estimated temperature histories and ages

p. 5 L. 27-31: a self-consistent approach would be to use a critical-taper topography in the models – it is not clear if the "Python topography" is based on such an approach, but the link between the imposed topography and a critically tapered wedge model could be outlined here.

> The "Python Topography" (now Responsive Topography) may be viewed as a simplified critical taper approach, with the first order angle of topography estimated from modern topographic angles in the Himalayas. A key difference is that we do not systematically vary the topography angle based on the décollement angle. Please see further discussion response to p. 8 l. 22-24 comment below.

p. 7 l. 6-17: see general comment on variable shortening rates above. More justification and discussion of these rates is needed.

> As mentioned in the general comment above, a whole range of velocities were tested and we acknowledge that a full suite of parameters tested (including velocities) was not reflected in the previous version of this manuscript. We have addressed this in section 3.2.2 and Table 3. This is also more fully addressed in the discussion section 5.3.

p. 7 l. 16: it seems that this is the first time the Kuru Chu section is mentioned; it hasn't been introduced previously (but should be).

> The Kuru Chu section and corresponding studies are now mentioned in section 2.2, (multiple locations), and earlier in section 3.2.2, and quite a lot in section 5.3.

p. 7 l. 19 (and numerous other occurrences): why do you call the reconstructions "flexural models"? This is surprising and confusing, as flexure is only one component of these models; the structural reconstruction is at the heart of them. You could call them "kinematic models" or something like that.

> The decision to call the models "flexural models" stems from the multi-step process of achieving a viable "kinematic model" in Move – and from our suspicion that the flexural component is missing from most thermo-kinematic modeling approaches that use cross section kinematics (clarified in the revised end of section 3.1). Without accounting for flexure in the kinematic solution, the evolution of the décollement cannot be determined and thus the estimated depth history (and resulting thermal history) of a given rock becomes a complete guess. Thus a forward model taking into account flexure is critical. We are weighting the flexural component with the term 'flexural'. The work flow for any given kinematic model is to first find a pure kinematic solution (the "kinematic model") with only fault motion accounted for, the second round of iterations is the flexural component that requires an evolution of topography, erosion, foreland basin development, and décollement flexure.
>
> We have revised the name to include both adjectives, Flexural-kinematic model, to make the model name more intuitively descriptive. We also clarify the reasoning for this in the revised end of section 3.1.

p. 7 l. 30: the INDEPTH lines were shot in the Yadong rift, which overlies the Yadong cross-structure – a probably important lateral ramp in the Main Himalayan décollement. Is the 4° dip you cite here relevant for the décollement west or east of the Yadong structure? In any case, this would be valid for western Bhutan and not necessarily for eastern Bhutan. It is not obvious that comparing the décollement dips with data that are not from the same region is very informative, given the probable lateral segmentation of the MHT.

> We have removed this reference and added Singer et al. (2017), which has estimates for both the décollement and Moho for this region of eastern Bhutan.

p. 8 l. 1-4: this is counter-intuitive. The flexural response should be driven by the topographic loading, not by the kinematic scenario. Therefore, if the different kinematic models lead to differences in flexural loading profiles, it must be because the (imposed) topographic response to the kinematics is different between these models.

> Yes, this is correct. We have rephrased this to make it much more clear and more accurate. See revised section 4.1

p. 8 l. 15-19: why do you not simply use the present-day topography as the final topography in the model? This is a known entity, and at least that would help in comparing kinematic and thermal histories at the right structural and topographic levels for the data points.

> While at first impression it seems that using present-day topography as the final topography would improve the integrity of the models, that is only true of a model that can 'predict' a topographic evolution where the next to final topography is almost identical to the modern topography. If there is significant discrepancy between the penultimate predicted topography and the present-day topography (if inputted as the final step) the result would be unrealistic "deposition" of material in areas that are modeled in the prior step with a lower topographic elevations than actual topography. Simultaneously, in areas that have lower actual topography than modeled, using present-day topography could simulate several km of unexplainable erosion.
>
> We recognize that topography of the Earth's surface is altered by more processes than are accounted for in our simplified, first-order estimation of topography such as river incision, the geometry of interfluves, and the effect of axial or transverse drainages. Our approach to modeling topography is outlined in McQuarrie and Ehlers (2017): "the more simplified critical taper model that responds to regions of uplift or subsidence will account for the longest-wavelength, and most significant, topographic effect (i.e., valley and ridge topography) in the thermal calculation."
>
> Each kinematic scenario prescribes a different evolution of topography because as Reviewer 1 stated in the p.8, l. 1-4 comment, "topographic response to the kinematics is different between these models." Our goal is to determine if the estimation of modern topography using the

python script can successfully replicate the first-order patterns of present-day topography. This is why we compare where and how the modeled topography deviates from the actual topography.

p. 8 l. 22-24: this phrase is hard to read and also appears counter-intuitive. In the critical-wedge model, the surface topography (α) and décollement dip (β) are linked through the critical taper angle (which itself depends, among other things, on β). Therefore, it might be more self-consistent to try to find a surface topography angle that corresponds to the critical taper for each time step (and degree of topographic loading). This would be an iterative approach, but I'm sure it can be done. See comment on p. 5 l. 27-31 above.

This is an intriguing point and one that we have thought about. As elaborated on in our reply to Reviewer 3, *Move* is a purely kinematic model and thus not governed by mechanical responses. Critical taper is a mechanical response that is dependent on a ratio of internal rock strength to décollement strength (i.e. resistance to sliding) (Dahlen 1990; Suppe, 2007). Thus assuming constant critical angle (one in which the topography angle becomes smaller over time as the décollement angle becomes steeper) would most likely misrepresent the topography evolution of the fold-thrust belt because décollement strength changes as lithologies change. As pointed out by Stockmal et al. (2007), pure critical wedge solutions become more limited when evaluating the effect of material differences, particularly ones with original horizontal geometries, and the ways in which those initial planes of weakness impact the internal structural geometry, strain history patterns, etc. This non-uniform behavior alters the predicted erosional response. An example may be the front of the fold-thrust belt dramatically propagating forward (on a weak décollement) before the development of a duplex system. The jumping forward would dramatically reduce the taper angle and the duplex response would be to increase structural and topographic elevation to regain "critical" taper (so the system can move forward). Using a constant (say 2° topography angle) in a model suggests that the taper angle is increasing through time. A true self-similar response would argue that the initial topography angle of the cross sections presented here would be 2.5°- 3.5° with an initial décollement angle of 1.5° to produce a final critical taper of 6°- 7° (broadly similar to the modern 4-5° décollement and a 2° topographic slope).

What we do know is the geology that is at the surface today, the modern dip of the décollement, and the cooling ages of a suite of minerals. What we can test is a topographic evolution that best matches all of those constraints because the ability of the model to predict older and deeper thermochronometer ages reflects its ability to accurately estimate the relationship of those rocks to the evolving surface of the earth. Critical taper theory gives us broad bounds for what may be a realistic topographic evolution though time. And that is an evolution that can get tested (using a range of permissible topographic angles) to see how accurately it reproduces the first order features in the modern topography.

Regardless, a taper angle is topography plus décollement, and defines an area that is filled with folded and faulted rocks. If the area does not change, (because the taper angle des not change, then a lower topographic angle would require a steeper décollement. We have rephrased this in section 4.1 to make this clearer.

p. 9 l. 11: you may have modified your version of Pecube, but in the "standard" model, heat production is constant with depth, so that "surface heat production" is a bit of a confusing term in this context.

Following the approach and rationale summarized in McQuarrie and Ehlers (2017), we prescribe an exponential decrease in heat production with depth, as opposed to assuming a constant crustal heat production. An exponential decrease in heat production with depth requires definition of a surface heat production (Ao) and an e-folding depth. One caveat of this approach is that material properties are not exhumed during the simulations to modify the surface heat production value. However, an exponential decrease in heat production with depth has the advantage of honoring observations that heat production diminishes with depth through the crust and that this decline is not monotonic (Chapman, 1986; Ketcham, 1996; Brady et al. 2006). This approach not only allows honoring measured surface values of heat production in the Himalaya (e.g. see Whipp et al. 2007), but also produces reasonable mid and lower crustal temperatures that would not produce partial melts. This text has been added to section 3.2.1.

p. 9 l. 15: this seems a fairly obvious result, since the kinematics of the models do not change, only the thermal field. The samples have the same "normalized" thermal histories; the temperatures are simply somewhat higher throughout for the models with higher heat production.

Yes, we agree. We have added this phrase when we first talk about the differences in the predicted ages. i.e. "The most apparent trend among all three thermochronometer systems is that predicted cooling ages become younger as the radiogenic heat production increases from 1.0 to 3.0 $\mu W/m^3$ due to the higher temperatures throughout the model." In addition we now talk about how changing values of heat production effects the three thermochronometer systems differently.

Specifying the changes in predicted cooling ages as Ao values change is necessary to fully address the concern raised in p. 13 l. 31-32, when we altered both heat production AND geometry , Reviewer 1 was left wondering "OK, but how much of this improved fit can be ascribed to the new structure and how much to the increased heat production." The background we have expanded upon here is needed to emphasize what signals are a function of changing geometry and what signals are a function of changing heat production when both change later in the manuscript (sections 4.3.1, 5.1.2 and 5.2).

p. 9 l. 19: "ages" not "rocks", I think.

Corrected

p. 10 l. 3-5: a bit of a rambling phrase that is difficult to read/understand.

We revised this paragraph to make it easier to read.

p. 10 l. 24: “later” not “earlier” I think?

Revised to “more recent”

p. 10 l. 32-33: there are many free parameters in these models: not only an infinite number of shortening-rate histories, but also significant degrees of freedom in the imposed structure and the topographic evolution. I fully understand and appreciate the difficulties in exploring this complex parameter space, but how robust are the inferred rates really? This is not obvious, and given the important implications of the shortening-rate history, this should be discussed. An alternative approach would be to not allow shortening rates that are greater than the plate-scale convergence rates at any time (i.e. use the plate-convergence rates as a constraint) and try to find models that can explain the data using this constraint.

We agree that the sensitivity of the model to the prescribed rates needs to be more fully discussed. The questions that Reviewer 1 raises on how-well constrained shortening magnitudes are, helps to elucidate what additional information is needed.

To address this comment, we removed much of the last paragraph in section 4.2.2 that emphasized the variations in shortening rates. Instead we ended with the very important observation that even with dramatic changes in shortening rate, the model still can not accurately predict cooling ages through the greater Himalayan section. We return to the discussion of shortening rates and the sensitivity of the predicted ages to these rates in section 5.3. We discuss the sensitivity of the model to rates that are at plate convergence rates (~45 mm/yr) versus faster than plate convergence rates when we present the revised geometry. In the end, there is limited usefulness in evaluating rates with a geometry that will never reproduce the measured ages.

p. 11 l. 10-11: why is this your expectation? The erosional history would depend on the topographic history through time, rather than the final topography. In the no-topography scenario, if I understand well, there is no topographic change through time. If in the other topographic scenarios topography diminishes locally in the final timesteps, this will predict younger ages.

Yes, a topographic scenario where topography diminished with time would produce younger ages, and the expected exhumation difference would be approximately the change in topographic elevation (maximum 2-3 km). Our expectation that the No Topography scenario would produce younger ages is because these models always produced higher total exhumation where the final cross section was over eroded by 1-2.3 km. The age in which this exhumation happens is a function of the age that a given structural relief was being generated. As an example, some component of over-erosion happened as the upper Lesser Himalayan duplex

moved up and over the pronounced ramp at 65 km. Thus our expectation is that predicted AFT ages that show this exhumation would be younger. The conclusion is that since the magnitude of erosion that happens during this displacement in each topographic scenario is significant, the additional 1-1.5 km of extra erosion in the No Topography scenario is not significant – particularly when viewed incrementally (e.g. Valla et al., 2010).

p. 11 l. 14-15: a list of 6 adjectives ("Python topography model fully reset Mar ages") followed by another of 4 . . . Maybe rewrite?

This was revised.

p. 11 l. 20-23: this is an important point but it also seems fairly obvious. It clearly points to the need of a self-consistent treatment of topographic evolution. The best way forward may be to combine these models with simple surface-process models to erode the topography through time.

We agree, a self-consistent treatment of topographic evolution where the modeled topography is a function of the deformation is a key result from this work. Although this seems like an obvious result, it is also a common approach to use a DEM of modern topography in models and assume that topography is in steady state and not changing – this result highlights that assumption is not valid either (and may also cause burial of material where particle points are subsiding and topography is not, and produces over-erosion of material where rock uplift occurs but topography remains static.

Also, while it is obvious to Reviewer 1, how topography is estimated particularly over long time windows is still a rather new item of discussion and application for thermokinematic modeling in compressional orogens. As outlined in the introduction, several other studies that have used Pecube have not used a method of applying topographic evolution that account for localized structural uplift and isostatic subsidence. Rather, they apply a muted topography similar to present-day elevations, infer topographic changes that seem appropriate or increase/decrease topographic slope over time. Yes, a self-consistent way to estimate topography is critical.

While we see the value of using other surface-process models such as Cascade to erode topography over time, the Python code (or an equivalent Matlab code) we use in this study, which approximates the first order topographic slope and specifically accounts for increasing topography in regions of active uplift and subsiding topography, provides a critical first step for estimating topographic change particularly in the isostasy calculations in *Move*. What may not have come through in the paper was the iterative process of finding a flexural solution (which is why we referred to it as flexural modeling). The kinematic displacements are known, and we are searching for a solution where the sequential kinematic restoration in *Move* (using flexure) can reproduce the depth of the foreland basin, geology at the surface and the dip of the décollement. This may take 20+ iterations to achieve using 20 km shortening increments. Thus whatever mechanism is being used to generate an initial topographic estimate needs to evaluate the magnitude of topography change and predict a new topography in <1 minute to be

viable in the iterative process. In addition, 1D erosion models require an estimate of time (which would have to be approximated for the initial reconstructions). Of course if the velocity were to change then the flexural-kinematic reconstruction in move would need to be redone. 1D erosion models also do not account for sedimentation (in a growing foreland basin). Our thought process is that the thrust loading and erosional unloading are much more sensitive to the first-order component of topography and thus using the responsive topographic taper approach is the best approach for Move. Once the displacement field has been determined (and then the resulting velocity fields), Pecube can run in conjunction with Cascade, to predict a more realistic and variable topography. As a double check --this Cascade Topography can be imported again in Move – just to make sure the resulting isostatic load is the same. We are currently working on fully integrating our modified version of Pecube and Cascade.

p. 12 l. 2: I think you are discussing MAr ages specifically here? May be useful to state this.

Revised

p. 12 l. 30: “older ages” seems more correct than “earlier ages” in this context.

Corrected

p. 12 l. 31: you have been calling this the MHT throughout the manuscript. Better stick to this acronym so as not to confuse the readers.

Changed

p. 13 l. 1-2: another somewhat rambling phrase . . .

This has been revised

p. 13 l. 5: this ramp is rather located at _90 km in the present-day geometry (Fig. 2)?

No, this early ramp is no longer visible in the cross section. See figure 3 C.2a for ramp location. We have clarified this in the Manuscript by revising the first 2 paragraphs of section 4.3 and referring to the appropriate figure location and ramp locations in the text.

p. 13 l. 12-15: is the cross-section of Fig. 9 still balanced? There is all of a sudden 35 km more Baxa group in this cross-section, while the rest of it has not been modified. Could these additional 35 km be found by reducing shortening in the upper LHS duplex? In that manner you might also be able to reduce the problematic shortening rates necessary to produce this (and the associated ZHe ages).

The new cross-section in figure 9 is balanced. Forward modeling the kinematics of a cross section ensures that it is balanced. But Reviewer 1 is correct in that the distribution of shortening has changed. All ramps north of the new Baxa footwall cutoff were shifted 35 km

north, and thus 35 km of shortening was added. Yes, we agree this does not reduce the problem of the fast rates (it can make the rates higher).

Our modeling (and others) have highlighted the strong relationship between ramps and young cooling ages. We can use this relationship and what is required by the geology to figure out how far south we can place the southern ramp (through the Diuri) initially this was placed at its location because the pervasive northward dips in structurally higher units (the northward dipping boundary of the Shumar-Daling on Baxa, GH on Shumar-Daling and the northward limb of the STD all suggest a northward dipping ramp ~ in the location shown on both cross section). What we did was turn this large ramp in Long et al.'s (2011b) original section into two ramps to better match the cooling signal. We know that the Baxa formation *has* to be under the anticline of Shumar-Daling because of the along strike relationship shown in the Kuru Chu section of the map (figure 1 – the anticline shown in the cross section is underlain by the Baxa Group rocks repeated by faults). So, even though we could move this ramp farther south to 50 km (location of the youngest AFT age in this region -- figure 9), we can't remove either of the Baxa horses. In addition, moving the ramp farther south would make each of these horses longer, adding more shortening back into the geometry. The cross sections were constructed to minimize shortening while matching surface constraints – thus any modification to the cross section that also matches surface constraints will tend to increase shortening estimates.

This last point was added in the discussion section on rates, and we have included the restored modified cross-section below the deformed section in figure 9b.

p. 13 l. 25-29: this is problematic. First of all, you change two major inputs to the model (structural geometry and heat production) at the same time here, while previously you have carefully only changed one parameter at a time. Second, you introduce spatially variable heat production here, which you did not do previously and which could have led to better fits in the previous models. This is a large change in the thermal structure and it should be justified. Although I am sympathetic to the fact that heat production could be significantly higher in the GHS than in the LHS, to really model this properly you should ascribe heat-production values to the different units, and advect these with the units.

Yes, we agree that the jump was too large to independently see the effect of both, but our goal was to show the best fit and a reasonable number of models and iterations. Numerous kinematic and thermal model iterations were performed in addition to the specific model results presented in this paper. Most of these iterations were performed with the goal of obtaining an improved fit using the cross-section geometry published by Long et al. (2011b). Several new models (changing flexural and topographic parameters were run using the new geometry to produce several models with slightly different exhumational histories to test the sensitivity of the model results to changing these different parameters. All models run in Pecube were evaluated using heat production values ranging from 2.0 to 5.0. (in steps of 0.5) and a range of different velocity combinations. In all, nearly 100 forward modeling combinations of the Long et al. (2011b) geometry were run for this study, and over 100 for the new geometry. None of the

models from the original Long et al., (2011) cross section could reproduce the AFT age trend seen across the GH (younger ages farther north), even with significantly higher heat production values in Pecube. This unsuccessful result of not being able to match the cooling ages with the original section led to the decision to strategically explore new geometry options, beginning with the replacement of the Baxa footwall cutoff. After evaluating a range of velocities and heat production values, we concluded that it would be best to ascribe different heat production values for different units in the model – even though we agree the most accurate approach would be to characterize each unit with distinct heat-production values in a single model. However we were limited by the current capabilities of our model. Thus the simplest way forward was to combine the results of the two models at the surface location of the MCT. Using Supplementary Figure 2 and 3, one can infer the range of potential cooling ages that would be predicted if it were possible to implement unit-prescribed heat production in Pecube. This seems most important for units in the immediate hanging wall and footwall of the MCT (~52 km north of MFT) where GH rocks that are known to be hotter with higher radiogenic heat production are spatially juxtaposed with the cooler Daling-Shumar units. This area is also where the greatest amount of cooling data are available.

We have worked to make this as transparent as possible in the revised manuscript. These include figure revisions to figure 9 and supplementary figure 2 and 3, and clarifications throughout sections 4 and 5. Examples include (1) the final paragraph of section 4.2.4 which highlights what is controlling predicted AFT ages in the immediate footwall of the KT, (2) the fourth paragraph of 4.3 detailing the rationale and method for combining models with different Ao values, and (3) section 5.2 which re-emphasizes the point that, even with higher heat production, fit of AFT ages remain poor in the immediate footwall of the KT using the original geometry proposed by Long et al. (2011b).

p. 13 l. 31-32: OK, but we are left wondering how much of this improved fit can be ascribed to the new structure and how much to the increased heat production.

Supplementary figure 2 graphically presents the best results from the using the updated cross-section geometry with 2.0 and 4.0 $\mu W/m^3$ heat production values applied along the entire line of section. New supplementary figure 3 does the same with the original geometry. As mentioned in the response to the comment directly before this one, we have clarified this in the text.

p. 14 l. 5-6: following up on the previous comment; can the data really tell the difference between the improved structural geometry and the increased heat production? There is very little data in the "bump" region. You use a simple visual comparison of predicted and observed ages; it would be useful to provide a more objective and quantitative comparison to back up inferences such as this.

We have added discussion in the manuscript that quantitatively compares the predicted AFT ages from the Long et al. (2011b) geometry to the predicted AFT ages from new geometry presented in this paper in order to support our conclusions of improved fit.

p. 16 l. 10-12: this is introducing yet another unconstrained parameter. I am not sure it is the best strategy to further complexify the models to improve the fit; this seems like a bit of a "flight forward". A more complete sensitivity and resolution analysis might be a more productive way forward.

> There are no new parameters. The parameters being discussed are EET and topography (section 3.1.1 and 3.1.3), and any given solution presented in this manuscript is a function of both parameters that combine to affect the exhumation of rocks. Is the added complexity you mention changing the value of EET or topography with time? There are strong arguments that can be made that both may have changed with time- and reflects your point made previously (p. 11, l 10-11). A forward model where multiple parameters have to be evaluated, and it is impossible to see if the model is a match to present day conditions until the last step, will always be a "flight (fight) forward". Not all questions or problems can be addressed through inverse solutions.
>
> The reality (which is why this section is important) is that subtle changes in EET have a larger effect on the modeled cooling ages than subtle changes in topography (such as using a process based estimation of topography or a simplified critical taper relationship). The reason why, is that a 5 to 10 km change in EET can impart a 1-3 km difference in magnitude of exhumation. Unfortunately, the flexural response to fault motion and associated topographic displacement (solved in the kinematic model) is something that is not included in many models attempting to link cross section to thermokinematic models, yet it has a significantly larger control on the predicted cooling ages than topographic estimations. We have clarified this section to emphasize this point.

p. 17 l. 9-10: "the amount of exhumation in this model is just at the amount necessary to reset AFT ages" is strange and apparently incorrect. The ages record cooling through the closure temperature at a certain time in the past. The thermal structure is going to affect that time, but the total amount of exhumation is much larger than the AFT closure depth it would seem.

> We have rewritten and clarified this point in section 5.1.2

p. 18 l. 10-15: A bunch of hard-to-read phrases that are in need of a few commas. Also, "after 13 Ma" would be better than "longer than" and replace the colloquial "till" by "until".

> We have edited this text for clarity and grammar.

p. 18 l. 15-20: another potential issue that is not discussed concerns the diffusion kinetics of He in zircon. Recent work has shown that the effective closure temperature of the ZHe system can vary from as low as _120 _C to as high as _240 _C as a complex function of the degree of _-damage (e.g. Guenthner et al., 2013). If you have underestimated the ZHe closure temperature (I suppose you are using the "standard" ZHe diffusion parameters built into Pecube) you could significantly underestimate the duration of shortening on the upper LH duplex, and thereby overestimate the shortening rates.

The reviewer raises a very good point, and we have modified the manuscript to state this as a potential caveat, although we do not think this is important for our samples because of the high cooling rate. The text now added in Section 2.2 is as follows:

The predicted ZHe ages in this study do not account for the effects of radiation damage on the closure temperature (e.g. Guenthner et al., 2013). The potential effect of this could be to underestimate the ZHe closure temperature. However, the effects of radiation damage on ZHe (or AHe) closure temperatures are most pronounced for long durations at relatively low (~220°C) temperatures (Guenthner et al., 2013). The Lesser Himalayan samples evaluated here experienced temperatures greater than 350° (Long et al., 2011c, Long et al., 2012), have young ages (typically ~7-11 Ma), highly reproducible ages (for individual samples) and underwent extremely rapid cooling (e.g., or around 16.3-22.5 C /Myr cooling rate since closure at ~180 C), thereby leading us to infer that radiation damage effects are minimal.

p. 18 l. 25-28: the first part of this argument is somewhat circular, since the McQuarrie and Ehlers (2015) scenario was input in the models here, without extensively testing all other potential scenarios. So the fact that the model predicts these variations in rates should not come as a surprise. In contrast, the dissimilar timing between the two sections that are only _25 km apart should be worrying. How can the same structure be active at time intervals that are several million years different between two adjacent locations? Again, the reader is left wondering how much of this difference could be due to variable diffusion kinetics?

We agree that many more rates need to be evaluated and presented, and we have clarified that in the updated version of the manuscript (see section 5.3, figure 11 and Table 3). We do not think that variable diffusion kinetics play a significant role (see response to previous comment) but elevation differences might. In addition, a revised geometry for the Kuru Chu section (two ramp scenario) may allow for an older age of transition from lower to upper LH duplexing which would decrease the fast rates.

p. 19 l. 2: given the numerous unexplored degrees of freedom in the models, it appears risky to assess the validity of the data based on the modelling outcomes.

That was not quite our point—thus we have revised and removed this sentence.

p. 20 l. 1: not sure what is meant with this phrase; what is “the spatial nature of thermochronometry”?

Wording was edited to clarify this point. The second part of the sentence is the important part: “the importance of considering the aerial distribution of cooling ages in the direction of transport and their relationship to the structural evolution of a landscape.”

Figures

Fig. 1: the inset geological map of Bhutan (panel B) is very small and not very readable. You should either increase its size or decrease the amount of detail on it. Also, in the legend of the main panel (C),

the Chekha Formation should be above the Greater Himalaya to keep all units in their structural order. Finally, it would help the reader if the colours used for the different thermochronometers were consistent between this figure and the following.

> Figure 1 has been revised. The colors of data points on the map are assigned based on the original studies due to overlap in sampling (e.g. ZHe and AFT data collected at same location). Colors used to label ages from thermochronometers at each sampling location do match colors used in subsequent figures.

Figs. 5-10: much more data appears to be plotted in these figures than in Figs. 1 and 2. What do the lighter-coloured data points refer to? For clarity it would be better to take them out. In Fig. 7, why does the "template topography" model not predict AFT ages everywhere?

> Figures 9, 10, and 11 include data from the Kuru Chu region (50% transparent) as well to help evaluate similarities and differences between the two sections. This has been clarified on the figure captions and expanded on in the text. Published data are presented in Figures 1 and 2. Are plotted on figure 5-8.
>
> Template Topography in Figure 7 does predict ages along the cross-section as completely as the other two models' output shown. In some areas, there is significant overlap with the other modeling results. In the AFT output plot, the Template Topography output lines are discontinuous because predicted ages were more scattered.

Author Response to SE-2017-117-RC2 (Anonymous Referee #2, 2018)

This manuscript analyzes the impact of variable radiogenic heat production, convergence rate, topographic estimates and out-of-sequence thrusting in determining the pattern of previously published thermochronologic ages along a transect across the Bhutan Himalaya. The authors utilize their results to validate a revised cross-section geometry of the study region.

The manuscript is generally well written. The topic is of potential interest for a broad international audience. However, it would benefit from a more comprehensive discussion of the whole range of geologic processes that may have an impact on the thermochronologic record of the study area.

The modelling approach utilized in this work is based on flexural and thermal-kinematic models. The authors sequentially deform the study cross section, and apply flexural loading and erosional unloading at each step to develop a high-resolution evolution of deformation, erosion, and burial over time. In other words, their approach only considers relatively shallow geologic processes. Deeper tectonic processes (e.g., channel flow exhumation and slab breakoff) that may also affect the thermochronologic record, especially higher temperature systems such as Ar-Ar on mica, are not discussed. This may puzzle part of the potential readership. I suggest to improve on the discussion, and possibly the modelling, in order to include these issues.

A discussion of more ductile processes on the higher temperature thermochronometer systems was raised by Reviewer 2 and Reviewer 3. The flexural and thermokinematic model looks at the evolution of rocks from 30 km depth and ~ 600-700 °C (peak temperature produced in Greater Himalayan rocks in the thermokinematic model, Pecube). As mentioned in the reply to Reviewer 3, the kinematic model will not capture all of the deformation processes, but it can evaluate if the cooling through the closure temperature of the MAr system was simply a function of shallower fold-thrusts belt processes — or if deeper processes (such as channel flow or slab break off) are needed to explain the data. Also, channel flow (if active) is interpreted to be reflected in the much higher temperature monazite data, which is not modeled in this study. What is key to note is that the kinematics described here can reproduce the peak temperatures and cooling history recorded in the rocks.

We have made minor revisions in multiple sections of the manuscript to incorporate this discussion raised in RC2 and RC3: 1) *2.1 Tectonostratigraphy* states that the Greater Himalaya was deformed through ductile processes, and that MCT shear is pervasive above and below the fault, 2) *3.2 Thermal Model* includes clarification on the depth and temperature range of the model as well as how isotherms are advected by motion along faults, 3) The discussion section clarifies permissible processes to reproduce the measured ages (including MAr).

The dataset of previously published thermochronologic ages, which is utilized as a benchmark for modelling, is not homogeneous. AFT and ZHe data are available in most of the transect, but Ar-Ar data are not. This would suggest more caution in the conclusions based on modelling results.

Moreover, these ages are invariably interpreted as cooling ages during exhumation across the closure temperature of the Ar-Ar system. Petrologic studies demonstrate that micas in metamorphic rocks often preserve disequilibrium textures, and their Ar-Ar age may thus record fluid-induced recrystallization below the closure temperature, rather than monotonic cooling (e.g., Villa 1998 - Terra Nova). Why mica Ar-Ar ages are so different in samples that are so close each other? What is the potential role of recrystallization during deformation? These issues should be discussed in the revised main text.

The available MAr data for this transect are very limited and were previously published by Stüwe and Foster (2001). The ^{40}Ar-^{39}Ar age spectra show relatively flat but slightly discordant age spectra that were interpreted to represent cooling ages for all 4 samples. The two sets of 11 Ma and 14 Ma ages were interpreted to record the same cooling signal that had been repeated by a fault. Our interpretation is broader and proposed that the 11-14 Ma ages represents a permissible age range in which rocks have passed through their closure temperature due to the short spatial scales between samples. Recent work from Sikkim Himalaya across the same Lesser Himalaya to Greater Himalaya transition highlights natural variability in MAr ages due to both the thermal conditions experienced by micas and the residence time at those temperatures. They measured both single grain ages (for 5-11 grains) as well as more traditional plateau age (Mottram et al., 2015) across a transect that spanned a temperature gradient over ~ 5 km. They found a significant spread in the single grain ages (2-5 Ma not including errors) and that the spread decreased (to 1.5-2 Ma) with higher temperatures and longer predicted residence times

at those temperatures, suggesting that the duration of metamorphism and the temperatures reached affected the loss of Ar from mica. In each case the MAr plateau ages spanned over a much narrower age range (13- 13.4 M) with significantly more precise error bars (0.05-0.2 Ma) than the single grain ages. The ~ 5 km transect crossed temperatures that ranged from 580°c to 650°C, while the maximum temperature range for the MAr samples presented here were between 600° and 700°C (Daniels et al., 2003). Their study also showed that a dispersion of +/- 2 Ma would be expected due to diffusive differences caused by grain size variations. We do not have access to the samples to go back and examine the textures of the mica that produced the cooling ages. However we have looked at many similar rocks from almost the exact same area and have found no textures indicative of fluid flow or alteration. While this does not rule out an age spread from post-cooling fluid flow or recrystallization during deformation, we are confident that the 11-14 Ma age range encompasses the actual cooling age of these rocks because of strong similarities in age to data available directly to the east near the Kuru Chu section (~12 Ma, Long et a., 2012; Figure 9 in this manuscript), as well as the range in ages measured by Mottram et al. (2015 in Sikkim (12-16 Ma). These ages are all younger than the youngest age for south-directed shear in GH rocks, 16-18 Ma (Grujic et al., 2002; Daniel et al., 2003; Kellett et al., 2009). In our model, the age and rate of deformation in the northern duplex of lower Lesser Himalaya most prominently control the predicted MAr ages modeled in this area of the Greater Himalaya.

Text was revised to address this point in sections 2.1, 2.2, 3.2, and 5.3. New citations are also included, i.e.:

Mottram, C. M., Warren, C. J., Halton, A. M., Kelley, S. P., and Harris, N. B. W.: Argon behaviour in an inverted Barrovian sequence, Sikkim Himalaya: The consequences of temperature and timescale on 40Ar/39Ar mica geochronology, Lithos, 238, 37–51, doi: 10.1016/j.lithos.2015.08.01, 2015.

Some of the findings of the authors are not surprising for an active orogenic belt such as the Himalaya, notably the minor effect of radiogenic heat production and topography compared to tectonics. Nevertheless, the authors' conclusion should be supported by more robust thermochronologic data. The addition of a new ramp under the Greater Himalaya does better explain available thermochronologic ages. However, this is just one of the possibilities, given the degree of freedom of the models.

Compared to other regions, even in the Himalaya, the dataset shown in this paper is rich, especially when including the data immediately east along the Kuru Chu transect as shown in Figures 9-11. MAr and AFT data are more limited than ZHe data due to cost and appropriate samples respectively. The reviewer raises an important point and that is, the models highlight regions where the predicted thermochronologic ages are very sensitive to the geometry or radiogenic heat production or velocity. Knowing these areas prior to collecting thermochronology samples would strongly influence where sampling would be the most useful for delineating geometry. Regrettably many of the gaps in the AFT data are a function of the apatite-poor lithology. Resampling and additional analyses are beyond the scope of this paper. However, the model process we present is useful for directing future thermochronologic work in the Himalaya and other mountain ranges. Although many geoscientists model data following the

collection of samples, this work suggests that initial thermokinematic modeling of an area prior to collecting data can direct and inform sampling strategies.

We are not sure what other possibilities the reviewer envisioned for changes to the cross-section to also explain the published dataset. We chose to highlight an obvious additional structural solution that was proposed to the east in Arunachal Pradesh: an out-of-sequence fault at the trace of the MCT (Adlakha, V. A., Lang, K. A., Patel, R. C., Lal, N., and Huntington, K. W.: Rapid long-term erosion in the rain shadow of the Shillong Plateau, Eastern Himalaya, Tectonophysics, 582, 76–83, doi: 10.1016/j.tecto.2012.09.022, 2013.). As expanded on in section 5.2, *Using Thermochronology to Evaluate Structural Geometry*, we evaluate whether an out-of-sequence fault can explain all of the observations. While it may be able to address the younger cooling ages, having a second, more southern out-of-sequence fault that post-dates the Kakhtang Thrust would have a pronounced effect on the topography (as highlighted in our response to reviewer 3, specific comment 2), that is not seen in the model topography or geomorphic metrics of active/ recent uplift. In addition, see response to RC1 for further comments on systematic approach to structural and thermal modeling.

We have revised this manuscript to clarify these points in sections 5 (*Discussion*) and 6 (*Conclusion*s).

Is the stratigraphy predicted by modelling consistent with the geologic record? This may provide independent constraints to the reconstructions illustrated in this work, that are prone to remain otherwise speculative. I suggest to describe in more detail the stratigraphic evolution of the foreland basin, as well as all of the other geologic evidence that may be useful to support the authors' conclusions.

One of the key parameters that we match through this process is the depth of the foreland basin. The modeling process also makes strong predictions regarding the detrital sedimentary signal recorded in the basin and the potential detrital thermochronologic record. Most of this research was accomplished as another research group was examining the details of the detrital climate, provenance, and sediment accumulation signal in the Siwaliks of Bhutan (e.g. Coutand, I., Barrier, L., Govin, G., Grujic, D., Dupont-Nivet, G., Najman, Y., and Hoorn, C.: Late Miocene-Pleistocene evolution of India-Eurasia convergence partitioning between the Bhutan Himalaya and the Shillong plateau: New evidences from foreland basin deposits along the Dungsam Chu section, Eastern Bhutan, Tectonics, 35, 2963–2994, doi:10.1002/2016TC004258, 2016. and, Govin, G., Najman, Y., Copely, A., Millar, I., van der Beek, P., Huyghe, P., Grujic., D., and Davenport, J.: Timing and mechanism of the rise of the Shillong Plateau in the Himalayan foreland, Geology, doi:10.1130/G39864.1, 2018). As with any provenance or stratigraphy study, most information is gained when there is a unique signal that enters the foreland basins, and these papers highlight that much of that signal is associated with the rise of the Shillong Plateau or ages that have a Tibetan origin.

The paper by Govin et al. (2018) highlights that at 6.35 Ma, there is significant input of Lower LH detritus into the foreland basin. Our models show both the age (6.35 Ma) and the signal (lower LH detritus), and the depth of the basin at this time (2.75 km), are all consistent. We agree with Reviewer 2 that matching the predicted foreland basin with the measured foreland basin is a

powerful tool for evaluating the flexural-kinematic modeling and rates of deformation. We are currently working on a fully-integrated detrital provenance and thermochronologic cooling set for the Siwalik basin, but a detailed description of the stratigraphic evolution of the foreland with respect to detrital provenance cooling signals and rates is well beyond the scope of this paper to do it properly.

The abstract should be improved. The first two sentences are not relevant to introduce the focus of the manuscript. The Introduction and section 2.1 are biased by excessive self-referencing.

Abstract issues were raised by multiple referees and have been addressed.

Introduction and section 2.1 have been revised to include more references to other research groups as available. In general, 26 new references (not self-citing) have been added to the manuscript.

I will be happy to read a revised version of this potentially interesting manuscript.

Author Response to SE-2017-117-RC3 (D. Grujic, 2018)

Dear Colleagues In this manuscript the authors present results of sensitivity of predicted thermochronological age distribution on several parameters: prescribed topographic evolution, geometry of the basal detachment and kinematics of the related fold-and-thrust belt and crustal heat production. The authors conclude that "this study presents a successful approach for using thermochronometer data to test the viability of a proposed cross section geometry based on forward models of the kinematic, exhumational, and thermal history of an area". I fully agree with this statement but have several comments that could help authors improve the manuscript and help reader better evaluate the contributions. I concur with the comments by referee #1 and try not to repeat them here. I apologise for several self-citations, but my research group has been working in the area and applying similar research techniques since couple of decades.

General Comments:

1. The general limitation of the kinematic models is that the geometry and kinematics is prescribed -- Therefore despite their best efforts dependent on authors' interpretation.

This is true, the geometry and kinematics are both prescribed, but they are also testable. Following this approach, a cross-section can be invalidated by not matching available cooling data --which is an important step forward. Although this approach seems limiting, it has the potential to refine the geometry of the active décollement in addition, or as a compliment to inverse methods. The determination of a décollement through searching a parameter space (see response to general comment 3 below) provides low broad posterior probability density functions (PPDFs) that may have a permissible range in depth of 3-5 km (Coutand et al., 2014). Within that range we can test a specific geometry and require it to match additional known constraints such as the surface geology.

See additional comments to RC1 and RC2 on cross-section solutions.

Multiple sections of the manuscript discuss the ability to test different geometries and as well as different (albeit prescribed) kinematics using the approach of this study. The revised manuscript retains this emphasis.

1, continued. I agree that this is still the best approach to interpret the spatial pattern of thermochronological data, and couple of authors of this manuscript have made significant progress with their previous publications (McQuarrie and Ehlers, 2015) in reducing these limitations. Unfortunately, the additional problem with the Pecube is that it cannot generate simultaneous movement on faults with opposite sense of slip. In the Himalaya, and in particular for the GHS, the cooling and exhumation were affected by the simultaneously motion along the MHT at the base and the South Tibetan Detachment (STD) at the top. The STD in the eastern Himalaya was active as a ductile shear zone until 11 Ma, which is half of the period of the here presented experiments. Could the "tectonic denudation" affect the cooling pattern of the northern part of the section?

There are two important points here.

1) Using the modified version of Pecube as presented in this paper, we actually can generate simultaneous motion on both the MCT and the STD. This can be done in Move by first applying 10 km of motion to the MCT, then 10 km of motion to the STD, and finally accounting for the flexural load and resulting change in topography. The resulting displacement field would show pure extrusion of Greater Himalayan rock in prescribed 10-km increments (or increment value of choice).

2) Although we could, we did not include simultaneous motion of the STD. This choice was made for a variety of reasons; 1) early STD magnitude is largely unconstrained and predates the ages preserved in the thermochronometers systems used in this manuscript, 2) not including STD motion (i.e. potentially more recent activity) allows us to evaluate what component of the low-temperature (ZHe or AFT) exhumation required extensional exhumation from 10-0 Ma. Tectonic denudation could absolutely affect the cooling in the northern part of the cross section. However, based on the match between our best-fitting models and measured cooling ages, we argue that any recent (7-0 Ma) tectonic denudation is minimal. The critical dataset needed in the north would be MAr ages. These data should record the earlier (~ 11 Ma ??) cooling signal of the STD.

We do suggest potential links between the periods of rapid shortening and STD activity in section 5.3 of the resubmitted manuscript.

2. The shape of isotherms and their effect on the cooling rates. Himalaya are an active contractional orogen, therefore, the isotherms are deformed and the geothermal gradient is not constant in space and time. Was this accounted for in the experiments when calculating the eroded material or when calculating the exhumation rates? For example the same rock uplift rate, minus same surface erosion

rate will not yield the same cooling rate. Therefore because the exhumation rates are based on thermochronology, i.e., cooling rates, thermochronological data cannot be simply converted into exhumation rates based on an assumed geothermal gradient. The exhumation rates will depend on local instantaneous geothermal gradient at different times. This is not discussed in the manuscript.

> Geothermal gradients and the resulting shape of isotherms in the model are dynamic and change at each incremental time-step based on 1) thermal parameters prescribed to each model in Pecube; 2) locations and magnitudes of fault displacement; 3) locations and magnitudes of erosion as dictated by structural uplift, isostatic flexure, topographic evolution, and erosion in the flexural-kinematic model; and 4) the rates of deformation and exhumation which are dictated by the absolute timing of each step which we assigned as input in Pecube. We reproduce the same inverted thermal gradients at the MCT (when active) and KT (when active) that have been both proposed and modeled for these structures.
>
> Reviewer 3 is correct in that this point should be explicitly stated in the manuscript for clarity. Revisions were made in sections 3.2 and 5.1.

3. The authors write that they have performed a sensitivity analysis. However they have performed a limited number of experiments changing one or two parameters at the time (I concur with the related comments by referee #1). However it would have been better to perform a systematic search through the parameter "space" by providing the ranges of variables and searching for the most optimal value – the lowest misfit. I agree that this is a very time consuming approach, which requires tens of thousands of experiments. However this is the only approach that can provide a statistically relevant evaluation of any of the parameters. Pecube produces posterior probability density functions (PPDFs) for each model parameter, (Braun, J., P. Van Der Beek, P. Valla, X. Robert, F. Herman, C. Glotzbach, V. Pedersen, C. Perry, T. Simon-Labric, and C. Prigent (2012), Quantifying rates of landscape evolution and tectonic processes by thermochronology and numerical modeling of crustal heat transport using PECUBE, Tectonophysics, 524-525, 1–28, doi:10.1016/j.tecto.2011.12.035.â˘A´l) I admit that I do not know if this can be implemented by the technique presented here (combination of Pecube thermokinematic modeling and Move kinematic modeling).

> The variables that are assigned in Pecube (in particular heat production properties) can be determined by a systematic search through parameter space. However, the much more interesting and debated properties such as cross section geometry, kinematics, velocity, and topography are all a function of the flexural-kinematic model generated in *Move*. For these models, designing a parameter search or graphically representing a parameter search is much more complicated. For example, supplementary data Figure 1 shows 9 different models where topography, kinematics, or geometry were varied. These 9 models all produced a foreland basin, dip of the decollement and surface geology that were all considered acceptable (within 1 km of modern thickness; +1/ -0.5° of modern dip; and 1 km of modern surface geology). Over 50 other flexural models were tested that did not match these criteria. Of the 9 models that are presented in this study, each model was run using 4-7 different velocities to 1) see predominant

trends on the predicted cooling ages and 2) determine which combination of velocities resulted in predicted cooling ages that best matched the measured data. For all of the different velocities and the different kinematics and geometries we examined a range of thermal properties, specifically Ao (surface radiogenic heat production – see response to comments from supplementary document (annotated manuscript) p. 9, l. 8 below), which has a large, known range of measured values (i.e. Ray and Rao, 2000; Menon et al., 2003; England et al., 1992; Whipp et al., 2007; Herman et al., 2010 – all references in manuscript). Ao was varied in 0.25 to 0.5 $\mu W/m^3$ increments. Note that we do not test the effect of basal heat production, but rather hold that fixed at 1300°C at the asthenosphere ~110 km (Table 2). While the number of variations we tested is not an infinite number (or 10's of thousands) it is respectably above 500 simulations (in Pecube). The challenge is of course visually showing that range.

We understand, based on comments by reviewer 1 and reviewer 3, that the full range of parameters tested was not clear and we have rectified this in the new version of the manuscript, particularly in section 3.

4. The GHC is not a thrust sheet-the rocks in this lithotectonic unit were affected by pervasive and heterogeneous ductile deformation. Similarly the MCT is not a fault but a several kilometers thick ductile shear zone with mylonites derived both from footwall block rocks and the hanging wall block rocks. All these rocks deformed as viscoelasto-plastic thermally activated materials and ought to be modeled as such not as Mohr-Coulomb materials. I do not question the applicability of cross section balancing and thermokinematic modeling for the rocks and structures that were dominantly deformed as the latter mechanisms. Therefore the particle displacement paths were not as simple as implemented by thermal-kinematic models. In conclusion, these models are applicable for the period after the cessation of pervasive ductile deformation. This is regardless weather the lithotectonic unit was emplaced according to the channel flow tectonic mode or to the classical fold nappe mode. In either case the pervasive ductile deformation occurred before the thermochronological record used here. Finally, the thermochronological data presented here and available in general cannot constrain the tectonic processes that occurred before them.

The short answer is that we completely agree with Reviewer 3 that "the thermochronological data presented here and available in general cannot constrain the tectonic processes that occurred before them." The available cooling age data we are evaluating are all younger (MAr ages of 11-14 Ma) than the MCT emplacement (23-16 Ma). However, what is interesting about the model process is that some of the models (such as our best fit model between 80-90 km from the MFT) predicts MAr ages that are a result of the proposed age and rate of the MCT. We do not have data in this region, so it would be interesting to see if they are in fact as old as what is predicted.

With respect to the MCT as a fault or a shear zone -- the boundary between uniquely Greater Himalayan rocks (by provenance) and Lesser Himalayan rocks (again by provenance) is actually quite discrete (<< 1 km). However, we absolutely agree with Reviewer 3 that the shear imparted

to the rocks above and below this zone is pervasive and heterogeneous and that the emplacement of the MCT on the LH rocks occurred while both lithotectonic packages were not behaving in a purely elastic or brittle fashion. We also agree that the AFT, ZHe, and MAr cooling ages reproduced accurately by the model all reflect cooling after predominantly ductile deformation in these rocks. It is important to note that the models used (Move and Pecube) do not attribute any mechanical behavior to the rocks. They only describe kinematics, or the motion of material. The kinematics invoked here are just as discrete as the kinematics used in Coutand et al. (2014) at 600°-700°C at 20-30 km depth or Herman et al. (2010) at 600-700 °C and 20-30km depth. The kinematics modeled in *Move* do not differentiate how ductile or plastically the rocks are deforming internally. The emplacement of the Greater Himalayan rocks above Lesser Himalayan rocks is critical for the heating and cooling of the Lesser Himalayan rocks and thus needs to be in the model. If the data we were evaluating were sensitive to the compressed temperature gradient (~450-700°) across the MCT zone (~ 1 km below and above in Bhutan; e.g. Long et al., 2016), trying to replicate the magnitude of fault-parallel shear would be more critical. As stated in response to General Comment 1, with respect to sensitivity of the cooling ages to the STD, the model predicts a cooling history and exhumation age and rate for GH rocks that can be compared to measured histories to assess how close just the simple (albeit possibly ductile) thrust emplacement model can account for the measured temperatures before attempting to incorporate a much more complex process.

The manuscript was revised to clarify these points in Sections 2 and 3.

5. The authors analyze and discuss the effect of the thermophysical properties of the rocks on the spatial pattern of cooling ages. However only the values of heat production were changed (2 and 4 $\mu W/m^3$). However the thermal properties control the Péclet number, which dictates how strongly are the isotherms deflected because of the thrusting. This furthermore implies that the thermal properties have to include the study of sensitivity on thermal conductivity, heat capacity and density of the rocks.

We agree with Reviewer 3 that crustal thermal fields are sensitive to thermal conductivity, heat capacity, and density. In this study (and most exhumation studies), crustal thermal properties are assumed constant because most thermal models, including Pecube, solve the advection-diffusion equation on an Eulerian grid which is not capable of tracking moving material properties. This makes implementation of variable thermal conductivity in a highly deformed thrust belt impossible. Lagrangian grids circumvent this problem, but have shortcoming for exhumation studies. They cannot accommodate large amounts of deformation, such as in the Himalaya, without becoming unstable, and require frequent re-meshing and interpolation of model parameters and properties, thereby progressively introducing numerical uncertainty into the model. Although hybrid Eulerian-Lagrangian techniques exist, these are not commonly used and difficult to implement. Given these limitations, we (like most other studies) use average upper crustal thermophysical properties and assume they remain constant through time. However, please note that the thermophysical properties we do use are based on observations (largely from Whipp et al., 2007 and references therein).

To accommodate this reviewer's concern, we have modified the manuscript in the following ways:

1. We more clearly state in the model setup section 3.2.1 that we are using observed thermal physical properties for the lithologies present in this region (see Whipp et al. 2007, and Ehlers, 2005).

2. We add a caveat statement in the same section to say: "Although thermophysical properties such as thermal conductivity, heat capacity, and density vary between different lithologies within a fold and thrust belt, the implementation of variable material properties in areas of large deformation is not possible in programs such as Pecube which solve the advection diffusion equation on an Eulerian grid. Thus, we address this potential issue by using the best available average measurements of thermophysical properties for the lithologies in this region."

In addition, see response to RC1 (p. 9 l. 11) for surface radiogenic heat production.

Specific Comments:

1. Valla et al. [2010] have shown that relief development must be 2–3 times faster than the background exhumation/erosion rate to be recorded and quantitatively extracted from thermochronological data. Valla, P., F. Herman, P. A. van der Beek, and J. Braun (2010), Inversion of thermochronological age-elevation profiles to extract independent estimates of denudation and relief history I: Theory and conceptual model, Earth Planet. Sci. Lett., 295, 511–522. Please comment in your manuscript in the relevant places.

The approach and conclusions of Valla et al. [2010] is included in Introduction and Discussion.

2. What is the evidence in the field (i.e., petrological) for the burial by Kakhtang thrust? Kakhtang thrust appears very steep therefore the burial rate might not be high. In addition the KT emplaced some of the hottest rocks in the Himalaya therefore the isotherms might have been disturbed during its activity, in other words heating and cooling does not need to imply burial and exhumation.

We agree with the reviewer's comments. However, the flexural response of motion on the steep Kakhtang Thrust is subsidence in the footwall. Modeled isostatic accommodation of this thrusting dramatically lowered topography in the footwall of the thrust and reduced erosion rates south of the thrust. In some models, enough subsidence occurred during out-of-sequence thrusting that sedimentation occurred in the immediate footwall. A potential relict of this footwall subsidence is the enigmatic low-relief surface preserved in the Bhutan Himalaya (Duncan et al., 2003; Grujic et al., 2006). This low-relief landscape contains hundreds of meters of sediment infilling of paleo-relief and is now out of equilibrium with respect to where it was formed (Adams et al., 2016). In eastern Bhutan, the infilled sediment is derived from the structurally higher GH; conglomerate is common, thus making it easy to associate the clasts with rocks carried by the KT. As published by reviewer 3, the low-relief surface is in the immediate

footwall of the Kakhtang Thrust (Grujic et al., 2006). Our flexural modeling of this region and others (e.g. McQuarrie and Ehlers, 2015, 2017; Rak et al., 2017) has highlighted the ubiquitous response of footwall subsidence and the development of low relief in the footwall region of out-of-sequence faults, thrusts, etc. We do not think that the spatial relationship between the low-relief surface and the Kaktang thrust is coincidental.

Not only do slower erosion rates in the Kakhtang Thrust footwall alter thermal gradient, but the reduced topography limits the magnitude and rate of future erosion. The current model does take into account the deflection of isotherms as the KT moves and advects deep, hot material upward during fault motion. The amount of disturbance to isotherms in each time-step is related to the geometry of the fault and magnitude and rate of motion assigned in the time-step.

Section 3.1.2 has been revised to explain these observations in the footwall of the KT and our rationale for modeling different timings of out-of-sequence thrusting. Section 4 has also been revised based on these comments.

3. Technical corrections a) Vertical uplift and vertical exhumation. Both rock and surface uplift and exhumation concern the vertical component of the particle displacement (in three different reference frames). Therefore word vertical is superfluous. However one must make difference between rock uplift and surface uplift, in particular in an article like this one where both processes are discussed. Please adhere strictly to the definitions by England and Molnar, 1990. Surface uplift, uplift of rocks, and exhumation of rocks. Geology, 18(12), pp.1173-1177. b) There is no process named “surface radiogenic heat production”. Please correct the wording accordingly in the entire document.

Language was corrected to reflect England and Molnar definitions.

RC3: All the above comments and further technical comments are in the annotated file.

Please also note the supplement to this comment:

https://www.solid-earth-discuss.net/se-2017-117/se-2017-117-RC3-supplement.pdf

The corrections suggested in the supplementary document were all addressed. Specific comments raised in the Supplementary PDF that are not addressed above are included below.

p.3, l. 30-31 furthermore as indicated by thermo-kinematic experiments, like this study, the cooling rates were not steady in time and space.

We agree completely with this statement but feel the point is best addressed in the results and discussion sections. We have removed interpretations of “rapid cooling” and or processes and simply describe the age data.

p.4 line 5 Is there any effect of sample elevation? This is important since you are testing the model for the sensitivity on surface processes.

> There are very limited/ modest age elevation relationships as discussed in McQuarrie and Ehlers, 2015. The relationships that are present include 1) the samples from Coutand et al. (2014) that have an age-elevation relationship, and if used to determine an exhumation rate, suggest a very modest rate of 0.4 mm/yr; and 2) the southern ZHe samples when combining the data from the Kuru Chu and Trashigang transects, located ~30 km from the MFT. The younger ages (8.5 to 10 Ma) at lower elevations (0.5 to 1 km) in the Kuru Chu and older ages (11 to 11.6 Ma) at higher elevations (1.6 to 2.4 km) along the Trashigang transect suggests differential exhumation of 0.7 mm/yr. These are expanded on in sections 2.2 and in 5.3.

p. 4, l. 20 since it is an active convergent orogen the isotherms are deformed and the geothermal gradient is not constant in space and time. Was this accounted for in the model when calculating the eroded material?

> In this section we mention that advection-diffusion thermal models are used to calculate the evolving subsurface temperatures (i.e. modified isotherms and geothermal gradient) but discuss this more explicitly in section 3.2.

p. 7, l.30 What is the argument that the geometry along distant section is applicable to the study area? How do these values compare to the estimates by Coutand et al. (2014) and by Singer, J., Obermann, A., Kissling, E., Fang, H., Hetényi, G., Grujic, D. (2017) Along-strike variations in the Himalayan orogenic wedge structure in Bhutan from ambient seismic noise tomography. Geochemistry, Geophysics, Geosystems, 18, 4, 1483-1498. DOI: 10.1002/2016GC006742.

> We have removed the INDEPTH reference. We found that Singer et al. (2017, JGR Solid Earth) had the specific data on to the dip of the décollement and the dip of the Moho. The relationship between the décollement geometry of Long et al. (2011b) and Coutand et al. (2014) is no different than that described in McQuarrie and Ehlers (2015; figure 3C). However the modified décollement geometry is much closer to EB1 in Coutand et al. (2014), with more discrete ramp steps.

p. 9, l. 8 [“surface radiogenic heat production”] --There is no such physical process. Please correct the wording accordingly in the entire document.

> With due respect, yes, there is. Please see detailed response to comment: p. 9 l. 11 from Reviewer 1. Radiogenic heat production at the surface can vary spatially by large amounts (e.g., Mareschal and Jaupart, 2013) and is a function of the concentration of heat-producing elements in the crust. Systematic sampling of crustal rocks now exposed at the surface indicates that heat production diminishes with depth through the crust and that this decline is not monotonic (Ketcham, 1996; Brady et al., 2006). Thus we prescribe an exponential decrease in heat production with depth, as opposed to assuming a constant crustal heat production. An

exponential decrease in heat production with depth requires definition of a surface radiogenic heat production (Ao) and an e-folding depth.

p. 13, l. 25 there is no such a process. Do you mean surface heat flow or (radiogenic) heat production

Neither, please see response to p. 9, l. 8.

p. 15, l.2 The GHC is not a thrust sheet as the MCT is not a fault but a several kilometers thick ductile shear zone. Therefore the particle displacement paths were as simple as predicted by thermal-kinematic models. Therefore these models are applicable for the period after the cessation of pervasive ductile deformation.

In the end we may need to continue to agree to disagree with Reviewer 3 on this point. Our definition of a thrust sheet is not quite that rigid (literally and figuratively). We have added "ductile" in front of "thrust" because we agree with Reviewer 3 that the fault that places Greater Himalayan rocks on Lesser Himalayan rocks is part of a much broader shear zone with pervasive shear both above and below the tectonostratigraphic boundary between the two units.

p. 15, l.25-29 Do you consider also that the isotherms are less deflected above this ramp than above the major ramp? This influences how closely spaced are the isotherms and therefore even with the sample particle displacement vector and surface denudation rate, the cooling rate will be different.

Yes, absolutely. The version of Pecube that we are using calculates the evolving thermal field including the deflection (or lack thereof) of isotherms with ramps.

p. 16, l. 28 Is there a justification to increase the number of significant digits (i.e. topography angle of 1.75°)

Yes, small changes to small angles (0.25° is 12% of a 2° angle) have a large effect when applied over hundreds of kilometers.

p. 18, l. 5 [The sensitivity of the model to the age of MCT] --However this depends also on how is the MCT treated. As a single fault with a displacement of a slab above it or as it is in the field as broad ductile shear zone with pervasive deformation in the hanging wall block.

While we agree that how deformation in the broad MCT zone is treated may have an effect on the temperatures within a few kilometers above and below the thrust fault (within the shear zone), this deformation is not captured by any of the available cooling age data we are evaluating. All of the thermochronometers available are younger (11-14 Ma) than the MCT emplacement (23-16 Ma). Available geochronologic data for this region support ductile shearing on the lower STD between circa 23 and 16 Ma, and shearing and associated exhumation of GH rocks in the MCT sheet after circa 23 Ma and continuing until circa 18–16 Ma [Grujic et al., 2002; Daniel et al., 2003; Kellett et al., 2009, 2010; Chambers et al., 2011]. Thus

our statement that we cannot evaluate the MCT emplacement age or rate is correct.

Figure 2 and Figure 4: [pointing to northern part of cross-section]--Something is missing here, both the topography and the geology.

The geology and topography in the northernmost portion of the cross section was never a part of the original geologic cross section (Long et al., 2011b). This is why it is blank in this figure as well.

Testing the effects of topography, geometry and kinematics on modeled thermochronometer cooling ages in the eastern Bhutan Himalaya

Michelle E. Gilmore[1], Nadine McQuarrie [1], Paul R. Eizenhöfer [1], Todd A. Ehlers [2]

[1] Department of Geology and Environmental Science, University of Pittsburgh, Pittsburgh, 15260, USA
[2] Department of Geoscience, University of Tübingen, Tübingen, D-72074, Germany

Correspondence to: Nadine McQuarrie (nmcq@pitt.edu)

Abstract. In this study, reconstructions of a balanced geologic cross section in the Himalayan fold-thrust belt of eastern Bhutan are used in flexural-kinematic and thermal-kinematic models to understand the sensitivity of predicted cooling ages to changes in fault kinematics, geometry, topography, and radiogenic heat production values. The kinematics for each scenario are created by sequentially deforming the cross section with ~10-km deformation steps while applying flexural loading and erosional unloading at each step to develop a high-resolution evolution of deformation, erosion, and burial over time. By assigning ages to each increment of displacement, we create a suite of modeled scenarios that are input into a 2-D thermo-kinematic model to predict cooling ages. Comparison of model-predicted cooling ages to published thermochronometer data reveals that cooling ages are most sensitive to (1) location and magnitude of fault ramps, (2) variable shortening rates between 68-6.4 mm/yr, and (3) timing and magnitude of out-of-sequence faulting. The predicted ages are less sensitive to (4) radiogenic heat production, and (5) estimates of topographic evolution. We used the observed misfit of predicted to measured cooling ages to revise the cross section geometry and separate one large ramp previously proposed for the modern décollement into two smaller ramps. The revised geometry results in an improved fit to observed ages, particularly young AFT ages (2-6 Ma) located north of the Main Central Thrust. This study presents a successful approach for using thermochronometer data to test the viability of a proposed cross-section geometry and kinematics, and describes a viable approach to estimating the first-order topographic evolution of a compressional orogen.

1 Introduction

Cooling ages recorded by thermochronometers are a direct function of the timing, magnitude, and rate of exhumation in fold thrust belts (e.g., Ehlers and Farley 2003; Shi and Wang 1987; Huerta and Rodgers, 2006; Rahn and Grasemann, 1999; McQuarrie and Ehlers, 2017). However, the rate and magnitude of exhumation may be strongly controlled by the geometry and rate of deformation (Lock and Willett 2008, McQuarrie and Ehlers, 2015). Previous studies have shown that thermochronometers are most sensitive to the vertical motion of material, such as fault motion over a fault ramp, which focuses exhumation at that location (Whipp et al., 2007; Herman et al., 2010; Robert et al., 2011; Coutand et al., 2014; McQuarrie and Ehlers, 2015). Because of this, several hundred kilometers of horizontal shortening such as motion along a

Nadine McQuarrie 2/19/2018 4:16 PM
Deleted:

Michelle Gilmore 1/27/2018 6:37 PM
Deleted: The temporal and kinematic evolution of fold-thrust belts is a critical component for evaluating the viability of proposed plate tectonic, geodynamic and even climatic processes in regions of convergence. Thermochronometer data have the potential to provide temporal constraints, but interpretations of these data are sensitive to both exhumational and deformational processes.

Nadine McQuarrie 1/29/2018 12:15 PM
Deleted: a

Michelle Gilmore 1/30/2018 10:16 PM
Deleted: and

Nadine McQuarrie 1/29/2018 12:19 PM
Deleted: We

Nadine McQuarrie 1/29/2018 12:28 PM
Deleted: and

Nadine McQuarrie 1/29/2018 12:28 PM
Deleted: y

Nadine McQuarrie 1/29/2018 12:33 PM
Deleted: propose a

Nadine McQuarrie 1/29/2018 12:33 PM
Deleted: revised

Nadine McQuarrie 1/29/2018 12:34 PM
Deleted: that

Nadine McQuarrie 1/29/2018 12:34 PM
Deleted: s

Michelle Gilmore 1/30/2018 10:17 PM
Deleted: (

Michelle Gilmore 1/27/2018 7:24 PM
Deleted: decollement

Michelle Gilmore 1/30/2018 10:17 PM
Deleted:)

Nadine McQuarrie 1/29/2018 12:34 PM
Deleted: cross section

Nadine McQuarrie 1/29/2018 12:38 PM
Deleted: based on forward models of the kinematic, exhumational, and thermal history of an area, as well as an

Nadine McQuarrie 1/29/2018 12:44 PM
Deleted: history along a line of section

Michelle Gilmore 2/3/2018 9:41 PM
Deleted: s

flat décollement, a phenomenon commonly observed in fold-thrust belts, may occur without a significant thermal cooling signal (e.g., Batt and Brandon, 2002; Huntington et al., 2007; Whipp et al., 2007; Coutand et al., 2014). Thus potential variations in cross section geometry such as the spatial distribution of ramps, the order of faulting, and how fault and ramp positions change with time are predicted to have a significant impact on the exhumation history of fold-thrust belts.

The shape of subsurface isotherms and the cooling history of minerals are also controlled by the evolution of topography, something that is largely unknown and often modeled either in steady state (e.g. Coutand et al., 2014; Herman et al., 2010; Whipp et al., 2007) or as a muted topography that increases relief with time (e.g. Erdös et al., 2014). The spatial and temporal changes in cooling rate due to topographic relief depend on topographic wavelength and amplitude, exhumation rate and duration, and the thermochronometer system recording the change (Ehlers and Farley, 2003; Braun et al., 2002; Mancktelow and Grasemann, 1997; Stüwe et al., 1994). Attempts to predict past relief from thermochronometer ages using a non-linear inversion method (Valla, 2010), determined that relief development must be 2–3 times faster than the background exhumation/erosion rate to be recorded in the measured ages—a criterion that is hard to achieve in actively deforming and exhuming regions. These studies highlight the yet unresolved issues regarding the best approach in deciphering the topographic evolution of an actively deforming region. In this study, we evaluate the sensitivity of predicted cooling ages to the different parameters that control exhumation magnitude, rate and location in fold-thrust belts. We expand on the approach taken by McQuarrie and Ehlers (2015) and assess the control that cross section geometry, kinematics, shortening rates and topographic assumptions have on modeled cooling ages by systematically changing these features. We do this using a balanced geologic cross section and associated thermochronometer data from an adjacent section (30 km east) in the Bhutan Himalaya. This approach not only requires kinematic compatibility and the ability to match predicted cooling ages for each cross-section, but also allows us to evaluate compatibility in geometry, age and rate of deformation between the two adjacent sections.

2.1 Tectonostratigraphy

The Himalaya orogen initiated with collision of the Indian Plate with the Asian Plate c. 50-55 Ma (e.g., Patriat and Achache, 1984; Klootwijk et al., 1992; Leech et al., 2005; Najman et al., 2010) and is divided into four geomorphic and tectonostratigraphic zones that span much of the east-west extent of the orogen. From south to north, these are the Subhimalaya, Lesser Himalaya, Greater Himalaya, and Tethyan Himalaya (Fig. 1). All of these units were derived from sediments originally deposited on the Indian Plate (Heim and Gansser, 1939; Gansser, 1964). In the following section, we describe the tectonostratigraphy and intervening structures expressed along a section line near Trashigang in the Bhutan Himalaya (Fig. 1 and 2) (Long et al., 2011a; Long et al., 2011b).

The Subhimalayan zone is located north of the Main Frontal Thrust (MFT) and composed of synorogenic sedimentary deposits from the Himalayan foreland basin. In Bhutan the MFT emplaces a single thrust sheet of Miocene-Pliocene Subhimalayan units referred to as the Siwalik Group over modern foreland basin deposits (Gansser, 1983; Long et al., 2011b; Coutand et al., 2016).

Michelle Gilmore 1/27/2018 7:24 PM
Deleted: decollement

Michelle Gilmore 2/3/2018 9:47 PM
Deleted: Erdos

Michelle Gilmore 2/3/2018 9:39 PM
Deleted: Stuwe

Nadine McQuarrie 1/29/2018 2:10 PM
Deleted: Therefore the sensitivity of modeled cooling ages due to a prescribed topographic evolution becomes a critical component in evaluating fold-thrust belt exhumation.

Nadine McQuarrie 2/19/2018 4:15 PM
Deleted: we evaluate the effect of cross section geometry and kinematics as well as the effect of topographic assumptions on modeled cooling ages using a balanced geologic cross section and associated thermochronometer data from the Bhutan Himalaya.

Nadine McQuarrie 1/29/2018 12:57 PM
Deleted: Yin and Harrision, 2000; Hodges, 2000

Nadine McQuarrie 1/31/2018 10:54 AM
Deleted: .

Nadine McQuarrie 1/29/2018 4:53 PM
Deleted: Estimates for the initiation of motion on the Main Central Thurst (MCT) in the fold-thrust belt range from ~25 to 20 Ma (e.g., Hodges et al., 1996; Daniel et al., 2003; Tobgay et al., 2012). The Himalayan fold-thrust belt is composed of south- and north-verging structures and extends from suture zone in southern Tibet to the modern foreland in India. It comprises igneous, sedimentary, and metasedimentary rocks of Paleoproterozoic to Quaternary age (Gansser, 1964; Powell and Conaghan, 1973; LeFort, 1975; Mattauer, 1986; Hodges, 2000; DeCelles et al., 2002; Yin, 20 ... [1]

Nadine McQuarrie 2/19/2018 4:17 PM
Deleted: rocks

Nadine McQuarrie 1/31/2018 10:55 AM
Deleted: present

Nadine McQuarrie 1/31/2018 10:55 AM
Deleted: surrounding

Nadine McQuarrie 2/19/2018 4:17 PM
Deleted: the Trashigang line of cross section

Michelle Gilmore 2/5/2018 9:44 PM
Deleted: of

The Lesser Himalayan zone consists of a package of Neoproterozoic to Permian strata, collectively grouped as the Upper Lesser Himalaya, and a suite of Paleoproterozoic strata comprising the Lower Lesser Himalaya (Gansser, 1983; Bhargava 1995; Long et al., 2011a).

The youngest unit of the Upper Lesser Himalaya, the Permian Gondwana succession, is exposed north of the Subhimalaya zone in the hanging wall of the Main Boundary Thrust (MBT) and in the immediate footwall of the thrust sheet carrying the stratigraphically older Permian Diuri Formation. North of these units, multiple fault-bound packages of the Neoproterozoic-Cambrian Baxa Group are repeated in the Upper Lesser Himalayan duplex. The Shumar Thrust (ST) exposed immediately to the north is interpreted as the roof thrust of the system (McQuarrie et al., 2008; Long et al., 2011b).

In the hanging wall of the Shumar Thrust, the Paleoproterozoic Daling-Shumar Group overlain by the stratigraphically unconformable Neoproterozoic-Ordovician Jashidanda Formation. These strata are repeated multiple times to form the Lower Lesser Himalayan duplex with the Main Central Thrust (MCT) as the roof thrust (McQuarrie et al., 2008; Long et al., 2011a; Long et al., 2011b).

The MCT separates the southern Lesser Himalayan zone from the Greater Himalayan zone located north of the MCT (Heim and Gansser, 1939; Gansser, 1964). The Greater Himalaya is divided into two structural levels: the lower unit is above the MCT but below the out-of-sequence Kakhtang Thrust (KT), while the higher unit is in the hanging wall of the KT (Grujic et al., 2002). Estimates for the initiation of motion on the Main Central Thrust (MCT) range from ~25 to 20 Ma (e.g., Hodges et al., 1996; Daniel et al., 2003; Tobgay et al., 2012), with continued shearing in the Bhutan Himalaya through 18–16 Ma (Grujic et al., 2002; Daniel et al., 2003; Kellett et al., 2009). The age of motion on the KT is notably later (14-8 Ma; Daniel et al., 2003; Grujic et al., 2002, 2011; Coutand et al., 2014). Regional-scale upright, non-cylindrical antiforms and synforms mapped throughout the GH are interpreted to be a result of underlying Lesser Himalayan duplex formation (Long et al., 2011b). Both Greater and Lesser Himalayan rocks preserve pervasive ductile deformation above and below the MCT (Grujic et al., 1996; Long et al., 2011c; Long et al., 2016) During both initial emplacement of the MCT and active displacement on the MHT, ductile processes at depth transition to brittle processes as thrust and shear systems approach the surface, with a transition temperature of ~350° (Avouac, 2007). These cooler processes, friction on brittle faults, and erosional exhumation, control modeled fault rates (Beaumont et al., 2001; Jamieson et al., 2004; Avouac, 2007). Although our approach does not capture ductile deformation at depth, it does capture the displacement and cooling below 350–400 °C, the temperature we are interested in tracking. Even at temperatures below 350–400°C, almost all of the rocks in Bhutan have undergone some component of granular-scale strain (Grujic et al., 1996; Long et al., 2011c; Long et al., 2016). In the models we present here, all thrust sheets are treated as rigid bodies that were translated by discrete structures.

2.2 Thermochronologic Data

We limit the data used to test the cross section by Long et al. (2011b) to those within 15 km of the line of section (Supplemental Table 1). Cooling ages are shown in map view (Fig. 1) and plotted versus distance along the Trashigang cross section (Fig. 2). In order to maintain structural context along the cross section, sample locations are projected onto the cross

Nadine McQuarrie 2/7/2018 2:27 PM
Deleted: a

Nadine McQuarrie 1/31/2018 11:04 AM
Deleted: in

Nadine McQuarrie 1/31/2018 11:04 AM
Deleted: f

Nadine McQuarrie 1/31/2018 11:04 AM
Deleted: ure

Nadine McQuarrie 1/31/2018 11:05 AM
Deleted: in

Nadine McQuarrie 1/31/2018 11:05 AM
Deleted: f

Nadine McQuarrie 1/31/2018 11:05 AM
Deleted: gure

section along structure (i.e. in the direction of the fault trend, maintaining distance from structures). The $^{40}Ar/^{39}Ar$ (MAr) and apatite fission track (AFT) data used are from previous studies and are presented with 2σ analytical error (Supplementary Table 1) (Stüwe and Foster, 2001; Grujic et al., 2006; Long et al., 2012; Coutand et al., 2014). Previously published zircon (U-Th)/He (ZHe) data are determined from the mean age of replicates (typically 3 grains) and presented in this study with a 2σ error that encompasses the range in measured ages (Long et al., 2012). Thirty km west of the cross section modeled in this manuscript is the Kuru Chu cross section (Fig. 1), which has an accompanying suite of cooling ages (Long et al., 2011b, 2012). The Kuru Chu cross section and accompanying data were forward modeled by McQuarrie and Ehlers (2015) using the approach presented here.

MAr data are published only for Greater Himalayan rocks in the immediate hanging wall of the MCT and range from 14.1±0.4 to 11.0±0.4 Ma (Stüwe and Foster, 2001). The spatial extent of this dataset is limited to a 9-km span in the GHl including two cooling ages of 14.1 and 11.1 Ma from samples less than 0.5 km apart taken from the immediate hanging wall of the MCT. The range in ages could be a function of residence time at the highest temperatures reached (650-700 °C) or residence time near the closure temperatures of the minerals, as well as how rapidly the minerals cooled (e.g. Mottram et al., 2016). In a study that examined white mica ages immediately above and below the MCT in Sikkim, Mottram et al. (2015) showed that muscovite single-grain ages had a significantly larger age spread (2-5 Ma) that was not seen in MAr plateau ages. In addition to residence time and thermal conditions experienced by the rocks affecting argon loss, they suggested that a ± 2 Ma age dispersion would be expected due to diffusive differences caused by grain size variations. MAr ages from eastern Bhutan post-date the age of south-directed shear on the MCT in this region (Stüwe and Foster, 2001; Grujic et al., 2002; Daniel et al., 2003; Kellett et al., 2009; Long et al., 2012). Thus we interpret the age range of these four MAr samples as the window of permissible exhumation-induced cooling through the modeled closure temperatures of white mica (Ehlers et al., 2005; Braun, 2003).

The eight ZHe samples from Lesser Himalayan rocks that we use have cooling ages ranging from 11.6±0.1 to 7.3±0.8 Ma along a 40-km across-strike distance (~20-50 km N of the MFT). These ages were interpreted by Long et al. (2012) to indicate structural uplift, exhumation, and cooling of Lesser Himalayan rocks through the zircon (U-Th)/He closure temperature at ~11.5-9.5 Ma. Measured ZHe ages in the Kuru Chu are 1-2 Myr younger than the ZHe ages along the Trashigang section between 15 and 30 km from the MFT (Long et al., 2012)(Fig. 1,2). The predicted ZHe ages in this study do not account for the effects of radiation damage on the closure temperature (e.g. Guenthner et al., 2013), which could lead to potentially underestimating the ZHe closure temperature. However, the effects of radiation damage on ZHe (or AHe) closure temperatures are most pronounced for long durations at relatively low (~220°C) temperatures (Guenthner et al., 2013). The Lesser Himalayan samples evaluated here experienced temperature greater than 300-350° (Long et al., 2011c, Long et al., 2012), have young ages (typically ~7-11 Ma) and underwent extremely rapid cooling (e.g., or around 16.3-22.5 C /Myr cooling rate since closure at ~180 C), thereby leading us to infer that radiation damage effects are minimal. North of the MCT, ZHe cooling ages are limited to two samples, one from the structurally higher Greater Himalaya and one from

Michelle Gilmore 1/31/2018 12:25 AM
Deleted: in this study …re from previous ... [2]

Nadine McQuarrie 1/31/2018 11:11 AM
Deleted: Additional …ooling ages …(Long ... [3]

Michelle Gilmore 1/30/2018 10:36 PM
Deleted: Cooling ages are shown in map view in figure 1 and plotted versus distance along the Trashigang cross section in figure 2. We limit the data we evaluate to those within a 15 km distance from the cross section line. The AFT and ZHe data published by Coutand et al. (2014) north of the KT were projected 27 km 129° SE, maintaining the dataset's original distance between the KT and STD to evaluate modeled age predictions north of the KT (Fig. 1).

Michelle Gilmore 2/4/2018 8:45 PM
Deleted: …m span in the GHl along the lit ... [4]

Nadine McQuarrie 1/30/2018 3:56 PM
Deleted: …T ... [5]

Michelle Gilmore 2/3/2018 9:45 PM
Deleted: h

Nadine McQuarrie 1/30/2018 3:43 PM
Deleted: h

Michelle Gilmore 2/3/2018 9:45 PM
Deleted: e

Nadine McQuarrie 1/30/2018 3:56 PM
Deleted: cooling

Michelle Gilmore 1/30/2018 10:50 PM
Deleted: ages

Nadine McQuarrie 1/30/2018 3:43 PM
Deleted: is interpreted to

Michelle Gilmore 1/30/2018 10:50 PM
Deleted:

Nadine McQuarrie 1/30/2018 3:44 PM
Deleted: represent…cooling through the e ... [6]

Michelle Gilmore 2/4/2018 9:00 PM
Deleted: 35…km across-strike distance ... [7]

Nadine McQuarrie 2/9/2018 9:25 PM
Formatted ... [8]

Michelle Gilmore 2/4/2018 9:04 PM
Deleted: n

Tethyan rocks at the western end of the Sakteng Klippe. These samples recorded cooling ages of 7.4±1.6 Ma and 7.1±0.3 Ma respectively (Coutand et al., 2014; Long et al., 2012).

AFT cooling ages from the Lesser Himalaya are limited to four samples that range between 6.3±2.3 Ma to 4.2±1.0 Ma (Long et al., 2012; Grujic et al., 2006). The youngest age is from the Jashidanda unit in the immediate footwall of the MCT (Grujic et al., 2006). The three older ages from 6.3±2.3 to 5.7±1.0 are from Diuri and Baxa units ~25-35 km farther south. In the structurally lower Greater Himalaya, AFT cooling ages progressively decrease from south to north from 7.8±2.8 Ma to 3.7±0.6 Ma from ~70 to 90 km N of the MFT (Grujic et al., 2006). One young AFT age of 3.1±1.2 Ma is immediately north of the MCT (Stüwe and Foster, 2001) and two similar ages of 3.0±1.4 Ma and 3.6±1.0 are also found 10 km farther north (Grujic et al., 2006). The range in ages of six AFT samples from the structurally higher Greater Himalaya is 2.5±0.4 Ma to 4.2±0.8 Ma (Coutand et al., 2014). In order to avoid skewing the overall fit of models based on fit or misfit to these six cooling ages from the GHh (>25% of AFT data included in this study), we discuss these AFT data sampled north of the line of section as one collective sample point that includes the spatial and temporal variability of the entire cluster when comparing the data to model results in the following sections. We apply the same approach for the cluster of three AFT data from the immediate hanging wall of the MCT, where ages range from 7.8±2.8 Ma to 3.1±01.2 Ma in a span of less than 0.5 km along the line of section (Fig. 1 and 2) (Stüwe and Foster, 2001; Grujic et al., 2006). However, to allow for visual comparison of all individual cooling ages, all 22 AFT ages are shown in all figures plotting thermochronometers.

Few of the data along the Trashigang section display age-elevation relationships, similar to that shown and discussed by McQuarrie and Ehlers (2015) for the Kuru Chu section. AFT ages from the structurally higher Greater Himalaya exhibit a modest age elevation relationship, which suggests exhumation rates of 0.4 mm/yr. Examining both Trashigang and Kuru Chu datasets, an age-elevation relationship may be present in the ZHe data with younger ages (8.5 to 10 Ma) at lower elevations (0.5 to 1 km) in the Kuru Chu and older ages (11 to 11.6 Ma) at higher elevations (1.6 to 2.4 km) along the Trashigang transect. If so, the data suggest differential exhumation of 0.7 mm/yr.

3 Methods

3.1 Flexural and Kinematic Model

Long et al. (2011b) published a balanced cross section in the Trashigang region of Bhutan (Fig. 2). We used the structural modeling software *Move* (Midland Valley) to sequentially deform the Trashigang section using fault-slip amounts determined from the cross section. It is important to note that the models created in *Move* (and Pecube) do not attribute any mechanical behavior to the rocks; they only describe kinematics, or the motion of material. The cross section was deformed in ~10-km increments and included isostatic loading due to fault displacement and unloading due to erosion in each increment. The magnitude of isostatic load was determined from the difference between each increment of deformed topography and the topography of the previous step (McQuarrie and Ehlers, 2015). Erosional offloading was based the difference between the deformed, isostatically loaded profile and a new topographic profile generated at each deformation

Nadine McQuarrie 1/31/2018 11:26 AM
Deleted: were reset…ecorded cooling ages ... [9]

Michelle Gilmore 2/4/2018 9:05 PM
Deleted: ,

Nadine McQuarrie 1/31/2018 11:20 AM
Deleted: -

Michelle Gilmore 2/4/2018 9:09 PM
Deleted: …hat range between 6.3±2.3 Ma ... [10]

Nadine McQuarrie 2/19/2018 4:19 PM
Deleted: two similar ages of ~3 Ma

Michelle Gilmore 1/31/2018 12:02 AM
Deleted: ,…The range in ages of six AFT ... [11]

Nadine McQuarrie 2/19/2018 4:19 PM
Deleted: All 22 AFT ages are shown in figures though to allow for visual comparison if individual cooling ages

Michelle Gilmore 2/4/2018 8:54 PM
Deleted: …levation relationships, similar ... [12]

Nadine McQuarrie 2/8/2018 9:38 AM
Deleted: is

Michelle Gilmore 1/31/2018 12:03 AM
Deleted: 10 …0-km increments and ... [13]

step (McQuarrie and Ehlers, 2015). The methods used to estimate the new topographic profiles are discussed in section 3.1.3. Including isostatic response in the model produces a record of syn-deformational exhumation and deposition, facilitates the steepening of the décollement over time, and develops a foreland basin (McQuarrie and Ehlers, 2017). The process of linking kinematic models of deformation derived from balanced cross sections to advection diffusion thermal models to calculate the evolving subsurface temperatures and predict cooling ages has been explored recently by several research groups (Almendral et al., 2014; Erdös et al., 2014; Mora et al., 2015; McQuarrie and Ehlers, 2015; Castelluccio et al., 2016; Rak et al., 2017), The level of kinematic detail modeled in each of these examples varies greatly as well as how depths of measured samples were projected backwards in time. Each kinematic step can range from 5 to 30 km over estimated time steps of 0.25-15 Myr. The flexural response of deformation has either been calculated explicitly in the reconstruction software (McQuarrie and Ehlers, 2015; Rak et al., 2017) or estimated based on reconstructed paleodepths, foreland basin history and/or perceived flexural response by using the flexural-slip unfolding algorithm in Move (Erdös et al., 2014; Mora et al., 2015; Castelluccio et al., 2016). Due to this growing method of linking cross section kinematics to thermal models it is critical to examine how sensitive the predicted ages are to how flexure and topography are calculated, because both control the depth and thus thermal history of rocks through time (McQuarrie and Ehlers, 2017).

3.1.1 Model Parameters

During the flexural-kinematic modeling process, effective elastic thickness (EET), crustal density, and initial décollement dip were systematically varied to optimize the fit of the final modeled cross section to the observed geology at the surface, foreland basin thickness (6 km), and décollement dip (4°) (Long et al., 2011b). We placed highest priority on matching surface geology. Over 50 different flexural-kinematic models were created in which topography, EET, density, kinematics, or geometry were varied. Out of these models, nine presented in this study produced a foreland basin, dip of the decollement, and surface geology that were all considered acceptable: within 1 km of modern thickness; +1/ -0.5° of modern dip; and 1 km of modern surface geology (Supplementary Fig. 1).

Young's modulus and mantle density were held constant at 70 GPa and 3.3 g/cm^3 respectively. Best-fitting flexural models in this study used values of 65-70 km EET, correlating well with regional estimates for the Himalaya, but are high compared to estimates specifically for the Eastern Himalaya (Jordan and Watts, 2005; Hammer et al., 2013) which are strongly dependent on the width of the modern foreland basin and the location of the Shillong Plateau. The EET values in our best fit models are based on reproducing the depth of the foreland basin preserved in the Siwaliks (5.5-6 km) and the dip of the modern decollement (~ similar to the 5° dip of the Moho (Mitra et al., 2005; Singer et al., 2017), and thus take into account the estimated strength of the lithosphere over a much longer window of time. It is important to note that the particular values for EET and density are not unique, but represent a combination that are able to reproduce the surface data. Our modeling iterations evaluated EETs as low as 40-60 km, however these were unable to match foreland basin thickness, geology exposed at the surface, or decollement dip. Flexural-kinematic model parameters are presented in Table 1 along with the kinematic and topographic variations used in each flexural model. A two-dimensional grid of points spaced 0.5 km apart was

Michelle Gilmore 1/27/2018 7:24 PM
Deleted: decollement

Nadine McQuarrie 1/31/2018 12:18 PM
Deleted: Details of how the new topography was estimated are outlined in section 3.1.3 Several recent studies have used approaches to kinematic reconstruction similar to the incremental-deformation method used in this study (e.g. ... [14]

Nadine McQuarrie 1/31/2018 2:09 PM
Deleted: E

Michelle Gilmore 1/27/2018 7:24 PM
Deleted: decollement

Nadine McQuarrie 1/31/2018 2:09 PM
Deleted: adjusted…to optimize the fit of t ... [15]

Michelle Gilmore 1/27/2018 7:24 PM
Deleted: decollement

Nadine McQuarrie 1/31/2018 2:31 PM
Deleted: and values of 40-70 km in Nepal (Berthet et al., 2013). These va

Michelle Gilmore 2/6/2018 12:26 AM
Deleted: a

Nadine McQuarrie 1/31/2018 2:45 PM
Formatted ... [16]

Nadine McQuarrie 1/31/2018 2:32 PM
Deleted: lues for

Nadine McQuarrie 1/31/2018 2:45 PM
Formatted: Font:(Default) +Theme Body

Nadine McQuarrie 1/31/2018 2:33 PM
Deleted: EET

Nadine McQuarrie 1/31/2018 2:45 PM
Formatted: Font:(Default) +Theme Body

Nadine McQuarrie 1/31/2018 2:33 PM
Deleted: however more than double estim ... [17]

Nadine McQuarrie 1/31/2018 2:45 PM
Formatted ... [18]

Michelle Gilmore 2/6/2018 12:24 AM
Deleted: either

Nadine McQuarrie 1/31/2018 2:45 PM
Formatted ... [19]

Michelle Gilmore 2/6/2018 12:25 AM
Deleted: or surface exposure in the hinterland

Nadine McQuarrie 1/31/2018 2:45 PM
Formatted ... [20]

Nadine McQuarrie 1/31/2018 2:45 PM
Deleted: using EET this low in *Move* itera ... [21]

Michelle Gilmore 2/6/2018 12:25 AM
Deleted:

distributed across the section and sequentially deformed with the cross section to generate high-resolution displacement vectors describing how the kinematics of the system evolve in ~10 km increments. By assigning an age to each step, the displacement field is converted into a velocity field that is used in the thermal and cooling-age prediction model Pecube (Erdös et al., 2014; McQuarrie and Ehlers, 2015; Rak et al., 2017). Each model presented in this study was run using four to seven different velocities to 1) see predominant trends on the predicted cooling ages and 2) determine which combination of velocities resulted in predicted cooling ages that best matched the measured data.

Michelle Gilmore 1/30/2018 11:49 PM
Deleted: The

Michelle Gilmore 1/30/2018 11:48 PM
Deleted: that can be

Michelle Gilmore 1/30/2018 11:49 PM
Deleted: by assigning an age to each step

3.1.2 Kinematic Variations Considered

Out-of-sequence thrusting along the KT occurred sometime between 14 Ma and 8 Ma, significantly more recently than motion on the MCT (Davidson et al., 1997; Grujic et al., 2002; Daniel et al., 2003, Hollister and Grujic, 2006). However, uncertainty remains regarding the magnitude and age of slip along the KT. Long et al., (2011b) argued for 31-53 km of minimum KT displacement. We tested three kinematic scenarios in the flexural models by varying the relative timing of KT motion, called the Early KT, Split KT, and Late KT models (Fig. 3). Early KT is modeled with 45 km of motion along the KT immediately following motion on the Shumar Thrust (Fig. 3c.1). In Split KT, out-of-sequence thrusting is modeled in two separate stages with 25 km of motion applied after deformation along the Shumar Thrust, followed by 20 km of motion after Upper Lesser Himalayan duplexing (Fig. 3c.2). Late KT is modeled with 45 km of out-of-sequence thrusting after development of the Upper Lesser Himalayan duplex, similar to the proposed model of sequential deformation by Long et al. (2012) (Fig. 3c.3).

Nadine McQuarrie 2/7/2018 2:55 PM
Deleted: 2011a

An enigmatic low-relief surface is preserved in the Bhutan Himalaya in the immediate footwall of the KT (Duncan et al., 2003; Grujic et al., 2006). This low-relief landscape contains hundreds of meters of sediment infilling of paleo-relief and is now out of equilibrium with respect to where it formed (Adams et al., 2016). In eastern Bhutan, the infilled sediment is derived from the structurally higher Greater Himalaya; conglomerate is common, thus making it easy to associate the clasts with rocks carried by the KT. Previous studies have highlighted the ubiquitous response of footwall subsidence and the development of low relief in the footwall region of out-of-sequence faults and thrusts (e.g. McQuarrie and Ehlers, 2015, 2017; Rak et al., 2017). Given the uncertainty of magnitude and timing of KT motion, we tested multiple kinematic scenarios of out-of-sequence thrusting in this study. We hypothesized that changing the relative timing of out-of-sequence KT motion in relation to the evolution of the décollement would alter the topographic evolution and isostatic history of the modeled cross-section, and associated thermochronometer ages predicted along it.

Nadine McQuarrie 2/19/2018 4:23 PM
Formatted: Normal, Line spacing: single

3.1.3 Topographic History Estimation

To model the isostatic response to deformation and erosion, we tested three different methods of estimating the topographic evolution in Move. Each method was variable in profile resolution and in its ability to account for common factors of fold-thrust belt development such as deformation front migration, localized topographic uplift, and structural subsidence. The three topographic models were evaluated in the thermal-kinematic model to determine the sensitivity of the predicted

thermochronometric data to each topographic scenario. The "no topography" scenario is the simplest of the three estimations with a topographic profile that remained at sea level throughout the entire section reconstruction. We also tested a "static topography" scenario with a topographic profile similar to the modern topographic gradient of Bhutan (Duncan et al., 2003) that maintains a steep gradient in the first 25 km behind the active deformation front, followed by shallower gradient with elevation increasing along a two-degree slope to a maximum of 5 km. This shape of the topographic profile remains identical throughout the kinematic evolution. The static topographic profile is spatially translated as the location of the deformation front is adjusted progressively southward throughout the sequential development of the fold-thrust belt. A critical caveat to the Static Topography method is that topographic elevations are not perturbed by isostatic loading. Thus the grid points in the model subside due to deformation-induced loading, but the topography does not. The third topographic model is a "responsive topography" that estimates a topographic profile for each flexurally loaded ~10-km deformational step using a Python-based computer script (McQuarrie and Ehlers, 2015). New topography is defined by a northward increasing slope similar to modern topography in regions of active structural and topographic uplift, while in areas without active uplift, the program follows existing, isostatically loaded topography. This approach allows topography to respond to deformational loading and erosional unloading. For models using the static and responsive topographies, the initial topography assigned to the restored section simulates a pre-existing fold-thrust belt in the Tethyan sequence before the initiation of the MCT (Ratschbacher et al., 1994; Murphy and Yin, 2003; Webb et al., 2011). This topography maintains 0 km elevation from the southern end of the restored cross section to the Lower Lesser Himalaya. Across the Lesser Himalaya, topographic elevation increases to 5 km across a distance of 140 km and reaches a maximum elevation of 5 km above the lower Greater Himalaya, which at its southernmost extent is buried at a depth of 16 km below sea level.

3.2 Thermal and Cooling Age Prediction Model

The velocity field and topography for each increment of deformation, after displacement, isostasy, and erosion have been applied, is input into a University of Tübingen modified version of the thermal-kinematic predictive model Pecube (Braun, 2003; Whipp et al., 2009; McQuarrie and Ehlers, 2015). The thermal-kinematic model functions as: (1) a kinematic model that uses fault geometries and high-resolution point tracking inputs from the Move software to calculate rock transport (advection) velocities; (2) a transient thermal model that calculates the thermal field using fault motion, erosion above the topographic surface, rock thermophysical properties, and thermal boundary conditions; and (3) a set of age prediction algorithms (Ehlers et al., 2005) that calculate a suite of thermochronometer ages for material at the topographic surface for each deformation step using the thermal histories of particles as they are exhumed and cooled from depth to the model surface (e.g. Coutand et al., 2014; McQuarrie and Ehlers, 2015). Modeled results highlight that increased rates of thrusting and exhumation advect isotherms upward while basin subsidence in the foreland locally depresses isotherms. Motion on the MCT and Kakhtang Thrust produce the same inverted thermal gradients at these faults that have been both observed and reproduced in previous modelling studies (Henry et al., 1997; Bollinger et al., 2006; Hollister and Grujic, 2006; Herman et al., 2010).

Michelle Gilmore 2/8/2018 8:14 PM
Deleted: N

Michelle Gilmore 2/8/2018 8:14 PM
Deleted: T

Michelle Gilmore 2/8/2018 8:10 PM
Deleted: "Template Topography"

Michelle Gilmore 2/8/2018 8:10 PM
Deleted: Template Topography

Michelle Gilmore 2/8/2018 8:11 PM
Deleted: the same north of the deformation front, and th

Michelle Gilmore 2/9/2018 12:51 AM
Deleted: Template

Michelle Gilmore 2/8/2018 8:15 PM
Deleted: , "Python Topography",

Michelle Gilmore 2/8/2018 8:09 PM
Deleted: (Python Topography)

Michelle Gilmore 2/8/2018 8:12 PM
Deleted: The n

Nadine McQuarrie 2/7/2018 3:01 PM
Deleted: N

Nadine McQuarrie 2/7/2018 2:59 PM
Deleted: is generated using a user-defined

Michelle Gilmore 2/8/2018 8:13 PM
Deleted: (e.g. Duncan et al., 2003)

Nadine McQuarrie 2/7/2018 3:01 PM
Deleted: slope (e.g., two degrees) where active uplift occurs

Michelle Gilmore 2/8/2018 8:09 PM
Deleted:

Michelle Gilmore 2/8/2018 8:14 PM
Deleted: Python and Template

Nadine McQuarrie 2/8/2018 3:40 PM
Deleted: The model predicts the cooling ages of rock samples that could hypothetically be collected from the surface at each deformation step, up to the modern deformed cross section geometry and topography

3.2.1 Radiogenic Heat Production

The thermal state of the crust depends on the basal heat flow from the mantle and the material properties of the crust (e.g., thermal conductivity, density, heat capacity, and radiogenic heat production). Following the approach and rationale summarized in McQuarrie and Ehlers (2017), we prescribe an exponential decrease in heat production with depth, as opposed to assuming a constant crustal heat production. An exponential decrease in heat production with depth requires definition of a surface heat production (Ao) and an e-folding depth. One caveat of this approach is that material properties are not exhumed during the simulations to modify the surface heat production value. However, an exponential decrease in heat production with depth has the advantage of honoring observations that heat production diminishes with depth through the crust and that this decline is not monotonic (Chapman, 1986; Ketcham, 1996; Brady et al. 2006). This approach not only allows matching measured surface values of heat production in the Himalaya (e.g. see Whipp et al. 2007), but also produces reasonable mid and lower crustal temperatures that would not produce partial melts. We varied Ao to test the sensitivity of predicted cooling ages to variations in rock thermophysical properties. Calculated values of radiogenic heat production in the Himalaya are highly variable. A low radiogenic heat production estimate of 0.8 $\mu W/m^3$ for the entire Indian Shield was calculated based on observed low in heat flow by Ray and Rao (2000), but other measurements have been estimated as high as 1.5-5.5 $\mu W/m^3$ due to the abundance of potassium, uranium, and thorium in granitic and gneissic rocks (Menon et al., 2003). Similar ranges of radiogenic heat production values from 1.5 to 6.0 $\mu W/m^3$, with clustering around 4 $\mu W/m^3$, have also been found for Greater Himalayan rocks (e.g., England et al., 1992; Whipp et al., 2007). Herman et al. (2010) concluded a best-fitting constant radiogenic heat production value of 2.2 $\mu W/m^3$ in their own thermal-kinematic model using a constant basal temperature of 750°C at 80 km depth. In this study we tested models of the Long et al. (2011b) cross-section geometry using Ao values ranging from 4.0 to 1.0 $\mu W/m^3$ in 0.25-0.5 $\mu W/m^3$ increments, and heat production decreases exponentially with depth (e-folding depth of 20 km). Thermal conductivity and heat capacity were held constant at values of 2.5 W/m K and 800 J/kg K (respectively) based on observed thermal physical properties for the lithologies present in the Himalaya (Whipp et al. 2007, and Ehlers, 2005). Although thermophysical properties such as thermal conductivity, heat capacity, and density vary between different lithologies, the implementation of variable material properties in areas of large deformation is not possible in programs such as Pecube, which solve the advection diffusion equation on an Eulerian grid. Thus, we address this potential issue by using the best available average measurements of thermophysical properties for the lithologies in this region. All thermal rock property parameters input in Pecube simulations are listed in Table 2.

3.2.2 Variable Deformation Age and Rate

To compare the effects of differing time and rate of fault motion on predicted cooling ages, several deformation ages and velocities were tested. Details for combinations of velocities, radiogenic heat production values, and flexural models are in Table 3.

Nadine McQuarrie 2/7/2018 3:15 PM
Deleted: radiogenic heat production (

Michelle Gilmore 2/4/2018 9:52 PM
Deleted: o

Nadine McQuarrie 2/7/2018 3:15 PM
Deleted:)

Nadine McQuarrie 2/19/2018 4:25 PM
Deleted: using radiogenic heat production values ranging from 4.0 to 1.0 $\mu W/m^3$

Michelle Gilmore 1/27/2018 7:26 PM
Deleted: ,

Michelle Gilmore 1/27/2018 7:37 PM
Deleted: A

Nadine McQuarrie 2/19/2018 4:26 PM
Deleted: age

A constant velocity of 17.3 mm/yr using the MCT initiation age of 23 Ma was tested to determine if a generalized long-term rate of shortening can adequately reproduce published cooling ages. This rate is comparable to the ~15-25 mm/yr estimates of modern convergence for the Himalaya (Bilham et al., 1997; Larson et al., 1999; Banerjee and Burgmann, 2002; Zhang et al., 2004; Bettinelli et al., 2006; Banerjee et al., 2008) and long-term rates of shortening through the Himalaya (DeCelles et al., 2001; Lavé and Avouac, 2000; Long et al., 2011b).

However, in Bhutan, variable rates of shortening have been proposed based on the integration of shortening estimates from balanced cross sections with thermochronometer data. These rates range from 4 mm/yr – 60 mm/yr (Long et al., 2012). Modeling rates of shortening along the Kuru Chu section using cross section kinematic in a thermal model McQuarrie and Ehlers (2015) found the best match to measured cooling ages with rates that varied from 7 mm/yr to as high as 75 mm/yr. We evaluate a suite of velocity simulations starting with these two published variable deformation rate scenarios. Velocity model A is based on rates proposed by Long et al. (2012) along the Trashigang section with pulses of rapid deformation during MCT motion (32 mm/yr) and the formation of the Upper Lesser Himalayan duplex (37-41 mm/yr), separated by slower periods of deformation during Lower Lesser Himalayan duplexing (15 mm/yr) and motion along the MBT and MFT (4-6 mm/yr). Velocity model B is broadly based on rates proposed by McQuarrie and Ehlers (2015), namely fast velocities (55-75 mm/yr) during formation of the Upper Lesser Himalaya duplex. In Velocity B, MCT motion initiates at 20 Ma with a slower velocity (21 mm/yr), duplexing of the Lower Lesser Himalaya is at similar rates (22-25 mm/yr), while the Upper Lesser Himalaya duplex deforms at rate of 69-75 mm/yr. Other rates of motion in this scenario are comparable to velocity model A. In addition to these rates, we varied rates of shortening for the formation of the Lower Lesser Himalaya duplex (16-25 mm/yr) formation of the Upper Lesser Himalaya duplex (45-75 mm/yr) and emplacement of the MBT and MFT (4-10 mm/yr). Inherent in the suite of velocities is testing the sensitivity of cooling ages to the start and end date of these different structural systems.

4 Results

4.1 Flexural-kinematic Model

Summaries of the final output of all seven flexural-kinematic models to the published Trashigang cross section (Long et al., 2011b) are presented in Table 1; supplemental figure 1 contains images of the results of each model. Because the flexural-kinematic models control locations and magnitudes of erosion and burial that are input into the thermal model, we evaluate the effects of estimated topographic evolution, different proposed kinematics, and amount of subsidence (illustrated by the final shape of the décollement) on exhumation magnitudes and the geology exposed at the present-day surface.

The difference between model results are subtle but show local variations in total erosion of 0.5-4 km that is reflected in the final geology exposed at the surface of the model and depth to stratigraphic markers within the model. All models produced foreland basin depths within 2 km of the 5.5-6 km thick Siwalik section exposed in Eastern Bhutan (Long et al. 2011a, Long et al.2011b). Average décollement dips varied from 3.75° to 5.4°. Six out of seven models are within the 4-7° décollement

Nadine McQuarrie 1/31/2018 3:46 PM
Deleted: concluded by Long et al. (2012)

Michelle Gilmore 1/31/2018 12:55 AM
Deleted: e

Nadine McQuarrie 1/31/2018 3:47 PM
Deleted: as low as … mm/yr – 60 mm/yr (... [22]

Nadine McQuarrie 1/31/2018 4:37 PM
Deleted:

Michelle Gilmore 1/27/2018 7:16 PM
Deleted: in this section

Nadine McQuarrie 1/31/2018 6:02 PM
Deleted: describe …valuate in this section ... [23]

Michelle Gilmore 1/27/2018 7:18 PM
Deleted: sensitivity of the vertical path of points and the resulting geology that is exposed at the surface to the

Nadine McQuarrie 1/31/2018 6:05 PM
Deleted: total magnitude…mount of subsi ... [24]

Michelle Gilmore 1/27/2018 7:25 PM
Deleted: decollemen…écollement)t ... [25]

Nadine McQuarrie 1/31/2018 6:03 PM
Deleted: particle…xhumation magnitudes ... [26]

Michelle Gilmore 1/27/2018 7:20 PM
Deleted: the …odel ing ... [27]

Nadine McQuarrie 1/31/2018 6:06 PM
Deleted: local

Michelle Gilmore 1/31/2018 1:02 AM
Deleted: estimated

Nadine McQuarrie 1/31/2018 6:06 PM
Deleted: -

Michelle Gilmore 1/31/2018 1:02 AM
Deleted:

Nadine McQuarrie 1/31/2018 6:06 PM
Deleted: ness estimated by…iwalik sectio ... [28]

Michelle Gilmore 1/27/2018 7:24 PM
Deleted: decollement…écollement dips va ... [29]

Nadine McQuarrie 1/31/2018 5:48 PM
Deleted: 6

angle estimated for the Main Himalayan Thrust (Ni and Barazangi, 1984; Mitra et al., 2005; Schulte-Pelkum et al., 2005; Singer et al., 2017).

Each of the different kinematic scenarios produced different flexural responses (Table 1). Models using Late KT deformation produced the deepest foreland basins and steepest décollement dips, along with under-eroded geology at the surface compared to the published section. These results are a function of the different kinematic scenarios imposing variations in the distribution of uplifted topography and consequently different flexural loading profiles over the evolution of the cross section. Early KT and Split KT scenarios have décollement dips shallower than Late KT models and result in a better match the surface geology data, except when using No Topography. Differences among Early KT and Split KT décollement dips and surface geology are not systematic, indicating these differences are less driven by kinematics and appear to be more sensitive to slight variations in flexural isostasy parameters and the profile of the topographic load. The poorest fit to surface geology was produced by the model combining Split KT with No Topography (Supplemental Fig. 1). In all other model combinations, exposed geology is within 1 km of the modern geology observed at the surface, with particularly good fits combining Early KT deformation with the Static Topography, and Split KT with Responsive Topography.

Topographic profiles from the final deformation step of each model vary in fit and misfit to observed topography along the Trashigang line of section (Fig. 4). The sea-level No Topography profile is obviously the worst fit of the three estimations. Static Topography fits the steep topographic rise from the MFT to the southern trace of the Shumar thrust; however to the north of the Shumar Thrust, estimated elevations are ~1 km greater than observed. Responsive Topography provides a better fit for the northern half of the section, including a local drop in elevation from 77-90 km along section north of the MFT. However, the average 2° slope assigned to the topographic profile resulted in under-predicted elevations from 13-55 km, where the average observed topographic slope of the range is steeper (4.5°). Overall, Responsive Topography best reproduces the observed topography along the cross section.

For models using responsive and static topographies, we attribute the differences in décollement dip to the lower topographic relief produced using a 2° angle with Responsive Topography, compared to the steeper topographic angle near the deformation front and overall higher elevations with Static Topography (Fig. 4). The shallower topography from the Responsive Topography requires a steeper décollement to accommodate the same amount of material between the surface and the décollement (i.e. broadly maintaining the same taper angle). The most significant result of flexural modeling was identifying the relationship between uplift or subsidence of rock (as represented by the two-dimensional grid of points) and the uplift, subsidence or static position of topography. The static profile used when modeling with Static Topography or No Topography can result in regions of non-erosion and burial (with respect to the topographic surface). When the deformation front shifts toward the foreland, higher topography is translated southward with no direct relationship for where structural uplift is occurring. Additionally, material (as represented by the grid) will subside in areas responding to flexural loading while topography does not. This latter example is especially relevant south of the Kakhtang Thrust during out of sequence thrusting. While using Responsive Topography, both points and topography subside in front of the Kakhtang Thrust, which

Nadine McQuarrie 1/31/2018 5:48 PM
Deleted: Hauck et al., 1998; Pandey et al., 1999;

Michelle Gilmore 1/27/2018 7:24 PM
Deleted: decollement

Nadine McQuarrie 2/9/2018 12:17 PM
Deleted: s

Michelle Gilmore 1/31/2018 1:07 AM
Deleted: out-of-sequence thrusting producing a greater magnitude of late-stage loading in the hinterland of the models. … Early KT and S… [30]

Nadine McQuarrie 2/9/2018 12:24 PM
Deleted: r…sponsive Tt … [31]

Michelle Gilmore 2/9/2018 12:51 AM
Deleted: Template…tatic Topography fits … [32]

Nadine McQuarrie 2/9/2018 12:24 PM
Deleted: t

Michelle Gilmore 2/8/2018 8:17 PM
Deleted: Python Topography …opographi… [33]

Nadine McQuarrie 2/9/2018 12:24 PM
Deleted: r…sponsive Tt … [34]

Michelle Gilmore 2/8/2018 8:18 PM
Deleted: Python …esponsive and Templat… [35]

Nadine McQuarrie 2/9/2018 12:25 PM
Deleted: y

Michelle Gilmore 1/27/2018 7:24 PM
Deleted: decollement…écollement dip to … [36]

Nadine McQuarrie 2/9/2018 12:26 PM
Deleted: r…sponsive Tt … [37]

Michelle Gilmore 2/9/2018 12:51 AM
Deleted: Template…tatic Topography (Fi… [38]

Nadine McQuarrie 2/9/2018 12:26 PM
Deleted: r…sponsive Tt … [39]

Michelle Gilmore 1/27/2018 7:24 PM
Deleted: decollement

Nadine McQuarrie 2/9/2018 12:27 PM
Deleted: within …etween the surface and … [40]

Michelle Gilmore 2/9/2018 12:51 AM
Deleted: Template…tatic Topography or … [41]

allows for minor amounts erosion to occur across the entire section during fault motion. Using the Static Topography, points subside due to the imposed load but topography does not which simulates burial in this region. Thus the Static Topography disconnects the topographic evolution from the kinematic and flexural evolution by not accounting for structural uplift and subsidence. The thermal consequences of the different flexural-kinematic models are explored in Section 4.2.

4.2 Predicted Cooling Ages Across the Cross-section

4.2.1 Effect of Radiogenic Heat Production and Constant Shortening Velocity on Predicted Ages

By holding velocity constant and testing multiple values of radiogenic heat production in Pecube, we can discern the effect that adjusting radiogenic heat production may have on the output of predicted cooling ages as well as the viability of a constant rate of shortening with time. We compare predicted cooling ages for AFT, ZHe and MAr systems to published ages using a range of surface radiogenic heat production (Ao) values from 1.0 to 3.0 $\mu W/m^3$ (Fig. 5). The kinematic input is from the flexural-kinematic model combining Split KT and Responsive Topography, coupled with a constant velocity of 17.3 mm/yr from 23 Ma to the present.

The most apparent trend among all three thermochronometer systems is that predicted cooling ages become younger as the surface radiogenic heat production increases from 1.0 to 3.0 $\mu W/m^3$ due to the higher temperatures throughout the model. In addition, for the MAr system, the modeled heat production values determine if the subsurface temperatures are hot enough crust to yield reset ages at the modeled present-day surface. When Ao is low (1.0 $\mu W/m^3$), the only reset MAr ages are north of the Kakhtang Thrust, while output with higher Ao (3.0 $\mu W/m^3$) include MAr ages as young as 5.8 Ma in the upper Lesser Himalaya (Fig. 5a). Changes in Ao have the smallest effect on predicted AFT cooling ages for range of Ao values tested. Predicted AFT ages are controlled by the motion of rocks over the active ramp located ~65-75 km from the MFT. The relatively rapid shortening rate produces a very shallow-dipping predicted age curve from 30-65 km from the MFT, with the youngest ages focused at the active ramp. Changes in radiogenic surface heat production slightly change the predicted age by 1-3 Myr, with larger predicted age differences (~5 Ma) for Greater Himalayan rocks that have not been transported over the ramp. These ages are significantly older (5-15 Myr) until 90 km from the MFT, the location of the Kakhtang Thrust (Fig. 5). For the ZHe system, changing Ao values notably changes the pattern of predicted cooling ages. The hottest surface radiogenic heat production value (Ao = 3.0 $\mu W/m^3$), produced a signal identical to the AFT, but slightly older. However, the coolest value (Ao = 1.0 $\mu W/m^3$) generated a markedly different trend from ~25-65 km along section, where the youngest predicted ages are at the southern limit of the upper Lesser Himalayan duplex and become gradually older to the north. This north-to-south younging of the predicted cooling ages is the expected signal for a hinterland-dipping duplex (Lock and Willett, 2008; McQuarrie and Ehlers 2017). The predicted age range, 10-5 Ma, closely matches the ages of upper Lesser Himalayan duplex formation (12.8-3.5 Ma) in the constant velocity model (Table 2 or 3). In AFT and ZHe predicted ages, the trend of older predicted cooling ages 65-85 km north of the MFT forms an upside-down U shape in the Greater Himalaya section between the Main Central and Kakhtang thrusts regardless of surface radiogenic heat production value (Fig. 5).

Michelle Gilmore 2/9/2018 12:51 AM
Deleted: Template…tatic Topography, po… [42]

Nadine McQuarrie 2/7/2018 3:37 PM
Deleted:

Michelle Gilmore 2/9/2018 12:48 AM
Deleted: Python…esponsive Topography, … [43]

Nadine McQuarrie 2/7/2018 3:54 PM
Deleted: radiogenic …urface radiogenic … [44]

Michelle Gilmore 2/4/2018 9:54 PM
Deleted: of ….0 $\mu W/m^3$) yields … [45]

Nadine McQuarrie 2/9/2018 2:29 PM
Deleted: U

Michelle Gilmore 2/4/2018 9:55 PM
Deleted: U…per Lesser Himalayan … [46]

Nadine McQuarrie 2/2/2018 12:17 PM
Deleted: The difference in predicted reset MAr ages in structurally higher Greater Himalaya rocks north of the Kakhtang Thrust is 3-7 Myr between simulations with Ao values of 1.0 and 3.0 $\mu W/m^3$. Similar differences in cooling ages are observed in ZHe and AFT plots as well (Fig. 5b,c)…han… [47]

Michelle Gilmore 2/4/2018 9:58 PM
Deleted: 5…6…75 km from the MFT. Th… [48]

Nadine McQuarrie 2/7/2018 3:59 PM
Deleted: spatially reaching

Michelle Gilmore 2/4/2018 10:09 PM
Deleted: of…3.0 $\mu W/m^3$), produced a sign… [49]

Nadine McQuarrie 2/7/2018 4:01 PM
Deleted: 30…65 km along section, where … [50]

Michelle Gilmore 1/27/2018 7:31 PM
Deleted: surface radiogenic heat

Nadine McQuarrie 2/2/2018 1:25 PM
Deleted: c

Evaluating the fit between measured and modeled ages predicted by the different thermal models using this constant velocity we observe that all three models reproduce less than half of all measured cooling ages. The best match to published AFT ages out of these three models is Ao = 1.0 μW/m^3; however, this is still a rather poor fit. Even with a cool crust, we find that predicted ages are too young to fit most published AFT and ZHe ages but significantly too old to match published MAr data. While MAr prediction improves slightly with high surface radiogenic heat production (Ao = 3.0 μW/m^3), even younger modeled AFT and ZHe ages poorly fit most data. These simultaneous over- and under-estimations of published ages require more complex rates of deformation and exhumation.

4.2.2 Effect of Shortening Rate Variations on Predicted Ages

A constant rate of deformation described in the previous section does not produce cooling ages that match all three thermochronometer systems (Fig. 5). In this section we present modeled cooling ages from two variable velocity schemes that are compared to published cooling ages: velocity model A (Long et al., 2012), and velocity model B (McQuarrie and Ehlers, 2015) (Table 3). All variable velocity models presented in this section used a surface radiogenic heat production value of 2.5 μW/m^3 with the flexural-kinematic model combining Split KT and Responsive Topography as input.

Using velocity model A in Pecube results in a visibly improved fit compared to the constant deformation rate. Cooling ages predicted in the model are within the range of error or variability of 16 out of 28 published cooling ages (57%) fit. Predicted AFT ages fit 7 out of 15 published samples (47% fit), with 5 of the samples not matched by the predicted ages located between 70 km to 120 km from the MFT (Fig. 6). Only 3 of the youngest measured AFT ages (3.0-3.6) matched modeled ages in the GH rocks 55-65 km from the MFT, while predicted AFT ages were 3-4 Myr older than the cluster of AFT ages in the structurally higher GH. Predicted ZHe ages match 8 out of 13 samples (62% fit), while predicted MAr ages are 2 Myr older than the olderst measured age of 14.1 Ma. Modeled MAr ages pass through the cooling window during Lower Lesser Himalayan duplex formation and motion on the Shumar Thrust, which ceases activity at 15 Ma for velocity model A.

During the formation of the Upper Lesser Himalayan duplex, a faster rate of deformation (37.3 mm/yr) than in the constant velocity model produces older ages across the Upper Lesser Himalaya (~10 Ma) and a better match to published ZHe data (Fig. 6a). Due to the large amount of shortening accommodated by the Upper Lesser Himalayan duplex, fast shortening is also required to predict the pattern of ZHe ages that do not young towards the south 15-35 km from the MFT (Fig. 5b). Only one of two measured ZHe ages from the structurally lower Greater Himalaya could be reproduced. Topographic uplift and increased exhumation as rocks are structurally uplifted over the décollement ramp 65 km from the MFT results in young predicted ZHe ages (and a match the measured ZHe age) at the ramp, but notably older predicted ages to the north. Southward displacement of rocks over the ramp produces the south-to-north younging of ZHe ages 35-58 km from the MFT (Fig. 6).

Samples from the Upper Lesser Himalaya cool through the AFT closure temperature after out-of-sequence motion on the Kakhtang Thrust and during rapid deceleration in deformation rate from 37 mm/yr to 6 mm/yr at 10 Ma. Both the out-of-sequence thrusting and the slower deformation rate create a prolonged timeframe for rocks to cool (Fig. 6a). Similar to ZHe

Michelle Gilmore 2/4/2018 10:18 PM
Deleted: indicates that…we observe that ... [51]

Nadine McQuarrie 2/2/2018 1:40 PM
Deleted: this low rate

Michelle Gilmore 1/27/2018 7:46 PM
Deleted: cool thermal parameter… we fin ... [52]

Michelle Gilmore 2/4/2018 10:47 PM
Deleted: Velocity

Michelle Gilmore 2/4/2018 10:33 PM
Deleted: , …ith the flexural-kinematic mo ... [53]

Michelle Gilmore 1/31/2018 1:29 AM
Deleted: Velocity model A produces a noticeably better fit than a constant deformation rate. Modeled MAr ages are 2 Myr older that the 2 oldest published ages (14.1 Ma), and predicted cooling ages are within error of 16 out of 28 published AFT and ZHe cooling ages (57% fit) (Fig. 6a). Predicted AFT ages fit 7 out of 15 published samples (47% fit), with no fit to AFT data from 70 km to 120 km. Predicted ZHe ages match 9 out of 13 samples (69% fit). Predicted MAr ages are reset during Lower Lesser Himalayan duplex formation and motion on the Shumar Thrust, which ceases activity at 15 Ma for velocity model A. The MAr system records cooling during Lower Lesser Himalaya duplexing, regardless of its age or rate.

Nadine McQuarrie 2/2/2018 1:46 PM
Deleted: no fit to AFT data…f the sample ... [54]

Michelle Gilmore 2/4/2018 10:50 PM
Deleted: age in the Greater Himalay

Nadine McQuarrie 2/9/2018 2:54 PM
Deleted: . …These m…deled MAr ages p ... [55]

Michelle Gilmore 2/4/2018 10:56 PM
Deleted: A … faster rate of deformation (... [56]

Nadine McQuarrie 2/2/2018 1:53 PM
Deleted: As the final two horses of the duplex are stacked along a large decollementdécollement ramp (Fig. 3c), the increased magnitude of uplift a ... [57]

Michelle Gilmore 1/27/2018 7:47 PM
Deleted: isotherm

Nadine McQuarrie 2/7/2018 4:21 PM
Deleted: cool through closure temperature

Michelle Gilmore 2/4/2018 11:15 PM
Deleted: record …a r ... [58]

Nadine McQuarrie 2/2/2018 2:02 PM
Deleted: particles

Michelle Gilmore 1/27/2018 7:48 PM
Deleted: AFT ages

Nadine McQuarrie 2/7/2018 4:24 PM
Deleted: ,…causing scatter in predicted A ... [59]

ages, predicted Lower Lesser Himalayan AFT ages are controlled by motion of rocks over the active MHT ramp located 65 km from the MFT. The slope of the predicted AFT ages from 30-65 km is a function of the rate of shortening from 7 Ma to present. Predicted AFT ages in the Greater Himalaya systematically increase north of the ramp, similar to the pattern observed with the constant velocity output (Fig. 6). These older predicted AFT ages located 65-85 km from the MFT cool much earlier in the deformation history when rocks were structurally uplifted over a ramp in the Lower Lesser Himalaya during early stages of Upper Lesser Himalayan duplexing (Fig. 3c.2).

Velocity model B uses an earlier MCT initiation at 20 Ma and a rate of Upper Lesser Himalayan duplexing that is twice the rate used in velocity model A (Table 3). Despite this difference, fits to published data are remarkably similar to velocity model A, with a marginally improved fit to MAr data and Upper Lesser Himalayan ZHe data (Fig. 6b). Predicted MAr ages produce a better match to published data due to a younger age for the growth of the Lower Lesser Himalaya duplexing: 17-13.5 Ma with velocity B versus 20-15 Ma with velocity A. Faster and earlier Upper Lesser Himalayan duplexing, which ends at 11 Ma in this scenario versus 10 Ma in velocity A, predicted slightly older and better-fitting modeled ZHe data across the Upper Lesser Himalaya (11-10 Ma). Eleven out of 13 ZHe ages (85%) are reproduced within error. As in velocity model A, 7 out of 15 AFT ages are reproduced (47% fit). Predicted AFT ages still remain too old in the GH zone from 65 km northward. Although the timing and rates of deformation used in velocity model B result in a significantly better fit to published thermochronometer data than constant velocity and slightly better fit than velocity A, there is still a large discrepancy between predicted and measured AFT ages across Greater Himalaya that can not be resolved by changes in velocity. The sensitivity of predicted cooling ages to the age and rate of shortening is expanded on in section 5.

4.2.3 Effect of Topographic Estimates on Cooling Ages

We evaluate the sensitivity of the predicted thermochronometer ages to different topographic development approaches (Responsive, Static, and No Topography) using the Split KT kinematic scenario and velocity model B. The resulting predicted ages for different thermochronometer systems are shown in figures 6b and 7. The significant overlap of modeled cooling ages for the three methods of estimating topographic evolution indicates the predicted cooling ages are much less sensitive to how topography is approximated than to changes in deformation velocity, surface radiogenic heat production, or geometry (Section 4.3).

The No Topography model generated predicted ages that are remarkably similar to the Responsive Topography. In detail, No Topography yields identical or slightly older (0.5 to 3 Myr) predicted ages than the Responsive Topography, with greatest difference in the predicted lower Lesser Himalayan AFT ages. This is in contrast to our initial expectations that the over-eroded No Topography model would produce younger cooling ages than the other topographies because the No Topography scenarios always produced higher total exhumation: the final cross section was over-eroded by 1-2.3 km (Table 1, Supplementary Fig. 1). However this total exhumation accumulates over the modeled history, suggesting that the incremental over-erosion of the No Topography scenarios is always significantly less than the exhumation driven by

Michelle Gilmore 2/4/2018 11:20 PM
Deleted: P…edicted Lower Lesser Himal… [60]

Nadine McQuarrie 2/2/2018 2:12 PM
Deleted: again

Michelle Gilmore 2/4/2018 11:27 PM
Deleted: the fold and thrust belt …ocks w… [61]

Michelle Gilmore 2/4/2018 11:30 PM
Deleted: Using velocity B …aster and earl… [62]

Nadine McQuarrie 2/2/2018 2:20 PM
Deleted: . … [63]

Nadine McQuarrie 2/8/2018 1:56 PM
Deleted: **Development**

Michelle Gilmore 2/4/2018 11:38 PM
Deleted: scenarios

Nadine McQuarrie 2/9/2018 2:23 PM
Deleted: ; o. utput for Responsive Topography is from the same model used in figure 6b. …G… [64]

Michelle Gilmore 2/9/2018 12:48 AM
Deleted: Python…esponsive Topography. … [65]

Nadine McQuarrie 2/9/2018 3:28 PM
Deleted: L

Michelle Gilmore 2/4/2018 11:48 PM
Deleted: where…the final cross section w… [66]

Nadine McQuarrie 2/2/2018 2:35 PM
Deleted:

Michelle Gilmore 2/4/2018 11:48 PM
Deleted:

structural uplift. In other words, exhumation differences due to different estimates of topography (<1 km) are significantly less than that required (2-3 km) to be recorded in thermochronometer ages (Valla et al., 2010).

Results from Static Topography versus Responsive Topography models show greater differences in predicted cooling age trends. In ZHe and MAr plots, the largest difference between the models is the spatial width of the reset cooling ages. For example, reset MAr cooling ages in the Responsive Topography model start 33 km north of the MFT, versus 36-37 km north in the Static Topography model. For ZHe ages, reset ages from the Responsive Topography model start at 10 km north of the MFT while reset ages from the Static Topography start at 20 km. There is also a high degree of scatter in the predicted AFT ages from the Static Topography model. Between 35 and 90 km, these ages range from 13-3 Ma without any pattern, except for directly over the ramp at 55-65 km from the MFT. This highly irregular cooling history is a function of the topographic modelling method not accounting for structural uplift or structural subsidence with time. Static topography that is simply spatially translated as the MHT advances southward inaccurately models burial of material where particle points are subsiding and modeled topography is not subsiding, and produces over-erosion of material where particle points experience structural uplift but modeled topography remains static. These results highlight that estimates of topographic evolution must account for areas of structural uplift and isostatic subsidence when modelling fold-thrust belt evolution.

4.2.4 Effect of Kinematic Variation on Cooling Ages

Changes to the prescribed kinematic order used in forward modeling the cross section were tested using flexural-kinematic models with Responsive Topography, coupled with velocity model B and surface radiogenic heat production of 2.5 $\mu W/m^3$ in the thermal-kinematic model. Because different thrust structures have different slip magnitudes, it is not possible to have precisely the same velocities with different kinematics. To most closely evaluate the effect of kinematic variations in out-of-sequence thrusting, we kept the age at which velocities change the same whenever possible. Predicted cooling age output for Early KT and Late KT kinematic scenarios are plotted in figure 8 and compared with results from the same Split KT scenario used in Section 4.2.3.

Fits of modeled MAr ages to published data are unaffected by changes to the timing of out-of-sequence thrusting; all three scenarios resulted in predicted MAr ages of ~14 Ma in the hanging wall of the MCT. This is expected because all changes to out-of-sequence thrusting occur after the formation of the lower Lesser Himalayan duplex from 17-13 Ma. In all of the modeled scenarios, the age and rate of shortening in the lower Lesser Himalayan duplex set the predicted ages for the MAr system between 40 and 60 km from the MFT.

Each of the three kinematic scenarios predicted significantly different ZHe ages across the upper Lesser Himalaya duplex, implying that there is a particular kinematic order of deformation required in the flexural-kinematic model to generate the measured cooling ages. The pattern of predicted ZHe ages between 10 and 65 km from the MFT is controlled by age and rate of displacement of the upper Lesser Himalayan duplex, the final step of which places duplexed Baxa units over younger Gondwana rocks on a ramp in the MHT (Fig. 3d). This last step structurally elevates the entire duplex and increases local exhumation. Continued motion of the duplex over this ramp cools the rocks through the AFT system. In the Split KT

Deleted: modeled
Michelle Gilmore 2/3/2018 9:58 PM
Deleted: thermochronometry
Michelle Gilmore 2/4/2018 11:50 PM
Deleted: the…Template…tatic Topograp… [67]
Nadine McQuarrie 2/2/2018 3:14 PM
Deleted: that are predicted …n the Respon… [68]
Michelle Gilmore 1/31/2018 1:40 AM
Deleted: For example, the Python Topogr… [69]
Nadine McQuarrie 2/2/2018 3:14 PM
Deleted: predicted
Michelle Gilmore 2/9/2018 12:48 AM
Deleted: Python…esponsive Topography … [70]
Nadine McQuarrie 2/2/2018 3:16 PM
Deleted: t…pography do not appear in res… [71]
Michelle Gilmore 1/31/2018 1:33 AM
Deleted: ….The wide discrepancy in predi… [72]
Nadine McQuarrie 2/2/2018 3:17 PM
Deleted: localized …tructural uplift,…ero… [73]
Michelle Gilmore 2/5/2018 12:00 AM
Deleted: rock…uplift but modeled topogr… [74]
Nadine McQuarrie 2/7/2018 4:58 PM
Deleted: should
Michelle Gilmore 2/5/2018 12:01 AM
Deleted: that …ccount for areas of structu… [75]
Michelle Gilmore 2/5/2018 12:53 AM
Deleted: Influence
Michelle Gilmore 2/9/2018 12:48 AM
Deleted: Python
Nadine McQuarrie 2/7/2018 4:59 PM
Deleted: radiogenic a …urface radiogenic… [76]
Nadine McQuarrie 2/2/2018 3:28 PM
Deleted: appear
Michelle Gilmore 1/31/2018 1:42 AM
Deleted: Modeled fits to published MAr d… [77]
Nadine McQuarrie 2/7/2018 5:05 PM
Comment [1]: This has to be consistent t… [78]
Nadine McQuarrie 2/2/2018 3:31 PM
Deleted: L
Nadine McQuarrie 2/8/2018 9:47 AM
Deleted: L
Michelle Gilmore 2/5/2018 12:18 AM
Deleted: l
Nadine McQuarrie 2/2/2018 3:28 PM
Deleted: when most of the rocks in this pa… [79]
Michelle Gilmore 1/31/2018 1:43 AM
Deleted: se particles have
Nadine McQuarrie 2/2/2018 3:31 PM
Deleted: cooled through the…et the predi… [80]
Michelle Gilmore 2/5/2018 12:18 AM
Deleted: different
Nadine McQuarrie 2/8/2018 9:47 AM
… [81]

kinematic model, displacement over this ramp occurs at 11 Ma, just before the second stage of motion on the Kakhtang Thrust. In the Early KT and Late KT models, Upper Lesser Himalayan duplexing is immediately followed by motion of the duplex over this ramp between 10 and 7 Ma, after a marked decrease in shortening velocity at 10-11 Ma (Table 3). The altered timing of this displacement results in young (7-10 Ma) ZHe ages and AFT ages (Fig. 8). Compared to Split KT model results (Fig. 6b), the younger ZHe ages predicted in Early KT and Late KT models are a poorer fit to published data at 10-40 km from the MFT. The 4-5 Myr gap between published ZHe and AFT data in the Upper Lesser Himalaya is only reproduced using the Split KT kinematic model. The second stage of out-of-sequence thrusting in this model postdates the development of the Upper Lesser Himalaya duplex but predates motion of the duplex over the ramp of younger rocks, causing a 4-5 Myr delay between these two processes that focus exhumation in the Lesser Himalaya. In addition, none of the ZHe ages from the Greater Himalaya could be reproduced by Early KT and Late KT models using velocity B, while the Split KT model results fit two out of three data. To reproduce the 7.42 Ma ZHe age from the structurally higher Greater Himalaya, the absolute age of out-of-sequence thrusting would need to be at least two million years younger in both models to create a mechanism of exhumation and cooling through ZHe closure. This would consequentially alter shortening rates and cooling ages both before and after out-of-sequence thrusting, producing younger modeled ZHe ages in the Lesser Himalaya, which are already too young in the Early and Late KT models.

The fit of predicted ages to published AFT data across the Upper Lesser Himalaya 10-30 km north of the MFT is similar in all three models (Fig. 6, 8). The matching AFT curves are due to the same age and rates of fault motion along the MBT and MFT from ~7.3 Ma to the present, when Upper Lesser Himalayan rocks cool through the AFT closure isotherm in the models. Though the magnitude and timing of out-of-sequence thrusting impacts the predicted AFT ages in GH rocks directly south of the Kakhtang Thrust, none of these three kinematic scenarios reproduced the observed south-to-north younging in AFT ages from the Greater Himalaya 70-90 km from the MFT (Figs. 6 and 8). In this area, the predicted AFT ages were set during Upper Lesser Himalayan duplexing, when GH material is carried over a ramp in the MHT. Cooling ages were subsequently modified by motion on the Kakhtang Thrust, which structurally uplifted Greater Himalayan rocks along a steep fault. The magnitude of subsidence produced in the Late KT model prevents any significant erosion from occurring in the model after out-of-sequence thrusting. Because the Split KT model applies smaller magnitudes of out-of-sequence thrusting twice, predicted ages from the model are between the ages from Early KT and Late KT. The out-of-sequence thrusting prior to upper Lesser Himalayan duplexing in the Early KT allows for structural uplift of GH material after KT motion, which induces topographic uplift and erosion and predicts AFT ages 3-4 Myr younger than the Late KT scenario (Fig. 8). However, Early KT predicted cooling ages are still 5 Myr older than the measured ages. The strong gradient from recently reset AFT ages predicted 50-70 km north of the MFT to older AFT ages 70 km to the north is a function of the prescribed geometry of the MHT. To change this erosional history and pattern of cooling ages, a mechanism of structural and/or topographic uplift in this region is required.

Nadine McQuarrie 2/8/2018 9:48 AM
Deleted: 7a,b

Michelle Gilmore 2/5/2018 12:26 AM
Deleted: 35…km from the MFT. … [82]

Nadine McQuarrie 2/8/2018 9:49 AM
Deleted: particularly …eproduce the 7.42 … [83]

Michelle Gilmore 2/5/2018 12:33 AM
Moved (insertion) [1]

Nadine McQuarrie 2/8/2018 9:51 AM
Deleted: across

Michelle Gilmore 2/5/2018 1:01 AM
Deleted: .

Nadine McQuarrie 2/8/2018 9:53 AM
Deleted: is…similarity…re is…due to sim… [84]

Michelle Gilmore 2/5/2018 12:33 AM
Deleted: across this area… none of these … [85]

Nadine McQuarrie 2/7/2018 5:11 PM
Deleted: along section any AFT data from the GH north of ~70 km from MCT…rom the MFT … [86]

Michelle Gilmore 2/5/2018 12:33 AM
Moved up [1]: The fit of predicted ages to published AFT data across the Upper Lesser Himalaya 10-30 km north of the MFT is similar across all three models. This is due to similar ages and rates of fault motion along the MBT and MFT from ~7.3 Ma to the present, when Upper Lesser Himalayan rocks cool through the AFT closure isotherm in the models.

Nadine McQuarrie 2/2/2018 3:42 PM
Deleted: emplacement…otion on of …he… [87]

Michelle Gilmore 2/3/2018 9:59 PM
Deleted: ted

Nadine McQuarrie 2/2/2018 3:43 PM
Deleted: of…deep, hot rocks …reater Hi… [88]

Michelle Gilmore 2/5/2018 1:15 AM
Deleted: Ages predicted using Late KT and Split KT kinematic scenarios in this region are older than Early KT model predictions because thrust induced subsidence postdates AFT closure in Late KT and Split KT models. …he strong gradient from recently reset AFT ages predicted 50-70 km north of the MFT to earlier … [89]

Nadine McQuarrie 2/7/2018 6:14 PM
Deleted: north of

Michelle Gilmore 1/31/2018 1:49 AM
Deleted: ain Himalaya Thrust

Nadine McQuarrie 2/2/2018 4:08 PM
Deleted: , which cannot reproduce the AFT signal in the Greater Himalaya north of 70 km

4.3 Effect of Cross-Section Geometric Variations on Ages

Multiple studies have shown that thrust geometry has a first-order control on cooling ages in convergent orogens (e.g. Lock and Willett, 2008; McQuarrie and Ehlers, 2015; 2017; Rak et al., 2017). Our thermokinematic modeling of the Long et al. (2011b) cross-section shows that motion over a footwall cutoff in the Daling formation (Fig. 3 C.2a) facilitated AFT cooling in the model from 13-11 Ma, too early to produce the measured ages of 3-6 Ma 65-90 km from the MFT. More recent motion over a footwall cutoff in Baxa and Diuri units set the young AFT ages modeled at 50-65 km from the MFT (Fig. 6). We hypothesized that modifying the geometry of the cross section, specifically changing the locations of décollement ramps, would result in an improved model of the young observed AFT ages across the Greater Himalaya.

In a new, modified and re-balanced version of the Trashigang cross section, the décollement has been adjusted to partition the large ramp cutting through the Diuri and Baxa units into two separate ramps (Fig. 9). The footwall cutoff of the Diuri has remained in its same position along the décollement (65 km north of the MFT), but the footwall cutoff of the Baxa unit has been shifted ~35 km north to the present-day northern end of the Lower Lesser Himalayan duplex (105 km north of the MFT). In balancing this modified geometry, an additional 35 km of slip was added to the amount of overall shortening along section. This shortening occurs after the formation of the duplexed Baxa Group and before motion on the MBT.

Several flexural-kinematic models with this new décollement geometry were evaluated in Pecube to find the best fit to the geology exposed at the surface, dip of the décollement and the depth of the foreland basin. All models use the Split KT kinematic scenario, modified to accommodate updated magnitudes of displacement. The models varied slightly in topographic evolution and assigned EET. Multiple velocity and radiogenic heat production combinations were coupled with these models in Pecube to evaluate the sensitivity of the predicted cooling ages to changing these parameters (Table 3).

Unlike previous models shown in this paper that used one surface radiogenic heat production (Ao) value, the best fit was achieved using a higher surface radiogenic heat production of 4.0 $\mu W/m^3$ in the region of exposed Greater Himalaya rocks and a lower 2.0 $\mu W/m^3$ value for Lesser Himalaya rocks. Using different values for radiogenic heat production is consistent with previous studies that have noted the higher radiogenic heat production capacity of Greater Himalaya rocks which cluster around 4.0 $\mu W/m^3$, while Lesser Himalayan rocks have a lower average radiogenic heat production value of 2.5 $\mu W/m^3$ (Roy and Rao, 2000; Menon et al., 2003; England et al., 1992; Whipp et al., 2007; Herman et al., 2010). Because Pecube is currently not designed to accommodate multiple Ao values within a single model, the model results shown in figures 9-11 merge the predicted ages using both Ao 2.0 $\mu W/m^3$ and 4.0 $\mu W/m^3$ at the surface trace of the MCT. The full extent of each of these predicted cooling age trends is shown in the Supplementary Fig. 2.

4.3.1 Fit of Predicted Cooling Ages Using Modified Geometry

The modified geometry model using the Responsive Topography resulted in a noticeably different and better-fitting predicted age trend in the region north of the MCT (Fig. 9b). Because changing values of Ao can shift predicted ages to older or younger values as well as change the across strike pattern of predicted ages (Fig. 5), both the original and the modified

Deleted: .
Michelle Gilmore 2/5/2018 1:32 AM
Deleted: Influence
Nadine McQuarrie 2/2/2018 4:10 PM
Deleted: such as the Himalaya and Andes
Michelle Gilmore 1/31/2018 1:51 AM
Comment [2]: I'd suggest something like ... [91]
Michelle Gilmore 1/31/2018 2:00 AM
Deleted: Because geometry of the cross se ... [90]
Nadine McQuarrie 2/2/2018 4:11 PM
Deleted: In…results from the best- fitting ... [92]
Michelle Gilmore 1/31/2018 2:02 AM
Deleted: using current cross section geom ... [93]
Nadine McQuarrie 2/2/2018 4:14 PM
Deleted: ,
Michelle Gilmore 1/31/2018 1:56 AM
Deleted: Greater Himalaya rocks are carri ... [94]
Nadine McQuarrie 2/2/2018 4:21 PM
Deleted: the…footwall cutoff inof…the D ... [95]
Michelle Gilmore 1/31/2018 2:01 AM
Deleted: We hypothesized that modifying ... [96]
Nadine McQuarrie 2/2/2018 4:19 PM
Deleted: in the original geometry
Michelle Gilmore 1/27/2018 7:24 PM
Deleted: decollement
Nadine McQuarrie 2/2/2018 4:23 PM
Deleted: of the Upper Lesser Himalaya
Michelle Gilmore 1/27/2018 7:24 PM
Deleted: decollement
Nadine McQuarrie 2/2/2018 4:30 PM
Deleted: ere
Michelle Gilmore 1/31/2018 1:58 AM
Deleted: , ~95 km north of the MFT.
Michelle Gilmore 2/5/2018 10:34 PM
Deleted: Two …everal flexural-kinematic ... [97]
Nadine McQuarrie 2/8/2018 11:03 AM
Deleted: tested …valuated in Pecube to fi ... [98]
Michelle Gilmore 2/5/2018 10:34 PM
Deleted: , one created using Python Topos ... [99]
Nadine McQuarrie 2/8/2018 11:25 AM
Deleted: a…uniform…ne surface radiog ... [100]
Nadine McQuarrie 2/8/2018 11:11 AM
Deleted: Figure 9a shows the results fron ... [101]
Michelle Gilmore 2/9/2018 12:48 AM
Deleted: Python
Nadine McQuarrie 2/8/2018 11:15 AM
Deleted: a

geometry are included in figure 9 using combined Ao values of 2.0 μW/m^3 and 4.0 μW/m^3 for the predicted ages.

Using the new geometry combined with higher radiogenic heat production from the trace of the MCT northward produced predicted MAr and ZHe ages that matched measured ages from the Trashigang section. In addition, the predicted ages matched measured MAr and ZHe ages from the Kuru Chu section except for 3 samples in the immediate footwall of the Kakhtang Thrust (77-87 km from the MFT). Perhaps most critically, the modified geometry provides an improved fit and matches 10 out of 12 AFT data from 53 to 120 km north of the MFT (83% fit). The notable difference with the new geometry is that the "U" shape in the immediate footwall of the KT is narrower (15 km across) and lower amplitude (3 Ma). The new geometry produces AFT patterns that are noticeably different than the patterns produced by the original geometry. For the original geometry (regardless of Ao value), the AFT age trend is set by the motion of rocks over a large footwall ramp, and continues to only match the youngest AFT ages and an additional sample at ~ 73 km from the MFT. On the north side of the ramp the ages reflect the last exhumation event. The ZHe pattern is completely set by the formation of the lower Lesser Himalayan duplex with oldest ages in the north that young in the direction of ramp propagation. Using a higher Ao value (4.0) for the original geometry is an improved match for all three ZHe ages. The across strike trend in predicted AFT and ZHe ages for the new geometry is a more subdued pattern that also gets younger towards the south (between 55 and 80 km north of the MFT). The ages set by the formation of the lower Lesser Himalayan duplex have been modified by motion and accompanying exhumation over the two smaller ramps. Note the youngest predicted AFT ages at 65 km and 105 km from the MFT, co-located with the top of each ramp. The comparison of the two cross section geometries and their predicted ages using the same Ao values specifically highlights the effect of geometry on the predicted cooling ages.

South of the MCT, predicted thermochronometer ages from the modified geometry do not have as strong of a match to the measured ages as with the previous best fit model (Responsive topography, Split KT, velocity B; Fig. 6b). The revised geometry matches half of the measured ZHe ages in the Lesser Himalaya using the lower surface radiogenic heat production of 2.0 μW/m^3 and fits all three published AFT ages within error. When including measured ages from the Kuru Chu region (Fig. 9), the fit improves to 70%. The most noticeable change to the fit of the original geometry using a lower Ao value is the markedly lower predicted AFT ages. With lower surface radiogenic heat production the AFT signal is not as sensitive to motion and associated exhumation over the MBT ramp located at ~ 25 km from the MFT. Similar to changing the kinematics, changing the cross section geometry alters the prescribed rates because the magnitude of shortening has changed (Table 3). In the best fit model of the original geometry, the Upper Lesser Himalaya duplex deforms quickly from 13 to 11 Ma. However in the revised geometry model, this duplex initially deforms quickly from 13-11 Ma, but the rate of deformation during the last 53 km of duplex formation is slower from 11-7.4 Ma. This slower rate and younger age limits the southern extent of the reset ZHe ages at the surface and results in slightly younger (8.5 to 10 Ma) predicted ZHe ages between 20 and 30 km from the MFT.

Michelle Gilmore 2/6/2018 12:38 AM
Deleted: Unlike previous models that used a uniform surface heat production (Ao) value, the best fit was achieved using a higher surface heat production of 4.0 μW/m^3 in the region of exposed Greater Himalaya rocks and a lower 2.0 μW/m^3 for Lesser Himalaya rocks, divided by the MCT. Using different values for radiogenic heat production is consistent with previous studies that have noted the higher heat production capacity of Greater Himalaya rocks which cluster around 4.0 μW/m^3, while Lesser Himalayan rocks have a lower average heat production value of 2.5 μW/m^3 (Roy and Rao, 2000; Menon et al., 2003; England et al., 1992; Whipp et al., 2007; Herman et al., 2010).

Nadine McQuarrie 2/8/2018 11:23 AM
Deleted: -

Nadine McQuarrie 2/8/2018 11:42 AM
Deleted: is

Nadine McQuarrie 2/9/2018 4:20 PM
Deleted: for both the MAr and ZHe systems

Nadine McQuarrie 2/8/2018 11:47 AM
Deleted: However as observed with the original geometry, although the values of the predicted ages are older with lower Ao radiogenic heat production values, the first-order shape of the predicted ages remains the same (Supplementary Fig. 2). Thus using the same radiogenic heat production value as the Lesser Himalaya rocks (2.0 μW/m^3) through the entire section, the predicted trend of AFT cooling ages that young northward between the MCT and KT is broadly 3-4 Ma older

Nadine McQuarrie 2/8/2018 11:48 AM
Deleted: but retains a similar shape.

Nadine McQuarrie 2/8/2018 12:30 PM
Deleted: This

Nadine McQuarrie 2/8/2018 12:41 PM
Deleted: indicates that the trend of cooling ages in this area is a function of the subsurface geometry of the decollementdécollement ramp

Michelle Gilmore 2/9/2018 12:48 AM
Deleted: Python

5 Discussion

5.1 Evaluating the sensitivity of predicted cooling ages

Geothermal gradients and the resulting shape of isotherms in the model, which dictate the spatial and temporal changes in predicted cooling ages, are dynamic and change at each incremental time-step in our models based on 1) thermal parameters prescribed to each model in Pecube; 2) locations and magnitudes of fault displacement; 3) locations and magnitudes of erosion as dictated by structural uplift, isostatic flexure, topographic evolution, and erosion in the flexural-kinematic model; and 4) the rates of deformation and exhumation which are dictated by the absolute timing of each step which we assigned as input in Pecube. Each component in the kinematics of a fold thrust belt system imparts a characteristic cooling pattern to the predicted ages at the surface. Emplacement of a large ductile thrust sheet as with motion of the MCT imparts a pattern of reset cooling ages that is the oldest at the thrust tip and decreases towards the active ramp (Lock and Willett, 2008; McQuarrie and Ehlers, 2015). A southward growing duplex will produce a pattern of cooling ages that young toward the south (Lock and Willett, 2008; McQuarrie and Ehlers, 2017). While rocks record cooling associated with every stage of structural evolution, the events that are recorded by any given thermochronometer system are dependent upon the magnitude of exhumation associated with each component of deformation and the thermal history of the rocks: length and magnitude of burial, speed of exhumation, and radiogenic heat production. If the magnitude of exhumation is particularly close to that necessary to reset a thermochronometer system, the predicted pattern of cooling ages can be significantly altered by small changes in modeled topography or radiogenic heat production. For example, minor changes to the prescribed topography or thermal parameters can shift the signal of preserved AFT ages to record the southward propagation of a duplex versus the displacement of material over a décollement ramp (which would have a northward propagating signal) when the magnitude of exhumation associated with the décollement ramp is small (Supplementary Fig 2). Below we discuss the effects of different topographic models, topographic evolutions, and thermal parameters on cooling ages predicted in Pecube.

5.1.1 Sensitivity of predicted cooling ages to prescribed topographic evolution and EET

Although our evaluation of different topographic models indicates a minor sensitivity in predicted cooling ages to how topography is estimated, modeling an evolving topography such as a topographic slope that either increases or decreases with time can significantly change the predicted pattern of cooling ages by controlling the magnitude of erosion that occurs at a given time and the exhumation event during which a thermochronometer is reset. This marked change in the pattern of cooling, such as recording an older southward propagating duplex rather than a northward migrating ramp, occurs if the magnitude of exhumation associated with an exhumation event is small (~2 km or less) and close to the amount necessary to reset a given thermochronometer. In the case of the young AFT ages across the Greater Himalayan (Fig. 9), the northward younging trend is imparted by recent motion over a décollement ramp that must be north of the youngest age. However, this ramp spans a vertical distance of 2.5 km, half the height of other décollement ramps farther to the hinterland such as the

Michelle Gilmore 2/5/2018 10:32 PM
Deleted: 4.3.2 Fit of Predicted Cooling Ages Using Modified Geometry with No Topo ... [102]

Michelle Gilmore 1/27/2018 7:24 PM
Deleted: decollement

Michelle Gilmore 1/27/2018 7:24 PM
Deleted: decollement

Nadine McQuarrie 2/8/2018 1:41 PM
Deleted: the prescribed

Nadine McQuarrie 2/8/2018 1:47 PM
Deleted: odest

Michelle Gilmore 1/27/2018 7:24 PM
Deleted: decollement

Michelle Gilmore 1/27/2018 7:24 PM
Deleted: decollement

ramp through the lower Lesser Himalayan. The smaller magnitude of vertical uplift and exhumation associated with this ramp makes cooling ages associated with it more sensitive to changes in other parameters.

The most basic requirement to reproduce observed cooling ages is to match the timing of exhumation with the structures that are producing the across strike exhumation pattern (McQuarrie and Ehlers, 2015; 2017). For a given flexural kinematic model this match is a function of the geometry, which is controls the location of uplift, EET which controls the location of rocks with respect to the mantle, and topography which controls the location of rocks with respect to the earths surface. In our best fitting flexural-kinematic and thermal model combination (Figs. 9a and 10a), ~2.0-3.5 km of exhumation, from 6 Ma to the present, was required to match the AFT ages that decrease in age from 6-3.5 Ma 65-90 km north of the MFT. To simulate this magnitude of exhumation following the decrease in topographic elevations south of the KT due to KT loading, the prescribed topographic taper angle was reduced from 2.0 to 1.5 degrees during MBT and MFT motion, with a maximum elevation of 3 km modeled in the final cross section. The magnitude and timing of this exhumation was critical to generate cooling ages across the Greater Himalayan that recorded the signal of recent motion over the décollement ramp and fit the published data (Section 5.4).

Other flexural-kinematic models evaluated in this study, did not predict cooling ages across the lower Greater Himalayan that matched published thermochronometer ages despite using the same geometry, kinematics and thermal properties. The difference in predicted and observed ages were a function of both slightly different topographic evolution scenarios that control magnitudes and timing of erosion and slightly different elastic thickness parameters that control the amount and timing of subsidence. Erosion angle and EET are features prescribed in the flexural-kinematic model before thermo-kinematic modelling. The flexural-kinematic model shown in figure 10b, is remarkably similar to our best fit model when comparing foreland basin thickness, dip of décollement, and surface geology (Supplementary Fig. 1f and 1h) This was obtained by an initial taper angle of 2° and an EET of 75 km. In comparison, the best fit model used an initial taper angle of 2° and an EET that increased from 60 km early in the deformation history to 85 km for the second pulse of motion on the KT and displacement on the MBT and MFT. Higher EET values early in the modeled deformation steps (Supplementary Fig. 1h; Fig. 10b) facilitated more erosion (0.5 to 1.5 km) between 17 and 8 Ma, thus resetting AFT ages at this time (Fig. 10b). In addition, the model displayed in figure 10b used a steeper topographic angle in the immediate foreland (3°) and a 2° angle in the hinterland to more closely match modern topography and the exposed geology (Fig. 10b, Supplementary Fig. 1h). This steeper topography resulted in less erosion from 8 Ma to present (~0.3-1.5) than the best fit model (Fig 10a, Supplementary Fig. 1f), however the predicted surface geology of both models is almost identical. The change in the exhumation history between the two models, although minor, produced a markedly different pattern of cooling ages at the surface between 55 and 85 km from the MFT. The model with 0.5 to 1.5 km of additional exhumation early in the model history produced cooling ages that record the age of older duplexing with southward younging of cooling ages (Fig. 10b).

Although matching the geology exposed at the surface is a critical test to evaluate the accuracy of the flexural-kinematic model, we were able to match the measured AFT data, with a predicted AFT age pattern using a flexural-kinematic model that is under eroded in the hinterland between 55 and 85 km from the MFT (Supplementary Fig. 1i). Structurally lower

Michelle Gilmore 1/27/2018 7:24 PM
Deleted: decollement

Nadine McQuarrie 2/9/2018 5:31 PM
Deleted: For example

Nadine McQuarrie 2/9/2018 5:31 PM
Deleted: , t

Nadine McQuarrie 2/3/2018 7:13 PM
Deleted:

Nadine McQuarrie 2/3/2018 7:16 PM
Deleted: results that was used to generate predicted ages shown in figure 10b used

Nadine McQuarrie 2/3/2018 7:17 PM
Deleted: compared to

Nadine McQuarrie 2/3/2018 7:17 PM
Deleted: that

Nadine McQuarrie 2/3/2018 7:18 PM
Deleted:

Nadine McQuarrie 2/3/2018 7:19 PM
Deleted: versus 10a

Nadine McQuarrie 2/8/2018 3:12 PM
Deleted: signal of an

Greater Himalayan material was under-eroded by ~2-3 km in the final step of the model with 1-2 km of Tethyan material preserved at the surface. Tethyan strata in the Sakteng Klippe is at the surface 10 km east of the Trashigang section line, but has been erosionally removed along the section (Figs. 1 and 2). Similar to the best fitting model, topography maintained a 2° taper until ~8 Ma, however the EET was 65 km. The lower EET allowed for more subsidence in the hinterland and thus less total erosion. From 6 Ma to present EET was increased to 70 km and the topographic angle was reduced to 1.75°. The stronger EET facilitated less subsidence particularly in the Greater Himalayan region. From 6 Ma to present the hanging wall of the MCT underwent 2.0- 2.5 km of exhumation (similar to our best fit model) and thus produced similar predicted AFT ages with the same pattern as observed data (Fig. 10). In summary, the AFT ages can be very sensitive to the evolution of topography and small changes (0.5-1.5 km) in exhumation magnitude as expected. They also can be very sensitive to slight changes in EET. Although the change in topographic taper angle from 2° to 1.5° may account for up to 0.5 km of exhumation, small, 5 km changes in EET which control the amount of subsidence had a larger effect (~ 1 km) on the age and magnitude of exhumation. Thus flexural-kinematic modeling that explicitly accounts for thrust loading and the resulting evolution of the décollement and associated foreland basin with time is a critical component of linking cross section kinematics to thermal models.

Nadine McQuarrie 2/7/2018 3:40 PM
Deleted: flexural…model with 1-2 km o ... [103]

5.1.2 Synthesis of the Effect of Thermophysical Properties on Cooling Ages

Altering the thermal history of the model by imparting a hotter or colder thermal field can also result in different cooling signals preserved at the topographic surface if the exhumation amount is close to a particular closure temperature for a thermochronometer system. For instance, the best fitting model run with exclusively a 2.0 $\mu W/m^3$ surface radiogenic heat production (Ao) value (Supplementary Fig. 2a), predicted AFT ages are reset at ~7-11 Ma from 65-85 km north of the MFT (Supplementary Fig. 2a), with a trend of younger ages toward the north from 85-105 km from the MFT. The pattern of AFT cooling ages, particularly between 75 and 90 km north of the MFT, is recording a signal of older structural uplift instead of recent motion over the décollement ramp.

Nadine McQuarrie 2/9/2018 5:34 PM
Deleted: radiogenic …urface radiogenic ... [104]

Michelle Gilmore 1/27/2018 7:24 PM
Deleted: decollement

Rocks at the surface in our best-fitting model (Fig. 9a) are at a critical thermal threshold where, when exhumed through a low thermal gradient, the rocks will preserve a different age pattern than if that same exhumation occurred through a higher thermal gradient. In the colder model, material that is at the present-day surface passed through the AFT closure temp prior to the motion over the new ramp. In the hot model, material at the present-day surface passed through the AFT closure isotherm during or after this structural uplift. If erosion were reduced by even a small amount in the hot model (0.5 to 1 km), the predicted ages from the model would produce a different trend in cooling ages more similar to a colder thermal model. Conversely, if erosion increased in the cold model, the signal at the surface may look similar to the warmer model. The difference in AFT cooling ages between surface heat production (Ao) values of 4.0 and 2.0 highlight that that magnitude of exhumation in the Greater Himalaya in this model is around the minimum amount necessary to record these younger AFT ages at the surface.

Nadine McQuarrie 2/9/2018 5:39 PM
Deleted: particles…ocks will preserve a ... [105]

5.2 Using Thermochronology to Evaluate Structural Geometry

Using traditional geologic and geophysical constraints to create balanced cross sections can often result in multiple interpretations of the subsurface geology with significant variations in proposed subsurface structures, décollement ramp locations, and total shortening estimates. While kinematic reconstructions of balanced cross sections can help in determining the viability and kinematic sequence of a cross section, thermochronometer data can offer additional insights into predicting subsurface geometry. The geometry of the subsurface and location of ramps in the décollement impart a first order control on the thermochronologic trends present at the surface (Herman et al., 2010; Robert et al., 2011; McQuarrie et al., 2014; Coutand et al., 2014; McQuarrie and Ehlers, 2015, 2017). In this study, Pecube output from two décollement geometries of the Trashigang cross section were compared, and an additional ramp in the MHT resulted in a noticeable change in cooling ages modeled. This finding is particularly evident in modeled AFT ages across the Greater Himalaya. Modeled AFT ages across the Greater Himalayan using the original cross section geometry reflected a cooling signal imparted by a larger ramp through the Lower Lesser Himalayan that did not fit the trend of published data (Fig. 6b). Even with a higher radiogenic heat production assigned to the models, the location and magnitude of this cooling signal did not change (Fig. 10b, Supplementary Fig. 3a). Modeling the modified geometry with an additional décollement ramp facilitated additional erosion across the Greater Himalaya and resulted in a different pattern of predicted ages that better matched the trend of published data (Fig. 9). Another possible structural solution to produce AFT young cooling ages preserved in Greater Himalayan rocks is an out of sequence fault at the modern trace of the MCT (e.g. Adlakha et al., 2013). This potential fault would have to post date motion on the Kakhtang Thrust and have enough throw (~3-5 km) to reset AFT ages. The strongest argument against this solution is the anticipated change in topography. As highlighted by our models of out-of-sequence motion on the Kakhtang Thrust, the topographic response would be a marked increase of topography in the hanging wall and much subdued topography in the footwall. This topographic response has been used to argue for out-of-sequence faulting in Nepal (Wobus et al, 2003) and is decidedly different than the topography of Bhutan (Adams et al., 2013; 2016).

5.3 Estimates of Timing and Rates of Deformation

We evaluated the new geometry using a suite of velocities to test the sensitivity of the predicted ages to prescribed shortening rates. As shown in figure 5, shortening rates of 17 mm/yr or higher in the last 10 million years produces AFT ages that are 2-3 Myr younger than measured ages. Similar to previous studies (Long et al., 2012; Coutand et al., 2014; McQuarrie and Ehlers, 2015), our modelling of the Trashigang data requires slow shortening velocities in eastern Bhutan (6.7-7.5 mm/yr) from 6 Ma to present to match the AFT ages 10-30 km from the MFT, with somewhat higher velocities (7.0-14.6) are permissible from 8.6 Ma. The earliest permissible age for slower velocities is 11 Ma, at a rate of 14.6 mm/yr from 11 Ma till 5.3 Ma (Table 3; Fig. 11). The 40 km south to north extent of ~8-11 Ma ZHe ages require fast shortening rates over this window of time. Acceptable rates of shortening range from 45-70 mm/yr which are at or exceeding plate tectonic rates respectively. 45 mm/yr rate require fast shortening to continue until 9 Ma or younger. Adding a period of

Michelle Gilmore 1/27/2018 7:24 PM
Deleted: decollement

Michelle Gilmore 1/27/2018 7:24 PM
Deleted: decollement

Nadine McQuarrie 2/8/2018 1:54 PM
Deleted: 2011

Michelle Gilmore 1/27/2018 7:24 PM
Deleted: decollement

Michelle Gilmore 2/5/2018 11:59 PM
Deleted: 5

Michelle Gilmore 1/27/2018 7:24 PM
Deleted: decollement

Michelle Gilmore 2/6/2018 12:00 AM
Deleted: ,

Nadine McQuarrie 2/9/2018 5:53 PM
Deleted: Applying a higher radiogenic heat production facilitated an improved fit to the data. By adjusting the decollementdécollement and creating vertical uplift and additional erosion in this area, we were able to successfully model the previously unmatched data across the lower Greater Himalayan

Nadine McQuarrie 2/9/2018 7:17 PM
Deleted: The thermal and flexural model

slightly faster rates (14.6 mm/yr) till 11 Ma increases the speed of shortening (65-70 mm/yr) from 11 Ma till ~13 Ma. The upper age for these modeled fast rates is controlled by predicted ages that are sensitive to the time period over which the lower Lesser Himalayan duplex forms (Fig. 11). These data are MAr ages between 11 and 14 Ma, and ZHe ages located 50-70 km from the MFT. Velocity models where lower Lesser Himalayan duplex is done by 15 Ma, produce the oldest MAr, ZHe and AFT ages north of the MCT and thus the poorest fits to the measured data. Conversely, extending shortening of the upper Lesser Himalayan duplex till 6 Ma predicts ZHe ages that are slightly younger than the measured ages between 10 and 25 km from the MFT (Fig. 11). The limited window of time (13-8 Ma) and high magnitude of shortening (146 km) requires fast shortening rates while the upper Lesser Himalayan duplex forms. Rates depend on both age and displacement and thus a critical question is, could shortening be reduced in the upper Lesser Himalayan duplex? The cross sections were constructed to minimize shortening, while matching surface constraints (Long et al., 2011b). We have re-examined the sections and any modification to the cross section, including moving a ramp as we suggest here, will increase shortening estimates and potentially increase rates. .

Comparison of the results from both the new cross-section geometry presented in this paper and the geometry originally proposed by Long et al. (2011b) indicate an insensitivity the age and rate of MCT displacement. We varied the start of the MCT from 23-20 Ma. Due to limited MAr data available along the Trashigang section, and their location close to the MFT thrust, the measured and predicted ages are all significantly younger than the age of MCT displacement. However, the modeled initiation and rate of displacement of the MCT control the predicted MAr ages between 60 to 90 km from the MFT (Figs. 6, 11) in the location of the Sakteng Klippe (Fig. 1and 2). These modeled ages provide a potential direction for future research that could confirm predicted ages, rates and exhumation amounts. In most of our models, MCT motion occurred from 20 Ma until 18 Ma, at a rate of 29 mm/yr.

The measured cooling ages along the Trashigang and Kuru Chu sections are largely consistent, with the most significant deviation at 10-30 km from the MFT. Here, the younger ages (8.5 to 10 Ma) are from the Kuru Chu and older ages (11 to 11.6 Ma) were collected along the Trashigang transect. As mentioned in section 2.2 the Kuru Chu samples are from elevations 1-1.4 km lower than the Trashigang samples. Our modeled elevation for this region is 0.5-0.7 km, similar to the sample elevations for the Kuru Chu, and our preferred model has a stronger match to the younger Kuru Chu ages, possibly suggesting a dependence on elevation in this region. The location that our modeled ages deviate from the measured ages along the Kuru Chu is between 75 and 90 km, in the immediate footwall of the Kakhtang Thrust. Two ZHe ages and one Mar age are notably younger than our predicted ages for these systems. Two of these samples (ZHe and MAr) are from lower Lesser Himalayan rocks in the Kuru Chu Valley and the other (ZHe) is from the immediate hanging wall of the MCT. All three samples would require a minimum of 4-7 km of addition exhumation to reach the exposure of the samples in the Kuru Chu region. However, similar arguments could be made for samples 65-75 km from the MFT, where similar magnitude of exhumation difference is projected between the Trashigang and Kuruchu sections but measured ages are markedly similar.

Nadine McQuarrie 2/9/2018 8:07 PM
Deleted: combination that best fit published thermochronometer data used rates of deformation that ranged from 68.4 to 6.7 mm/yr (Table 3). Our results provide estimates on the timing of motion along discrete structures present in the Himalayan fold-thrust belt of eastern Bhutan.

Nadine McQuarrie 2/19/2018 4:30 PM
Deleted: Our results are insensitive to

Nadine McQuarrie 2/9/2018 10:12 PM
Deleted: motion

Nadine McQuarrie 2/9/2018 10:12 PM
Deleted: as early as 23 Ma or as late as 20 Ma

Nadine McQuarrie 2/9/2018 10:13 PM
Deleted: d

Nadine McQuarrie 2/9/2018 10:13 PM
Deleted: the

Nadine McQuarrie 2/9/2018 10:13 PM
Deleted: location of

Michelle Gilmore 2/3/2018 10:03 PM
Deleted: Saktang

Nadine McQuarrie 2/9/2018 10:15 PM
Deleted: ,

Nadine McQuarrie 2/9/2018 10:15 PM
Deleted: and thus

Nadine McQuarrie 2/9/2018 10:16 PM
Deleted: and

Nadine McQuarrie 2/9/2018 9:17 PM
Deleted: our best fitting

Nadine McQuarrie 2/9/2018 9:18 PM
Deleted: model

Nadine McQuarrie 2/9/2018 9:19 PM
Deleted: The transition from lower LH to upper LH duplexing in our best fit velocity model of the Trashigang section occurs at 13.5-13.0 Ma suggesting formation of the lower LH duplex from ~18-13 Ma. The 11.1-14.1 Ma ages of MAr samples directly above the lower LH duplex provide the age constraints (Fig. 9). Our predicted MAr ages are closer to the younger end of the range of data present along the Trashigang section (12-14 Ma), suggesting that lower LH duplexing can not continue longer than 13 Ma. The 9-11 Ma ZHe signal present in the upper LH, requires an end to rapid shortening by 11.0 Ma to fit the measured cooling ages. As shown with our revised geometry, extending shortening of the LH duplex till 7.5 Ma predicts ZHe ages that are slightly younger than the measured ages. The limited window of time (13-9 Ma) and high ... [106]

Nadine McQuarrie 2/9/2018 9:30 PM
Deleted: younger predicted ages provide a better match to the ZHe ages measured directly to ... [107]

The age and rate of deformation from the best-fit model of the Trashigang region has noted similarities and differences to other thermokinematic models of the area. We found pronounced variation in shortening rates and magnitude of rates that are very similar to those presented by McQuarrie and Ehlers (2015), however, the window of time of rapid shortening (13-8 Ma; this study) is longer and the permissible rates slower than that proposed for the Kuru Chu section (11-8.5 Ma) immediately to the west (McQuarrie and Ehlers, 2015). The difference in the windows of rapid shortening is a result of the difference in ZHe ages and MAr ages between the two regions. In the Kuru Chu region ZHe and MAr ages continue to get younger to the north between 70 and 100 km from the MFT. The slope and age of the MAr samples was used to argue for the age and rate of deformation of the lower Lesser Himalayan duplex along the Kuru Chu section (McQuarrie and Ehlers, 2015). They found that extending the formation of the duplex until 11 Ma provided the best match to the data. However, their best-fitting model still did not reproduce the youngest cooling ages found 80-100 km from the MFT. The very old predicted ages in this region were a result of a large footwall ramp similar to the original Trashigang geometry (Fig. 6). A potential solution to both the proposed fast rates and the misfit of predicted ages 80-100 km from the MFT may be a change in ramp geometry, similar to the modified geometry proposed here for the Trashigang section. An additional driver of exhumation across the footwall of the Kakhtang thrust would promote younger ages there without the need for a young age of shortening in the lower Lesser Himalayan duplex. If the lower Lesser Himalayan duplex in the Trashigang region continued to ~12 Ma with a timing and rate of deformation more similar to those proposed by McQuarrie and Ehlers (2015), including a younger age in which the MHT slows (8-9 Ma), then the predicted ages would match observed ages as well as any modeled velocity (Fig. 11), but would suggest both sections deformed at rates of 55-75 mm/yr from 8-12 Ma. These rates are faster than plate tectonic rates and would only be permissible with coeval extension on the Southern Tibetan Detachment (STD) as proposed by McQuarrie and Ehlers, 2015. A 12.5 Ma Th-Pb monazite age from Kula Kangri (at the border of Bhutan and Tibet) and 7 Ma ZHe ages (Edwards and Harrison, 1997; Coutand et al., 2014) suggest STD activity over this time window. Even though the details of the rates may continue to evolve for both sections, general trends will remain the similar such as: slow velocities between ~18-13 Ma, fast (45-65 mm/yr) velocities between ~13-8 Ma, and slow velocities from ~8 Ma to present with perhaps a more significant decrease in the last 6 Myr. This post-6 Ma decrease in convergence is consistent with the significant decrease in erosion rate at 6 Ma in eastern Bhutan proposed by Coutand et al. (2014).

6 Conclusions

This study presents a successful approach for using thermochronometer data to test the viability of a proposed cross section geometry based on forward models of the kinematic, exhumational, and thermal history of an area. The cross section geometry imparts a model of the horizontal and vertical component of displacement. We found that the location and magnitude of vertical displacement has the most significant control on the trends of cooling signals recorded by a suite of thermochronometers. Mismatches between modeled and published thermochronometer ages provide insight into how cross sections can be modified and re-evaluated in order to create a more accurate solution to known geologic and

Nadine McQuarrie 2/9/2018 9:33 PM
Deleted: Similar to previous studies (Long et al., 2012; McQuarrie and Ehlers 2015) our results also suggest a slowing in the shortening rate to 14 mm/yr or less sometime between 11 and 9 Ma the shortening rate maybe as low as 5.4 mm/yr during MBT and MFT motion from ~6 Ma to the present to fit AFT data.

Nadine McQuarrie 2/9/2018 9:35 PM
Deleted: hile w

Nadine McQuarrie 2/9/2018 9:36 PM
Deleted:

Nadine McQuarrie 2/9/2018 9:36 PM
Deleted: 11

Nadine McQuarrie 2/9/2018 9:36 PM
Deleted: does not overlap with the period

Michelle Gilmore 2/3/2018 10:03 PM
Deleted: Kuri

Michelle Gilmore 2/3/2018 10:04 PM
Deleted: i

Nadine McQuarrie 2/9/2018 10:23 PM
Deleted: 25 km to the east, the ZHe ages cluster between 8.5 and 10 Ma.

Nadine McQuarrie 2/9/2018 10:24 PM
Deleted:

Nadine McQuarrie 2/9/2018 10:25 PM
Deleted: Along the Trashigang section (this study), the ages range from 9.5 to 11.5 Ma (Figs. 1, 9). If the lower LH duplex in the Trashigang region continued to ~12 Ma with a timing and rate of deformation more similar to those proposed by McQuarrie and Ehlers (2015), including a younger age in which the MHT slows (7.4 Ma versus 11 Ma) then the predicted ZHe ages are younger than the observed ages. The impact of velocity variations plotted in figure 6 highlight the change from an 11 Ma decrease in shortening rate versus a 10 Ma decrease. The difference in age of the fast rates between the Kuri Kuru Chu and Trashigang sections suggests that 8.5-11.5 Ma is the acceptable range in ZHe ages for both sections (Fig. 9). Thus revised thermokinematic models using this larger range of cooling ages for both regions would allow for matching velocities between the cross-sections. Even though the details of the rates would change in both sections, ... [108]

Nadine McQuarrie 2/19/2018 4:35 PM
Deleted: , more

Michelle Gilmore 2/5/2018 11:26 PM
Deleted: resulting

Michelle Gilmore 2/3/2018 10:05 PM
Deleted: themochronometers

Michelle Gilmore 2/3/2018 10:05 PM
Deleted: reevaluated

thermochronologic constraints. We found that the addition of a ramp under the Greater Himalaya in our flexural-kinematic model resulted in more accurately modeled cooling ages across this region while also preserving the modeled accuracy of other geologic and geophysical parameters.

Timing and rates of deformation in compressional settings can be quantified by coupling a high-resolution flexural-kinematic model of a balanced cross section with the thermokinematic model Pecube. Adjusting the timing of motion along structures changes the timing of corresponding exhumation and thus predicted mineral cooling ages. These changes to timing and rates of deformation control the absolute ages recorded by a thermochronometer as well as the slope of cooling ages with distance in the direction of transport. We applied a variable rate of deformation to obtain a best fitting model of the Trashigang cross-section in Bhutan. Acceptable velocities for periods of rapid shortening range from 45-70.0 mm/yr between 13 to as recently as 8 Ma. These alternate with periods of slow shortening. In particular, a significant slowing of shortening rates (7.5 to 6.7 mm/yr) is needed at ~8-6 Ma to present.

While geometry sets the pattern of permissible cooling ages and velocity controls the absolute ages recorded, changes to surface radiogenic heat production and topographic evolution can regulate which patterns of cooling are recorded in each chronometer. Increasing radiogenic heat production in our models generally produced younger cooling ages, with the pattern of predicted cooling ages critically altered in areas where rocks were close to the closure isotherm for a given system. As the timing of closure shifted in a hotter model, patterns of not just younger ages but younger structures were produced in predicted cooling ages, such as the trend of motion over a footwall ramp versus duplex formation. Our best-fitting model combined results from hot and cold thermal models for material north and south of the MCT respectively.

Although model results were less sensitive to the exact method of estimating topography, a responsive topographic method is critical for maintaining the relationship between structural uplift and subsidence and the resulting change in topography. In addition, an evolving topographic taper angle and/or an evolving EET, can alter the timing of exhumation and the predicted pattern of cooling ages. We found that the timing and magnitude of erosion controls which component of deformation and associated exhumation is recorded by a given thermochronometer system. Similar to changes in surface radiogenic heat production, structural signals such as duplex formation and ramp propagation maybe preserved in the cooling ages of different thermochronometer systems depending on the magnitude of exhumation. A pronounced change in the modeled pattern of cooling ages is most noticeable with lowest-temperature thermochronometers. Thus, small topographic changes can produce significantly different results in cooling age patterns for the same cross-section geometry, particularly when particles are at a temperature close to the closure temperature of a given mineral cooling system. While changes in topographic gradients over multi-million year time scales are often uncertain, we can use thermal-kinematic modeling coupled with flexural-kinematic models that estimate topographic evolution to better understand what is driving large- and small-scale changes in the pattern of exhumation over time and space.

This work highlights the importance of considering the aerial distribution of cooling ages, particularly in the direction of transport, to understand their relationship to the structural and topographic evolution of a landscape. Due to the predominant lateral transport of material that occurs in fold and thrust belts, the across-strike pattern of cooling ages from

Nadine McQuarrie 2/19/2018 4:37 PM
Deleted: While geometry sets the pattern of permissible cooling ages, Ao controls which pattern is recorded in which chronometer and changes to velocity controls the absolute ages (including the slope of cooling ages with distance in the direction of transport). Small changes in magnitude of erosion (such as is possible with small changes in EET or how topography is modeled through time) will have a similar effect as to changing Ao, more erosion will show the cooling pattern in a shallower chronometer and less erosion will produce the signal in a deeper chronometer. But the fundamental signal set by the geometry of structures is still there. ... [109]

Michelle Gilmore 2/5/2018 11:15 PM
Deleted: promotes a new perspective on the spatial nature of thermochronometers, particularly

Nadine McQuarrie 2/19/2018 4:39 PM
Deleted: i

Michelle Gilmore 2/5/2018 11:18 PM
Comment [3]: corrected/clarified

Nadine McQuarrie 2/19/2018 4:39 PM
Deleted: n the direction of transport and their relationship to the structural evolution of a landscape.

thermochronometers spanning a wide range of temperature and spatial coverage provide the most robust constraints to the structural geometry and rate of deformation. Forward modeling cross sections and cooling ages using high-resolution spatial and temporal scales reveals which structures are responsible for a given cooling pattern, their geometry, and the rate at which they move—insights that are unavailable with other modeling workflows.

Acknowledgements

The authors acknowledge research support from the Alexander von Humboldt Foundation (McQuarrie and Eizenhöfer), the University of Pittsburgh (McQuarrie, Eizenhöfer and Gilmore), and NSF EAR 0738522 to McQuarrie. Ehlers acknowledges support by European Research Council (ERC). Midland Valley provided software support and use of the program Move. We thank Willi Kappler (University of Tübingen) for his time and programming assistance, and Peter van der Beek, Djorjie Grujic, and one anonymous reviewer for their edits and suggestions. The data for this paper are available through contacting N. McQuarrie, while the modified version of Pecube that can be coupled to 2-D Move restoration files is available through T.A. Ehlers.

References

Adams, B. A., Hodges, K. V., van Soest, M. C., and Whipple, K. X., Evidence for Pliocene-Quaternary normal faulting in the hinterland of the Bhutan Himalaya, Lithosphere, 5, 438–449, doi:10.1130/l277.1, 2013.

Adams, B. A., Whipple, K. X., Hodges, K. V., and Heimsath, A. M.: In situ development of high-elevation, low- relief landscapes via duplex deformation in the Eastern Himalayan hinterland, Bhutan, J. Geophys. Res. Earth Surf., 121, 294–319, doi:10.1002/2015JF003508, 2016.

Adlakha, V.A., Lang, K.A., Patel, R.C., Lal, N., and Huntington, K.W.: Rapid long-term erosion in the rain shadow of the Shillong Plateau, Eastern Himalaya, Tectonophysics. 582, 76–83, 2013.

Avouac, J.-P.: Dynamic processes in extensional and compressional settings—Mountain building: From earthquakes to geological deformation, in: Crust and Lithosphere Dynamics, Treatise on Geophysics, 6, edited by Schubert, G. and Watts, A. B., Elsevier, Boston, 377–439, doi:10.1016/B978-044452748-6.00112-7, 2007.

Banerjee, P. and Burgmann, R.: Convergence across the northwest Himalaya from GPS measurement, Geophys. Res. Lett., 29(13), 1652, 2002.

Banerjee, P., Burgmann, R., Nagarajan, B., and Apel, E.: Intraplate deformation of the Indian subcontinent, Geophys. Res. Lett., 35, L18301, 2008.

Batt, G. E. and Brandon, M.T.: Lateral thinking: 2-D interpretation of thermochronology in convergent orogenic settings, Tectonophys., 349, 185 – 201, 2002.

Beaumont, C., Jamieson, R. A., Nguyen, M. H., and Lee, B.: Himalayan tectonics explained by extrusion of a low-viscosity crustal channel coupled to focused surface denudation, Nature, 414, 738–742, doi:10.1038/414738a, 2001.

Michelle Gilmore 2/5/2018 11:16 PM
Deleted: ,

Nadine McQuarrie 2/19/2018 4:40 PM
Deleted: McQuarrie Eizenhöferacknowledges research support from an Alexander von Humboldt Foundation fellowship, NSF (EAR 0738522) and the University of Pittsburgh. Gilmore acknowledges funding from NSF (EAR 0738522) and the University of Pittsburgh. Ehlers acknowledges supportted by European Research Council (ERC).

Michelle Gilmore 1/28/2018 10:58 PM
Deleted: reviewers

Nadine McQuarrie 2/3/2018 8:26 PM
Deleted: Kip

Nadine McQuarrie 2/3/2018 8:26 PM
Deleted:

Nadine McQuarrie 2/19/2018 4:46 PM
Deleted:

Nadine McQuarrie 2/19/2018 4:46 PM
Deleted:

Bettinelli, P., Avouac, J. P., Flouzat, M., Jouanne, F., Bollinger, L., Willis, P., and Chitrakar, G. R.: Plate motion of India and interseismic strain in the Nepal Himalaya from GPS and DORIS measurements, J. Geod., 80, 567–589, 2006.

Bhargava, O. N.: The Bhutan Himalaya: A Geological Account, in: Geological Society of India Special Publication 39, edited by Bhargavara, O. N., Calcutta, India, 64–78, 1995.

Bilham, R., Larson, K., Freymueller, J., and Project Idylhim Members: GPS measurements of present-day convergence across the Nepal Himalaya, Nature, 386, 61–64, 1997.

Bollinger, L., Henry, P., and Avouac, J. P.: Mountain building in the Nepal Himalaya: Thermal and kinematic model, Earth Planet. Sci. Lett., 244, 58–71, doi:10.1016/j.epsl.2006.01.045, 2006.

Brady, R. J., Ducea, M. N., Kidder, S. B., and Saleeby, J. B.: The distribution of radiogenic heat production as a function of depth in the Sierra Nevada batholith, California, Lithos, 86, 229–244, doi:10.1016/j.lithos.2005.06.003, 2006.

Braun, J.: Pecube: a new finite-element code to solve the 3D heat transport equation including the effects of a time-varying, finite amplitude surface topography, Computers & Geosci., 29, 787-794, 2003.

Castelluccio, A., Mazzoli, S., Andreucci, B., Jankowski, L., Szaniawski, R., and Zattin, M.: Building and exhumation of the Western Carpathians: New constraints from sequentially restored, balanced cross sections integrated with low-temperature thermochronometry, Tectonics, 35, 2698–2733, doi:10.1002/2016TC004190, 2016.

Chapman, D.: Thermal gradients in the continental crust, in: The Nature of the Lower Continental Crust, in: Geol. Soc. Spec. Pub., vol. 24, edited by Dawson, J. B., Carswell, D. A., Hall, J., and Wedepohl, K .H., 63–70, doi:10.1144/GSL.SP.1986.024.01.07, 1986.

Coutand, I., Whipp Jr., D.M., Grujic, D., Bernet, M., Fellin, M.G., Bookhagen, B., Landry, K.R., Ghalley, S.K., and Duncan, C.: Geometry and kinematics of the Main Himalayan Thrust and Neogene crustal exhumation in the Bhutanese Himalaya derived from inversion of multithermochronologic data, J. Geophys. Res, Solid Earth, 119, 2014.

Coutand, I., Barrier, L., Govin, G., Grujic, D., Dupont-Nivet, G., Najman, Y., and Hoorn, C.: Late Miocene-Pleistocene evolution of India-Eurasia convergence partitioning between the Bhutan Himalaya and the Shillong plateau: New evidences from foreland basin deposits along the Dungsam Chu section, Eastern Bhutan, Tectonics, 35, 2963–2994, doi:10.1002/2016TC004258, 2016.

Daniel, C. G., Hollister, L. S., Parrish, R. R., and Grujic, D.: Exhumation of the Main Central Thrust from lower crustal depths, eastern Bhutan Himalaya, J. Metamorph. Geol., 21, 317–334, doi:10.1046/j.1525- 1314.2003.00445.x, 2003.

Davidson, C., Grujic, D., Hollister, L. S., and Schmid, S. M.: Metamorphic reactions related to decompression and synkinematic intrusion of leucogranite, High Himalayan crystallines, Bhutan, J. Metamorph. Geol., 15, 593–612, 1997.

DeCelles, P.G., Robinson, D.M., Quade, J., Ojha, T.P., Garzione, C.N., Copeland, P., and Upreti, B.N.: Stratigraphy, structure, and tectonic evolution of the Himalayan fold–thrust belt in western Nepal, Tectonics, 20, 487–509, 2001.

DeCelles, P. G., Robinson, D. M., and Zandt, G.: Implications of shortening in the Himalayan fold-thrust belt for uplift of the Tibetan Plateau, Tectonics, 21(6), 1062, 2002.

Nadine McQuarrie 1/31/2018 2:21 PM
Deleted: Berthet, T., Hetényi, G., Cattin, R., Sapkota, S.N., Champollion, C., Kandel, T., Doerflinger, E., Drukpa, D., Lechmann, S., and Bonnin, M.: Lateral uniformity of India Plate strength over central and eastern Nepal, Geophys J. Int, 195(3), 1481-1493, 2013.

Nadine McQuarrie 2/19/2018 4:47 PM
Deleted:

Nadine McQuarrie 2/19/2018 4:47 PM
Deleted:

Nadine McQuarrie 2/19/2018 4:48 PM
Deleted: Célérier, J., Harrison, T.M., Beyssac, O., Herman, F., Dunlap, W.J., and Webb, A.G.: The Kumaun and Garwhal Lesser Himalaya, India. Part 2: Thermal and deformation histories, Geol Soc. Am. Bull., 121, 1281-1297, 2009.

Duncan, C., Masket, J., and Fielding, E.: How steep are the Himalaya? Characteristics and implications along-strike topographic variations, Geology, 31, 75–78, 2003.

Edwards, M. A., and T. M. Harrison: When did the roof collapse? Late Miocene north-south extension in the high Himalaya revealed by Th-Pb monazite dating of the Khula Kangri granite, Geology, 25, 543–546, doi:10.1130/0091-7613(1997)025<0543:WDTRCL>2.3.CO;2, 1997.

Ehlers, T. A.: Crustal thermal processes and thermochronometer interpretation, in: Low-Temperature Thermochronology: Techniques, Interpretations, and Applications, Rev. Mineral. Geochem., 58, 315–350, doi:10.2138/rmg.2005.58.12, 2012.

Ehlers, T. A., Chaudri, T., Kumar, S., Fuller, C. W., Willett, S. D., Ketcham, R. A., Brandon, M. T., Belton, D. X., Kohn, B. P., Gleadow, A. J. W., Dunai, T. J., Fu, F. Q.: Computational tools for low-temperature thermochronometer interpretation, Rev. Mineral. Geochem., 58, 589–622. doi:10.2138/rmg.2005.58.22, 2005.

Ehlers, T.A. and Farley, K.A.: Apatite (U–Th)/He thermochronometry; methods and applications to problems in tectonic and surface processes, Earth Planet. Sci. Lett., 206, 1–14, 2003.

England, P., Le Fort, P., Molnar, P., and Pêcher, A: .Heat sources for Tertiary metamorphism and anatexis in the Annapurna-Manaslu region (central Nepal), J. Geophys. Res., 97, 2107–2128, 1992.

Erdös, Z., Huismans, R. S., van der Beek, P., Thieulot, C.: Extensional inheritance and surface processes as controlling factors of mountain belt structure, J. Geophys. Res. Solid Earth, 119, 9042–9061, 2014.

Gansser, A.: Geology of the Himalayas, 289 pp., Wiley-Interscience, New York, 1964.

Gansser, A.: Geology of the Bhutan Himalaya, 181 pp., Birkäuser, Basel, 1983.

Grujic, D., Hollister, L. S., and Parrish, R. R.: Himalayan metamorphic sequence as an orogenic channel: Insight from Bhutan, Earth Planet. Sci. Lett., 198, 177–191, 2002.

Grujic, D., Coutand, I., Bookhagen, B., Bonnet, S., Blythe, A., and Duncan, C.: Climatic forcing of erosion, landscape, and tectonics in the Bhutan Himalayas, Geology, 34, 801–804, 2006.

Grujic, D., Warren, C. J., and Wooden, J. L.: Rapid synconvergent exhumation of Miocene-aged lower orogenic crust in the eastern Himalaya, Lithosphere, 3, 346–366, doi:10.1130/L154.1, 2011.

Guenther, W. R., Reiners, P. W., Ketcham, R. A., Nasdala, L., Giester, G.: Helium diffusion in natural zircon: Radiation damage, anisotropy and the interpretation of zircon (U-Th)/He thermochronology, Am. J. Sci., 313, 145–198, doi:10.2475/03.2013.01, 2013.

Hammer, P., Berthet, T., Hetényi, G., Cattin, R., DRupka, D., Chophel, J., Lechmann, S., Le Moigne, N., Champollion, C., and Doerflinger, E.: Flexure of the India plate underneath the Bhutan Himalaya, Geophys. Res. Lett., 40(16), 4225–4230, 2013.

Henry, P., Le Pichon, X., and Goffé, B.: Kinematic, thermal and petrologi- cal model of the Himalayas: Constraints related to metamorphism within the underthrust Indian crust and topographic evolution, Tectonophysics, 273, 31–56, doi:10.1016/S0040-1951(96)00287-9, 1997.

Nadine McQuarrie 2/19/2018 4:49 PM
Deleted: .

Nadine McQuarrie 2/19/2018 4:49 PM
Deleted: .

Heim, A. and Gansser, A.: Central Himalayas—Geological observations of Swiss expedition, 1936, Mem. Soc. Helv. Sci. Nat., 73, 1–245, 1939.

Herman, F., Copeland, P., Avouac, J.P., Bollinger, L.. Mahéo, G.. Le Fort, P., Rai, S., Foster, D., Pêcher, A., Stüwe, K., and Henry, P.: Exhumation, crustal deformation, and thermal structure of the Nepal Himalaya derived from the inversion of thermo-chronological and thermobarometric data and modeling of the topography, J. Geophys. Res., 115, B06407, 2010.

Hodges, K.V., Parrish, R.R. and Searle, M.P.: Tectonic evolution of the central Annapurna Range, Nepalese Himalayas: Tectonics, v. 15, p. 1264–1291, 1996.

Hollister, L. S. and Grujic, D.: Pulsed channel flow in Bhutan, Geol. Soc. Spec. Publ., 268, 415–423, 2006.

Huntington, K.W., Ehlers, T.A., Hodges, K.V. and Whipp Jr., D.M.: Topography, exhumation pathway, age uncertainties, and the interpretation of thermochronometer ages, Tectonics, 26, TC4012, 2007.

Jain, A.K., Kumar, D., Singh, S., Kumar, A., and Lal, N.: Timing, quantification and tectonic modelling of Pliocene–Quaternary movements in the NW Himalaya: Evidence from fission track dating. Earth Planet. Sci. Lett., 179, 437–451, 2000.

Jamieson, R. A., Beaumont, C., Medvedev, S, and Nguyen, M. H.: Crustal channel flows: 2. Numerical models with implications for metamorphism in the Himalayan-Tibetan orogen, J. Geophys. Res. Solid Earth, 109, B06407, doi:10.1029/2003JB002811, 2004.

Kellett, D. A., Grujic, D. and Erdmann, S.: Miocene structural reorganization of the South Tibetan detachment, eastern Himalaya: Implications for continental collision, Lithosphere, 1, 259–281, doi:10.1130/L56.1, 2009.

Ketcham, R. A.: Distribution of heat producing elements in the upper and middle crust of southern and west-central Arizona: Evidence from the core complexes, J. Geophys. Res. Solid Earth, 101, 13,611– 13,632, doi:10.1029/96JB00664, 1996.

Klootwijk, C. T., Gee, J. S., Peirce, J. W., Smith, G. M., and McFadden, P. L.: An early India□Asia contact: Paleomagnetic constraints from Ninetyeast Ridge, ODP Leg 121, Geology, 20, 395–398, doi:10.1130/0091-7613(1992)020<0395:AEIACP>2.3.CO;2, 1992.

Larson, K. M., Burgmann, R., Bilham, R. and Freymueller, J.: Kinematics of the India-Eurasia collision zone from GPS measurements, J. Geophys. Res., 104, 1077–1093, 1999.

Lavé, J. and Avouac, J. P.: Active folding of fluvial terraces across the Siwaliks Hills, Himalayas of central Nepal, J. Geophys. Res., 105, 5735–5770, 2000.

Leech, M. L., Singh, S., Jain, A. K., Klemperer, S. L., and Manickavasagam, R. M.: The onset of India-Asia continental collision: Early, steep subduction required by the timing of UHP metamorphism in the western Himalaya: Earth Planet. Sci. Lett., 234, 83–97, doi: 10.1016/j.epsl.2005.02.038, 2005.

LeFort, P.: Himalayas: The collided range, present knowledge of the continental arc, Am. J. Sci., 275-A, 1–44, 1975.

Lock, J. and Willett, S.: Low-temperature thermochronometric ages in fold-and-thrust belts, Tectonophysics, 456, p. 147–162, doi:10.1016/j.tecto.2008.03.007, 2008.

Nadine McQuarrie 2/19/2018 4:50 PM
Deleted: .

Nadine McQuarrie 1/29/2018 12:57 PM
Deleted: Hodges, K. V.: Tectonics of the Himalaya and southern Tibet from two perspectives, Geol. Soc. Am. Bull., 112, 324–350, 2000. .

Nadine McQuarrie 2/19/2018 4:50 PM
Deleted: .

Long, S., N. McQuarrie, N., Tobgay, T., Rose, C., Gehrels, G., and Grujic, D.: Tectonostratigraphy of the Lesser Himalaya of Bhutan: Implications for the along-strike stratigraphic continuity of the northern Indian margin, Geol. Soc. Am. Bull., 123, 1406–1426, 2011a.

Long, S., McQuarrie, N., Tobgay, T., and Grujic, D.: Geometry and crustal shortening of the Himalayan fold-thrust belt, eastern and central Bhutan, Geol. Soc. Am. Bull., 123, 1427–1447, 2011b.

Long, S., McQuarrie, N., Tobgay, T., and Hawthorne, J.: Quantifying internal strain and deformation temperature in the eastern Himalaya, Bhutan: Implications for the evolution of strain in thrust sheets, J. Struct. Geol., 33, 579–608, doi:10.1016/j.jsg.2010.12.011, 2011c.

Long, S.P., McQuarrie, N., Tobgay, T., Coutand, I., Cooper, F., Reiners, P., Wartho, J., and Hodges, K.V.: Variable shortening rates in the eastern Himalayan thrust belt, Bhutan: insights from multiple thermochronologic and geochronologic datasets tied to kinematic reconstructions, Tectonics, 31, TC5004, 2012.

Long, S. P., Gordon, S. M., Young, J. P., and Soignard, E.: Temperature and strain gradients through Lesser Himalayan rocks and across the Main Central thrust, south central Bhutan: Implications for transport-parallel stretching and inverted metamorphism, Tectonics, 35, 1863–1891, doi:10.1002/ 2016TC004242, 2016.

Mattauer, M.: Intracontinental subduction, crust-mantle décollemont and crustal-stacking wedge in the Himalayas and other collision belts, in Collision Tectonics, edited by M. P. Coward and A. C. Ries, Geol. Soc. Spec. Publ., 19, 37–50, 1986.

McQuarrie, N., Robinson, D., Long, S., Tobgay, T., Grujic, D., Gehrels, G., and Ducea, M.: Preliminary stratigraphic and structural architecture of Bhutan: Implications for the along-strike architecture of the Himalayan system, Earth Planet. Sci. Lett., 272, 105–117, 2008.

McQuarrie, N., Tobgay, T., Long, S.P., Reiners, P.W., and Cosca, M.A. Variable exhumation rates and variable displacement rates: documenting a recent slowing of Himalayan shortening in western Bhutan, Earth Planet. Sci. Lett., 386, 161-174, 2014.

McQuarrie, N. and Ehlers, T.A: Influence of thrust belt geometry and shortening rate on thermochronometer cooling ages: Insights from the Bhutan Himalaya: Tectonics, 34, doi:10.1002/ 2014TC003783, 2015.

McQuarrie, N. and Ehlers T.A.: Techniques for understanding fold-thrust belt kinematics and thermal evolution: in Law, R.D., Thigpen, J.R., Merschat, A.J., Stowell, H.H., (eds) Linkages and Feedbacks in Orogenic Systems. Geol. Soc. Am. Mem. 213. doi:10.1130/2017.1213(02), 2017.

Menon, R., Kumar, P., Reddy, G. and Srinivasan, R.: Radiogenic heat production of late Archaean Bundelkhand granite and some Proterozoic gneisses and granitoids of central India, Curr. Sci., 85, 634–638, 2003.

Mitra, S., Priestley, K., Bhattacharyya, A. and Gaur, V.K.: Crustal structure and earthquake focal depths beneath northeastern India and southern Tibet, Geophys. J. Int., 160, 227–248, 2005.

Mora, A., Casallas, W., Ketcham, R.A., Gomez, D., Parra, M., Namson, J., Stockli, D., Almendral, A., Robles, W., and Ghorbal, B.: Kinematic restoration of contractional basement structures using thermokinematic models: A key tool for petroleum system modelling, American Association of Petroleum Geologists Bulletin, 99, 1575–1598, doi:10.1306/04281411108, 2015.

Nadine McQuarrie 2/19/2018 4:51 PM
Deleted: .

Michelle Gilmore 2/3/2018 10:13 PM
Deleted: -

Nadine McQuarrie 2/19/2018 4:51 PM
Deleted: .

Michelle Gilmore 2/3/2018 10:13 PM
Deleted: o-

Michelle Gilmore 2/3/2018 10:13 PM
Deleted: l

Nadine McQuarrie 2/19/2018 4:51 PM
Formatted: Font:(Default) +Theme Headings, 10 pt

Nadine McQuarrie 1/29/2018 12:56 PM
Deleted: .

Michelle Gilmore 2/3/2018 10:14 PM
Deleted: -

Mottram, C. M., Warren, C. J., Halton, A. M., Kelley, S. P., and Harris, N. B. W.: Argon behaviour in an inverted Barrovian sequence, Sikkim Himalaya: The consequences of temperature and timescale on $^{40}Ar/^{39}Ar$ mica geochronology, Lithos, 238, 37–51, doi: 10.1016/j.lithos.2015.08.01, 2015.

Najman Y., Appel, E., Boudagher-Fadel, M., Bown, P., Carter, A., Garzanti, E., Godin, L., Han, J., Liebke, U., Oliver, G., Parrish, R., and Vezzoli, G.: Timing of India–Asia collision: Geological, biostratigraphic and palaeomagnetic constraints. J. Geophys. Res., 115, B12416, doi:10.1029/2010JB007673, 2010.

Patriat, P. and Achache, J.: Indian-Eurasian collision chronology has implications for crustal shortening and driving mechanisms of plates, Nature, 311, 615– 621, 1984.

Powell, C.M., and Conaghan, P.J.: Plate tectonics and the Himalayas, Earth Planet. Sci. Lett. 20, 1–12, 1973.

Rak, A. J., McQuarrie, N., and Ehlers, T. A.: Kinematics, Exhumation, and Sedimentation of the North Central Andes (Bolivia): An Integrated Thermochronometer and Thermokinematic Modeling Approach, Tectonics, 36, 2524–2554, doi:10.1002/2016TC004440, 2017.

Ray, L., Bhattacharya and A. Roy, S.: Thermal conductivity of Higher Himalayan Crystallines from Garhwal Himalaya, India. Tectonophys. 434, 71–79, 2007.

Robert, X., van der Beek, P., Braun, J., Perry, C., Dubille, M. and Mugnier, J.-L.: Assessing Quaternary reactivation of the Main Central Thrust zone (central Nepal Himalaya): New thermochronologic data and numerical modeling, Geology, 37(8), 731–734, 2009.

Singer, J., Kissling, E., Diehl, T., and Hetényi, G.: The underthrusting Indian crust and its role in collision dynamics of the Eastern Himalaya in Bhutan: Insights from receiver function imaging, J. Geophys. Res. Solid Earth, 122, 1152–1178, doi:10.1002/2016JB013337, 2017.

Stüwe, K. and Foster, D.: 40Ar/39Ar, pressure, temperature and fission track constraints on the age and nature of metamorphism around the Main Central Thrust in the eastern Bhutan Himalaya, J. Asian Earth Sci., 19(1–2), 85–95, 2001.

Thiede, R., Ehlers, T.A., Bookhagen, B., and Strecker, M.R.: Erosional variability along the northwest Himalayan Front, J. Geophys. Res., Earth Surface, 114, F01015, 2009.

Thiede, R. C. and Ehlers, T. A.: Large spatial and temporal variations in Himalayan denudation, Earth Planet. Sci. Lett., 371, 278-293, 2013.

Tobgay, T., McQuarrie, N., Long, S., Kohn, M. J., and Corrie, S. L., The age and rate of displacement along the Main Central Thrust in the western Bhutan Himalaya, Earth Planet. Sci. Lett., 319–320, 146–158, doi:10.1016/j.epsl.2011.12.005, 2012.

Valla, P., Herman, F., van der Beek, P. A., and Braun, J.: Inversion of thermochronological age-elevation profiles to extract independent estimates of denudation and relief history - I: Theory and conceptual model, Earth Planet. Sci. Lett., 295, 511–522, doi:10.1016/j.epsl.2010.04.032, 2010.

Whipp, D.M. Jr., Ehlers, T.A., Blythe, A.E., Huntington, K.W., Hodges, K.V., and Burbank, D.W.: Plio-quaternary exhumation history of the central Nepalese Himalaya: 2. Thermokinematic and thermochronometer age prediction model, Tectonics, 26, TC3003, 2007.

Nadine McQuarrie 2/19/2018 4:52 PM
Deleted: .

Nadine McQuarrie 2/19/2018 4:52 PM
Deleted: .

Whipp, D., Ehlers, T.E., Braun, and J., Spath, C.: Effects of exhumation kinematics and topographic evolution on detrital thermochronometer data, J. Geophys. Res. 114, F04021, 2009.

Wobus, C. W., Hodges, K. V., and Whipple, K. X.: Has focused denudation sustained active thrusting at the Himalayan topographic front?, Geology, 31, 861–864, doi:10.1130/G19730.1, 2003.

Zhang, P. Z., et al.: Continuous deformation of the Tibetan Plateau from global positioning system data, Geology, 32, 809–812, 2004.

Nadine McQuarrie 1/29/2018 12:56 PM

Deleted: Yin, A.: Cenozoic tectonic evolution of the Himalayan orogen as constrained by along-strike variation of structural geometry, exhumation history, and foreland sedimentation, Earth Sci. Rev., 76, 1–131, 2006. ... [110]

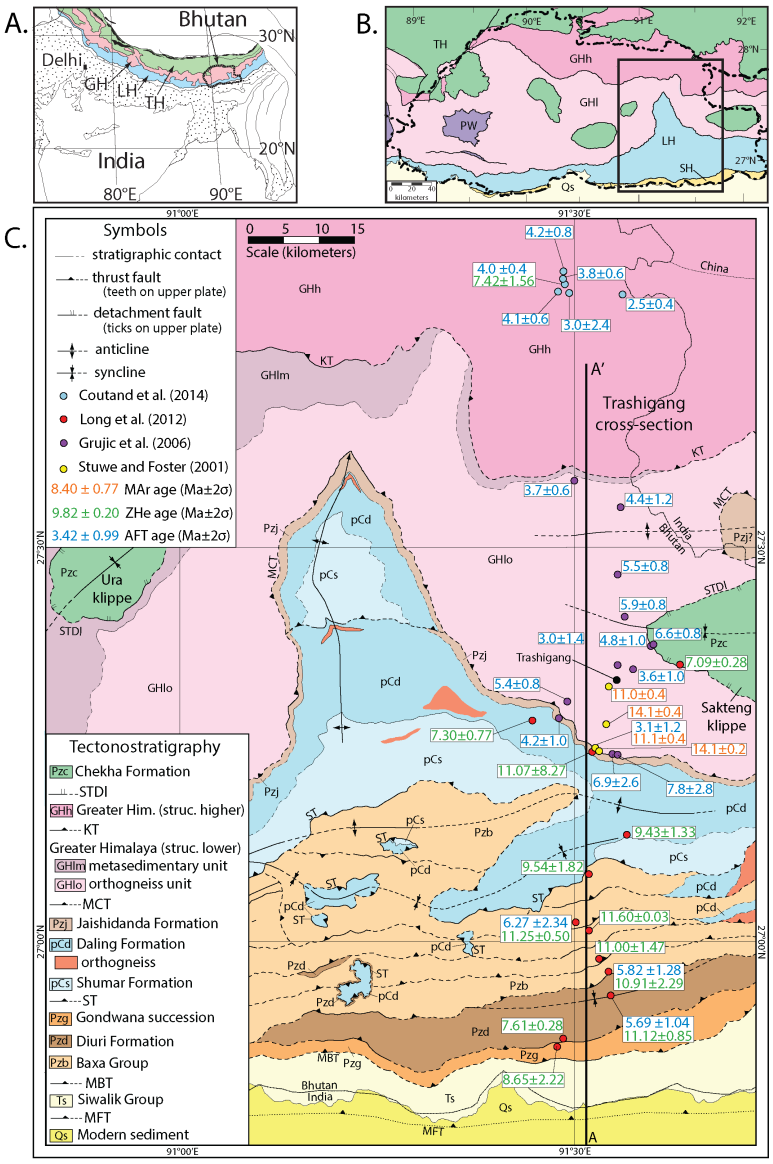
A.
Bhutan
30°N
Delhi
GH
LH
TH
India
20°N
80°E
90°E
B.
89°E
90°E
91°E
92°E
28°N
27°N
TH
GHh
GHl
PW
LH
SH
Qs
kilometers
C.
91°00'E
91°30'E
27°30'N
27°00'N
Symbols
stratigraphic contact
thrust fault
(teeth on upper plate)
detachment fault
(ticks on upper plate)
anticline
syncline
Coutand et al. (2014)
Long et al. (2012)
Grujic et al. (2006)
Stuwe and Foster (2001)
8.40 ± 0.77 MAr age (Ma±2σ)
9.82 ± 0.20 ZHe age (Ma±2σ)
3.42 ± 0.99 AFT age (Ma±2σ)
0 5 10 15
Scale (kilometers)
Tectonostratigraphy
Pzc Chekha Formation
STDI
GHh Greater Him. (struc. higher)
KT
Greater Himalaya (struc. lower)
GHlm metasedimentary unit
GHlo orthogneiss unit
MCT
Pzj Jaishidanda Formation
pCd Daling Formation
orthogneiss
pCs Shumar Formation
ST
Pzg Gondwana succession
Pzd Diuri Formation
Pzb Baxa Group
MBT
Ts Siwalik Group
MFT
Qs Modern sediment
China
India
Bhutan
Trashigang
cross-section
A
A′
Ura
klippe
Sakteng
klippe
4.2±0.8
4.0 ±0.4
7.42±1.56
3.8±0.6
2.5±0.4
4.1±0.6
3.0±2.4
3.7±0.6
4.4±1.2
5.5±0.8
5.9±0.8
6.6±0.8
3.0±1.4
4.8±1.0
7.09±0.28
3.6±1.0
11.0±0.4
5.4±0.8
14.1±0.4
3.1±1.2
11.1±0.4
7.30±0.77
4.2±1.0
14.1±0.2
11.07±8.27
6.9±2.6
7.8±2.8
9.43±1.33
9.54±1.82
6.27 ±2.34
11.25±0.50
11.60±0.03
11.00±1.47
5.82 ±1.28
10.91±2.29
7.61±0.28
5.69 ±1.04
11.12±0.85
8.65±2.22

Figure 1: A. Generalized geologic map of central and eastern Himalayan orogen, modified from Gansser (1983). Abbreviations are GH: Greater Himalaya, LH: Lesser Himalaya, TH: Tethyan Himalaya

B. Simplified tectonostratigraphic map of Bhutan, modified from Long et al. (2012). The border of Bhutan is marked as a dashed and bolded line, and the area of figure 1C is outlined as a solid black rectangle. Tectonostratigraphic groups shown are TH: Tethyan Himalaya (green); GHh: Greater Himalaya, structurally higher (dark pink); GHl: Greater Himalaya, structurally lower (light pink); PW: Paro Window (purple); LH: Lesser Himalaya (blue); SH: Subhimalaya Siwalik Group (dark yellow); Qs: modern sediment (light yellow).

C. Geologic map of eastern Bhutan with Trashigang section line A-A' and reported thermochronometer data shown (Fig. 2), modified from Long et al. (2012). Cooling ages are reported in Myr. Abbreviations of units are Pzc: Chekha Formation; GHh: Greater Himalaya, structurally higher; GHlm: Greater Himalaya, structurally lower, metasedimentary unit; GHlo: Greater Himalaya, structurally lower, orthogneiss unit; Pzj: Jaishidanda Formation; pCd Daling Formation; pCs: Shumar Formation; Pzg: Gondwana succession; Pzd: Diuri Formation; Pzb: Baxa Group; Ts: Siwalik Group; Qs: Modern sediment. Labled fault abbreviations are STDI: South Tibetan Detachment; KT: Kakhtang Thrust; MCT: Main Central Thrust; ST: Shumar Thrust; MBT: Main Boundary Thrust; MFT: Main Frontal Thrust.

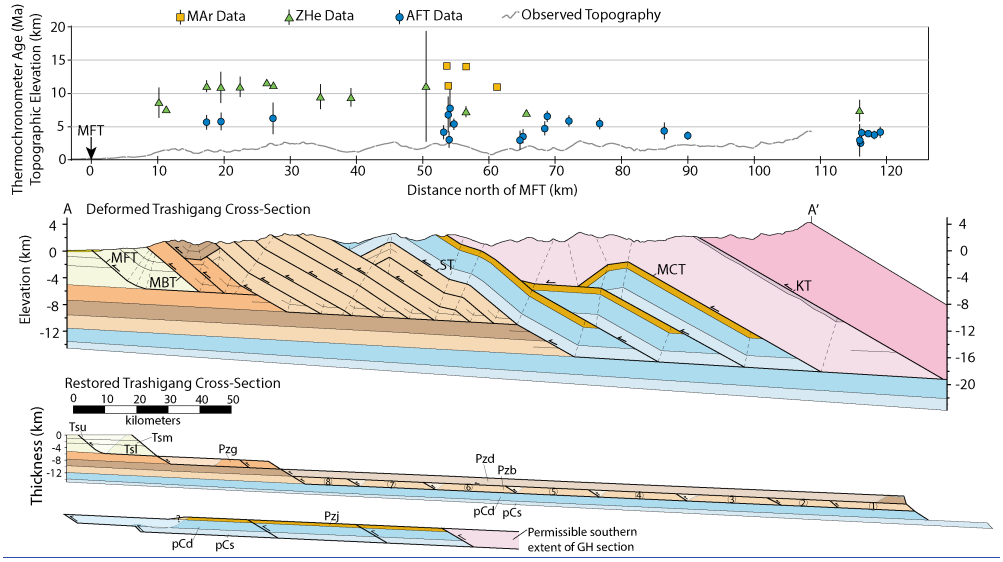

Figure 2: A. MAr, ZHe, and AFT thermochronometer data and elevation along the Trashigang section plotted in the direction of transport. B. Simplified balanced geologic cross section of the Trashigang region of Bhutan, modified from Long et al. (2011a). Scale of the deformed section is represented on the above graph. Unit abbreviations are shown in the stratigraphic column of figure 1. Abbreviations same as figure 1.

Michelle Gilmore 2/3/2018 10:36 PM
Deleted: Abbreviations of structures from north to south: YCS: Yadong Cross-Structure, STDh: structurally higher South Tibetan Detachment, LT: Laya thrust, KT: Kakhtang Thrust, STDl: structurally lower South Tibetan Detachment, MCT: Main Central Thrust, ST: Shumar Thrust MBT: Main Boundary Thrust, MFT: Main Frontal Thrust. Abbreviations of windows and klippen from east to west: LLW: Lum La window, SK: Sakteng klippe; UK: Ura klippe, TCK: Tang Chu klippe, PW: Paro window LS: Lingshi syncline.

Michelle Gilmore 2/3/2018 10:40 PM
Deleted: The border of Bhutan is marked as a dashed and bolded line, and the area of Fig 1C outlined as a solid black rectangle.

Michelle Gilmore 2/8/2018 7:44 PM
Deleted: shown

Michelle Gilmore 2/8/2018 7:44 PM
Deleted: with reported thermochronologic data

Michelle Gilmore 2/3/2018 10:19 PM
Deleted: Blue circles mark AFT and ZHe data from Coutand et al. (2014) that has been projected 27 km SE at 129 degrees, preserving distance of data between KT and STDh structures.

Michelle Gilmore 2/3/2018 10:20 PM
Deleted: in inset

Michelle Gilmore 2/3/2018 10:20 PM
Deleted: Pza: Chekha Formation;

Nadine McQuarrie 2/7/2018 3:44 PM
Deleted: e

Michelle Gilmore 2/8/2018 7:43 PM
Formatted: Normal, Line spacing: single

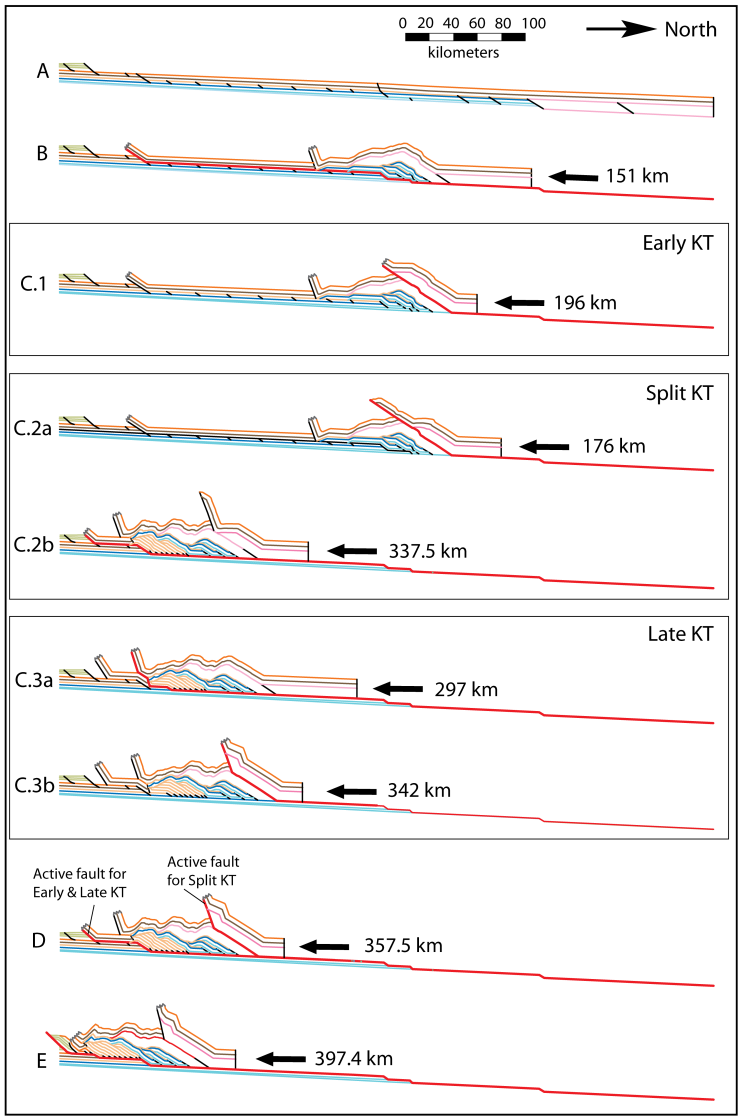
0 20 40 60 80 100
kilometers
North
A
B
151 km
Early KT
C.1
196 km
Split KT
C.2a
176 km
C.2b
337.5 km
Late KT
C.3a
297 km
C.3b
342 km
Active fault for Early & Late KT
Active fault for Split KT
D
357.5 km
E
397.4 km

Figure 3: Sequential kinematic reconstruction of the Trashigang cross section depicting three kinematic scenarios of out-of-sequence thrusting tested in this study. Net slip amounts are shown for each subfigure A: the restored section used in the kinematic model; B: deformation along the MCT and ST, including duplexing of the lower LH; C.1: KT motion prior to upper LH duplexing (Early KT); C.2: KT motion before and after upper LH duplexing (Split KT); C.3: KT motion after seven out of eight horses of upper LH duplex have been deformed (Late KT); D: completion of out-of-sequence thrusting and Upper LH duplexing. Note that the most recent active fault in this step for Split KT varies; E: deformation along MBT and MFT.

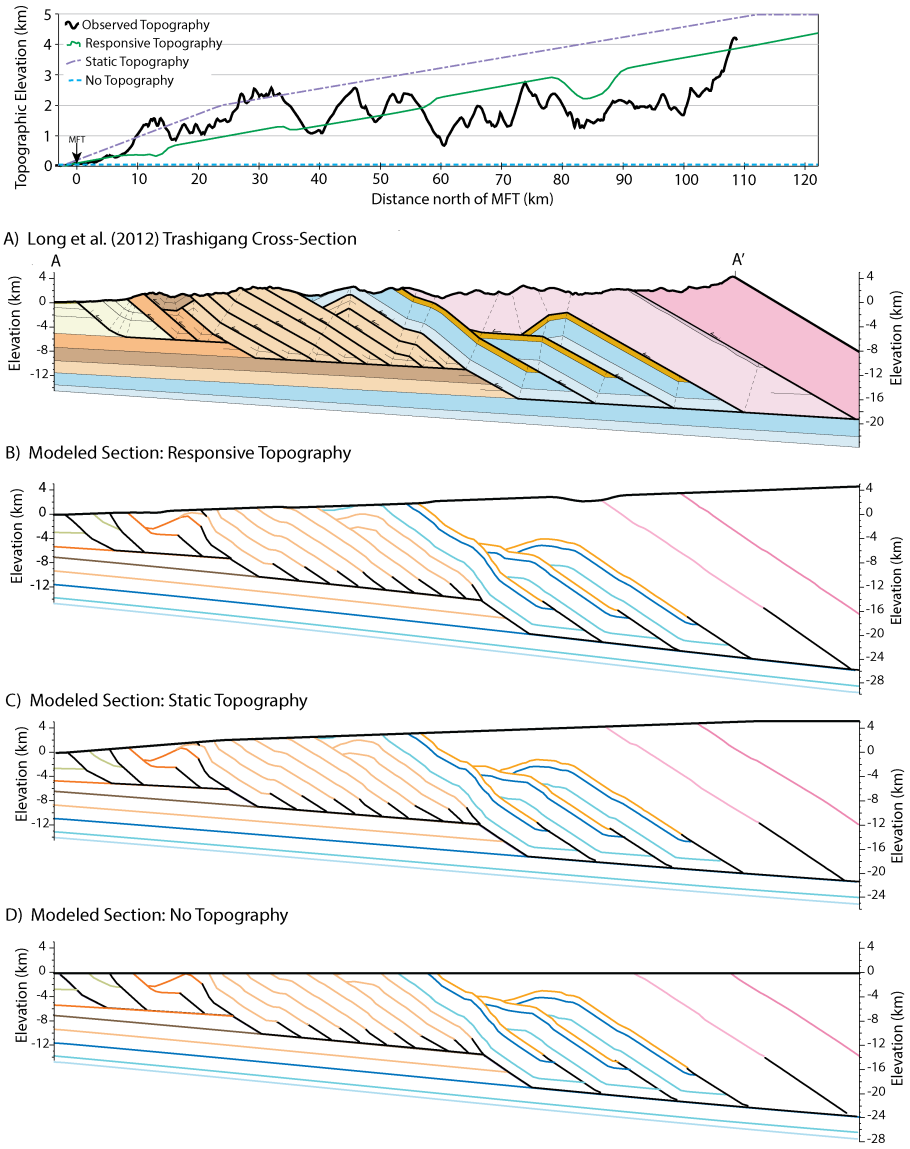
Topographic Elevation (km)
Observed Topography
Responsive Topography
Static Topography
No Topography
MFT
Distance north of MFT (km)
A) Long et al. (2012) Trashigang Cross-Section
A
A'
Elevation (km)
B) Modeled Section: Responsive Topography
C) Modeled Section: Static Topography
D) Modeled Section: No Topography

Figure 4: A) Vertically exaggerated topographic model elevations compared to observed topography of the Trashigang section, Long et al. (2011a) cross-section shown in A). Flexural-kinematic models were created using Split KT and B) Responsive, C) Static, and D) No Topography.

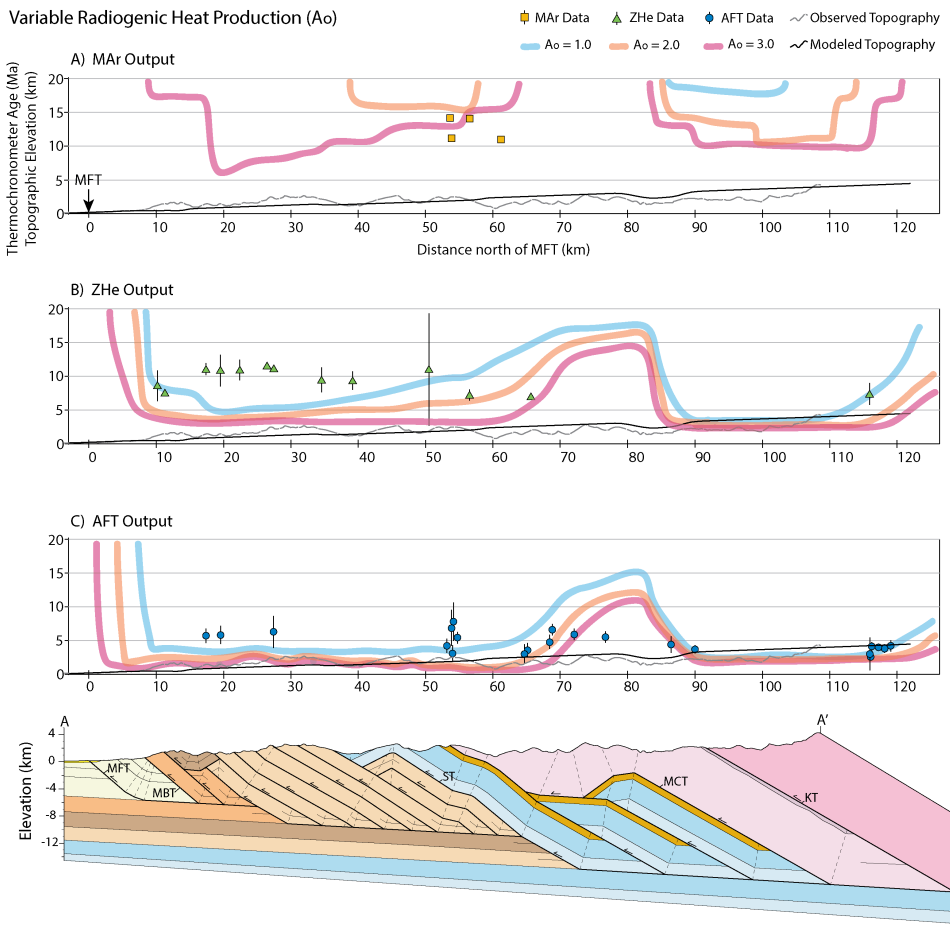

Figure 5: Predicted MAr (a), ZHe (b), and AFT (c) cooling ages from Pecube using variable surface radiogenic heat production (Ao) values of 1.0, 2.0, and 3.0 µW/m^3 compared to published cooling data. Other model variables are set as constant velocity, Split KT, Responsive Topography.

Michelle Gilmore 2/8/2018 9:51 PM
Deleted: s

Michelle Gilmore 2/8/2018 9:50 PM
Deleted: topographic elevations of the deformed cross sections using

Michelle Gilmore 2/8/2018 9:48 PM
Deleted: Python

Michelle Gilmore 2/8/2018 9:49 PM
Deleted: Template

Michelle Gilmore 2/8/2018 9:50 PM
Deleted: . B) Trashigang cross section simplified from Long et al. (2011a) compared to flexural-kinematic model outputs using Split KT and Python, Template, and No Topography.

Michelle Gilmore 2/8/2018 9:26 PM
Deleted: Python

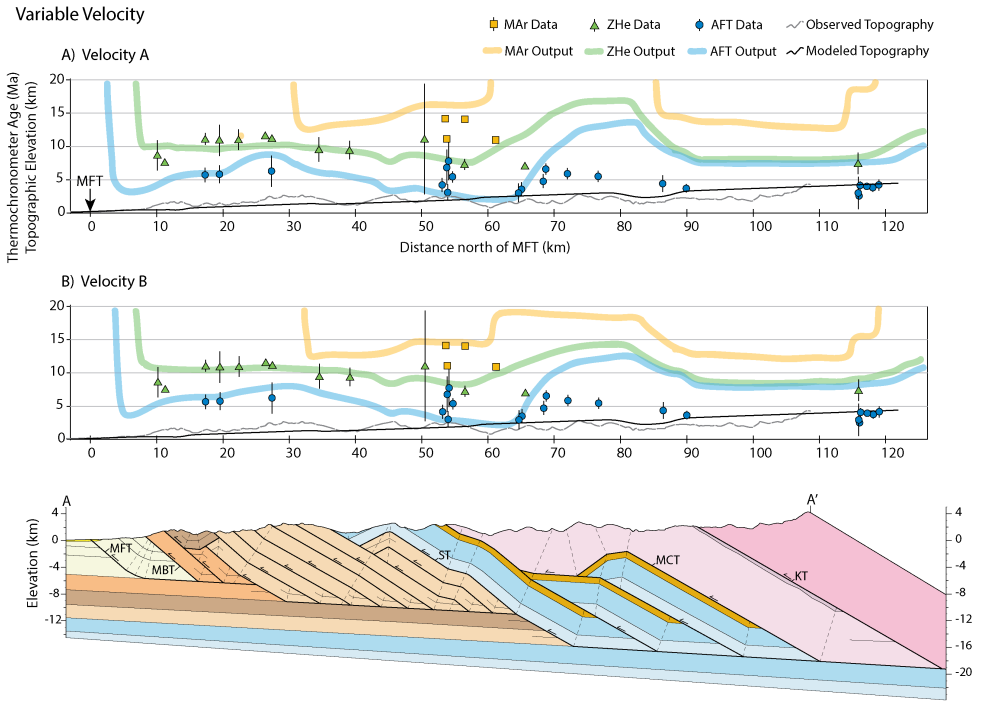

Figure 6: Predicted MAr (yellow), ZHe (green), and AFT (blue) cooling ages using variable velocities A (A) and B (B) compared to published thermochronometer data. Other model variables are set as Split KT, Responsive Topography, and Ao = 2.5 µW/m^3.

Michelle Gilmore 2/9/2018 12:48 AM
Deleted: Python

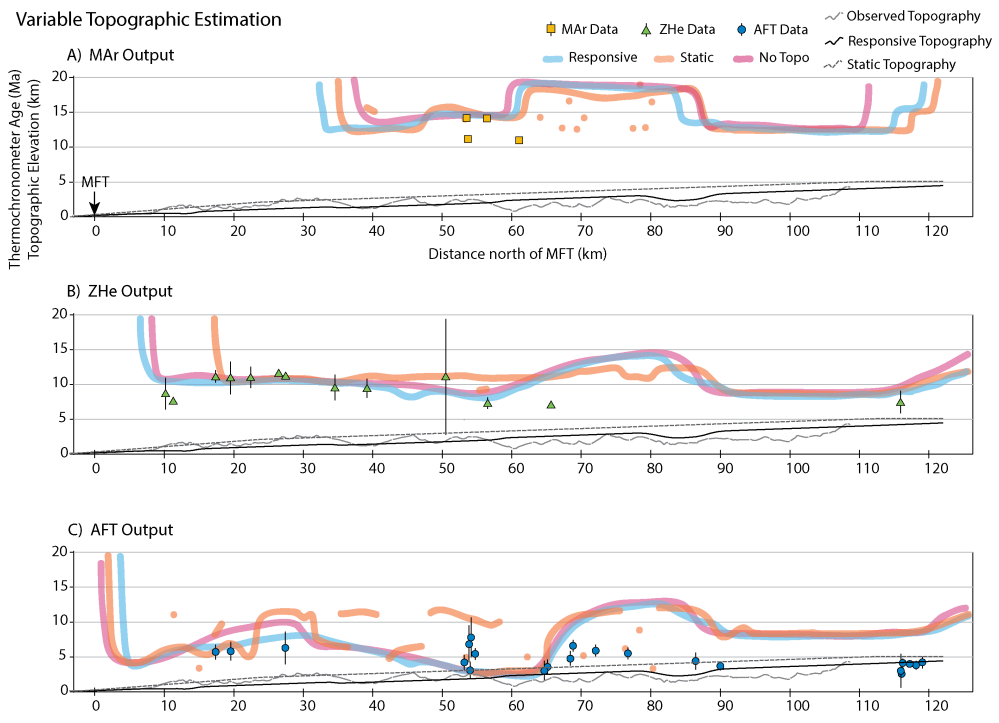

Figure 7: Predicted MAr (a), ZHe (b), and AFT (c) cooling ages using Responsive, Static, and No Topography models compared to published thermochronometer data. Other model variables are set as Split KT, Velocity B, and Ao = 2.5 µW/m^3.

Michelle Gilmore 2/8/2018 10:29 PM
Deleted: Python, Template

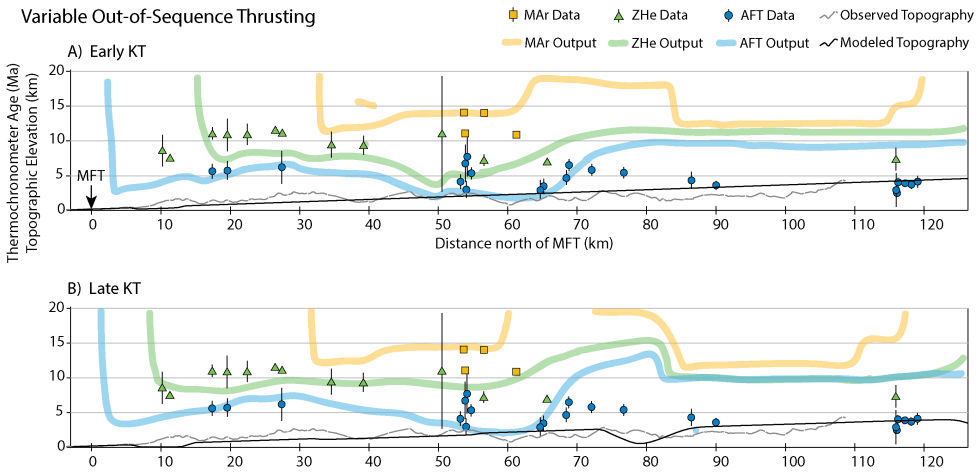

Figure 8: Predicted MAr, ZHe, and AFT cooling ages using Split KT (A), Early KT (B), and Late KT (C) kinematic scenarios compared to published thermochronometer data. Other model variables are set as Responsive Topography, Velocity B, and Ao = 2.5 µW/m^3.

Unknown
Formatted: Font:9 pt, Bold

Michelle Gilmore 2/8/2018 10:31 PM
Deleted: using flexural-kinematic models

Michelle Gilmore 2/8/2018 10:30 PM
Deleted: a

Michelle Gilmore 2/8/2018 10:30 PM
Deleted:

Michelle Gilmore 2/8/2018 10:30 PM
Deleted: b

Michelle Gilmore 2/8/2018 10:30 PM
Deleted:

Michelle Gilmore 2/8/2018 10:35 PM
Deleted: Python

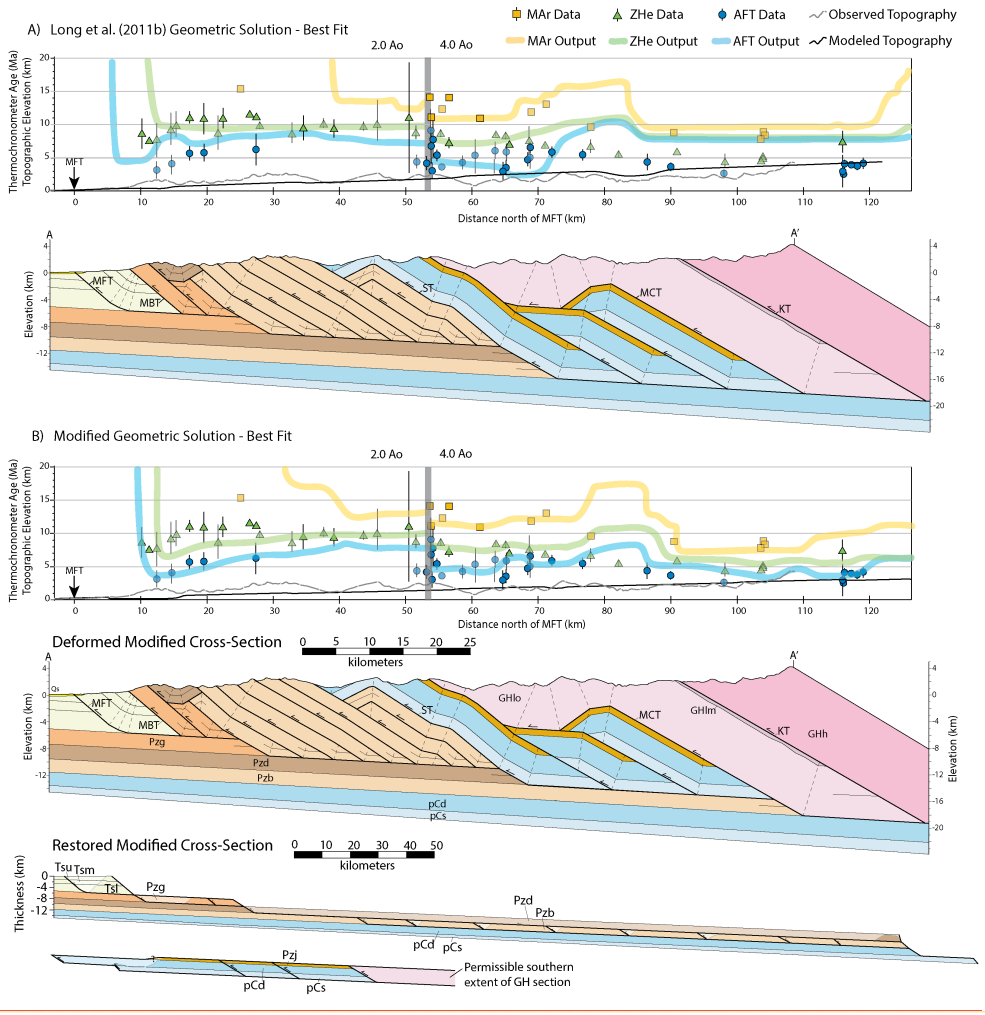

Figure 9: Predicted MAr, ZHe, and AFT cooling ages using a flexural model of the modified geometry with Responsive Topography (a) and No Topography (b) models compared to published thermochronometer data. The décollement ramp through the upper LH Baxa and Diuri units has been split, and the Baxa footwall ramp moved 35 km north. Published data include

Unknown
Formatted: Font:9 pt, Bold

Michelle Gilmore 2/9/2018 12:48 AM
Deleted: Python

Michelle Gilmore 1/27/2018 7:24 PM
Deleted: decollement

additional ages from the Kuru Chu line of section west of the Trashigang section (Long et al., 2012) shown in the transparent colors. The grey vertical line aligned with the location of the MCT shows the division between outputs from separate thermal models have been merged using 2.0 and 4.0 µW/m^3 to the south and north of the MCT respectively. Other model variables are set as Split KT and Velocity C.

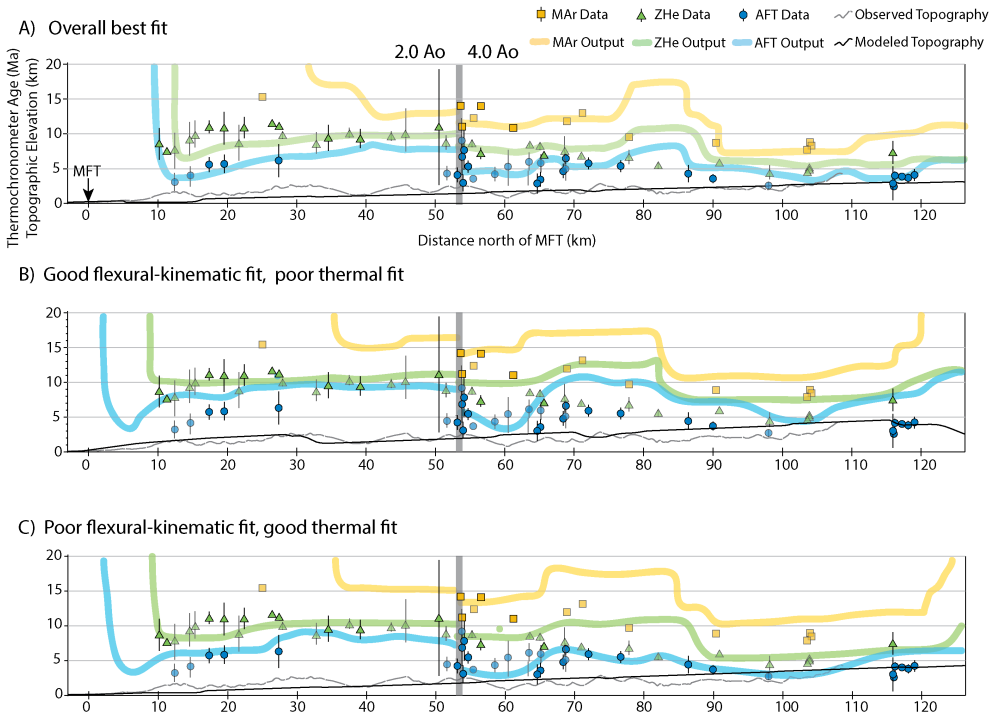

Figure 10: Comparison of predicted MAr, ZHe, and AFT cooling ages between the best fitting thermo-kinematic model combination present in figure 9a (a), a well-matched flexural-kinematic model that yielded a thermal model with poorly fitting predicted ages (b), and a poorly-matched flexural-kinematic model that yielded a thermal model with well-fitting predicted ages (c). Published data include additional ages from the Kuru Chu line of section west of the Trashigang section (Long et al., 2012). Predicted ages are presented with combined thermal models using Ao of 2.0 and 4.0 µW/m^3. Flexural models used Split KT and Responsive Topography.

Michelle Gilmore 2/3/2018 10:15 PM
Deleted: gray

Unknown
Formatted: Font:Bold

Nadine McQuarrie 2/7/2018 3:43 PM
Deleted: flexural-thermal

Michelle Gilmore 2/9/2018 12:48 AM
Deleted: Python

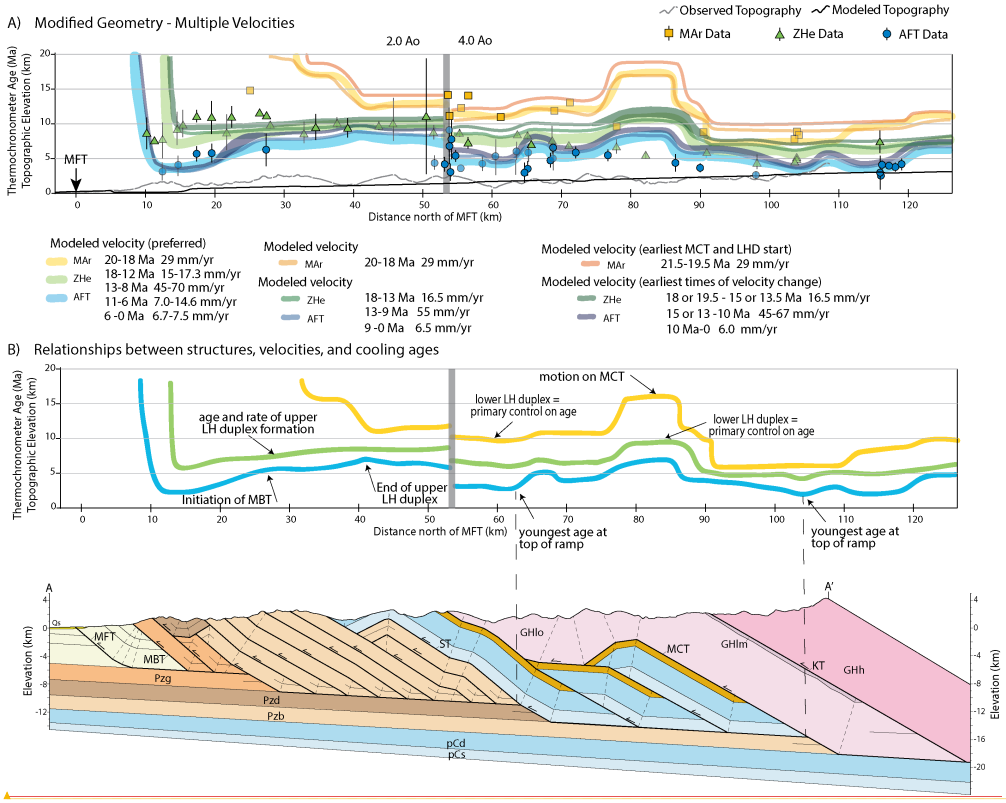

Figure 11: A) Predicted MAr (yellow), ZHe (green), and AFT (blue) cooling ages for velocities tested using the modified Trashigang cross-section geometry. Published data include additional ages from the Kuru Chu line of section, 30 km west of the Trashigang section (Long et al., 2012), which are indicated by thermochronometer symbols that are 50% transparent. Predicted ages are presented with combined thermal models using Ao of 2.0 and 4.0 μW/m^3. Flexural-kinematic models used Split KT and Responsive Topography. B) Relationships between structures, velocities, and predicted cooling ages.

Unknown

Formatted: Font:9 pt, Bold

Flexural-Kinematic Model Output

Geometry & Kinematics	Topography Estimation	EET (km)	Crustal Density (g/cm^3)	Foreland Basin Thickness (km)	Décollement Dip (°)	Surface Geology
Long et al. [2011a]	-	-	-	**5.6**	**4**	-
Long et al. Geometry						
Split KT	Responsive	65	2.60	5.2	5.1	GOOD
Split KT	Static	65	2.60	4.6	3.8	over-eroded by 0.3 km at hanging wall of ST
Split KT	NoTopo	65	3.20	5.1	4.6	over-eroded by 0.9 km at Diuri Fm and by 2.3 km at hanging wall of ST
Early KT	Responsive	65	2.60	4.3	5	over-eroded by 0.5 km at Diuri Fm and hanging wall of ST
Early KT	Static	65	2.60	4.5	4.4	GOOD
Late KT	Responsive	65	2.60	5.6	5.4	under-eroded by 0.4 km at Diuri Fm, hanging wall of ST, and GH synform
Late KT	Static	65	2.60	4.9	5.2	under-eroded by 1 km at Diuri Fm
Modified Geometry						
Split KT	Responsive	70	2.60	5.7	4.5	GOOD

Table 1: Comparison of the geologic constraints of the published Trashigang cross section to the final deformed cross section results of the flexural-kinematic models presented in this study.

Numerical model parameters

Property/parameter	Model input value
Material properties	
heat production	
crustal volumetric heat production	1.0 - 5.0 mW/m3
e-folding depth of crustal heat prod.	20 km
thermal conductivity	2.5 W/m K
specific heat capacity	800 J/kg K
crustal density	2700 kg/m3
mantle density	3300 kg/m3
Numerical properties	
temperature at base	1300°C
model base	110 km
surface temperature at 0 km	20 °
atmospheric lapse rate	0°/ km
kinematic grid spacing	0.5 km
displacement increment	~10 km
model domain	730 x 110 x 5 km
horizontal node spacing (numerical model)	0.5 km
vertical node spacing (numerical model)	1.0 km
model start time	50 Ma

Table 2: Thermal and rock property parameters assigned as input for Pecube.

Unknown
Formatted: Font:9 pt, Bold

Displacement Ages & Rates

A. Long et al. (2012) Geometric Solution

Split KT Models

			Constant Velocity $Ao = 1.00, 2.00, 3.00\ \mu W/m^3$			*Velocity A* $Ao = 2.25, 2.50, 2.75, 3.00\ \mu W/m^3$			*Velocity B* $Ao = 2.00, 2.25, 2.50, 2.75, 3.00, 4.00\ \mu W/m^3$		
Active Structure	**Slip on Structure (km)**	**Total Shortening (km)**	**Start Age (Ma)**	**End Age (Ma)**	**Velocity (mm/yr)**	**Start (Ma)**	**End (Ma)**	**Velocity (mm/yr)**	**Start (Ma)**	**End (Ma)**	**Velocity (mm/yr)**
MCT	63.2	63.2	23.0	19.3	17.3	23.0	21.0	31.6	20.0	17.0	21.1
Lower LH Duplex	87.9	151.1	19.3	14.3	17.3	21.0	15.0	14.7	17.0	13.5	25.1
KT	25.0	176.1	14.3	12.8	17.3	15.0	14.3	37.3	13.5	13.2	74.6
Baxa Duplex	161.4	337.5	12.8	3.5	17.3	14.3	10.0	37.3	13.2	11.0	74.6
KT	20.0	357.5	3.5	2.3	17.3	10.0	6.7	6.0	11.0	7.3	5.4
MBT	26.5	384.0	2.3	0.8	17.3	6.7	2.2	6.0	7.3	2.5	5.4
MFT	13.4	397.4	0.8	0.0	17.3	2.2	0.0	6.0	2.5	0.0	5.4

Early KT Models

			Velocity B $Ao = 2.25, 2.50, 2.75\ \mu W/m^3$		
Active Structure	**Slip on Structure (km)**	**Total Shortening (km)**	**Start (Ma)**	**End (Ma)**	**Velocity (mm/yr)**
MCT	63.2	63.2	20.0	17.0	21.1
Lower LH Duplex	87.9	151.1	17.0	13.0	22.0
KT	45.0	196.1	13.0	12.4	69.4
Baxa Duplex (1-7)	145.9	342.0	12.4	10.3	69.4
Baxa Duplex (8)	15.5	357.5	10.3	7.4	5.4
MBT	26.5	384.0	7.4	2.5	5.4
MFT	13.4	397.4	2.5	0.0	5.4

Late KT Models

			Velocity B $Ao = 2.25, 2.50, 2.75, 3.00, 3.25, 3.50\ \mu W/m^3$		
Active Structure	**Slip on Structure (km)**	**Total Shortening (km)**	**Start (Ma)**	**End (Ma)**	**Velocity (mm/yr)**
MCT	63.2	63.2	20.0	17.0	21.1
Lower LH Duplex	87.9	151.1	17.0	13.0	22.0
Baxa Duplex (1-7)	145.9	297.0	13.0	11.0	73.0
KT	45.0	342.0	11.0	10.0	45.0
Baxa Duplex (8)	15.5	357.5	10.0	7.2	5.5
MBT	26.5	384.0	7.2	2.4	5.5
MFT	13.4	397.4	2.4	0.0	5.5

B. Modified Geometric Solution

			Range of Velocities Tested $Ao = 2.00, 2.25, 2.50, 2.75, 3.00, 3.25, 3.50, 3.75, 4.00, 5.00\ \mu W/m^3$			*Range Best-Fitting Velocities* $Ao = 2.00, 4.00\ \mu W/m^3$		
Active Structure	**Slip on Structure (km)**	**Total Shortening (km)**	**Start Age Range (Ma)**	**End Age Range (Ma)**	**Velocity Range (mm/yr)**	**Start Age Range (Ma)**	**End Age Range (Ma)**	**Velocity Range (mm/yr)**
MCT	58.0	58.0	21.6 - 19.9	19.6 - 17.9	29.0	20.4 - 19.9	18.4 - 17.9	29.0
Lower LH Duplex	78.0	136.0	19.6 - 17.9	14.9 - 13.2	15.0 - 17.5	18.4 - 17.9	13.4 - 13.2	15.0 - 17.3
KT	25.0	161.0	14.9 - 13.2	14.4 - 11.8	15.0 - 68.4	13.4 - 13.2	13.1 - 11.8	15.0 - 68.0
Baxa Duplex (1-7)	146.0	161.0	14.4 - 11.8	11.2 - 9.6	45.0 - 70.0	13.1 - 11.8	11.0 - 9.6	45.0 - 70.0
Baxa Duplex (8)	53.0	360.0	11.2 - 9.6	10.0 - 7.3	8.0 - 67.0	11.0 - 9.6	8.6 - 7.3	8.0 - 65.0
KT	20.0	380.0	10.0 - 7.4	6.7 - 5.7	6.0 - 17.0	8.6 - 7.3	5.3 - 6.0	7.0 - 14.6
MBT	29.0	409.0	6.7 - 4.7	1.8 - 1.5	6.0 - 7.5	5.3 - 5.2	1.6 - 1.5	6.7 - 7.5
MFT	11.0	420.0	1.8 - 1.5	0.0	6.0 - 7.5	1.6 - 1.5	0.0	6.7 - 7.5

Table 3: Combinations of heat production values and deformation ages and rates tested for each flexural-kinematic model.

Michelle Gilmore 2/8/2018 5:33 PM

Deleted: Tested combinations of flexural, thermal, and deformation timing and velocity parameters.